NASA TECHNICAL NOTE

NASA TN D-8444

NASA TN D-8444

AERODYNAMIC AND ACOUSTIC PERFORMANCE OF HIGH MACH NUMBER INLETS

Edward Lumsdaine, Lorenzo R. Clark, Jenn G. Cherng, and Ismail Tag

Langley Research Center
Hampton, Va. 23665

NATIONAL AERONAUTICS AND SPACE ADMINISTRATION • WASHINGTON D. C. • AUGUST 1977

1. Report No. NASA TN D-8444	2. Government Accession No.
4. Title and Subtitle AERODYNAMIC AND ACOUSTIC PERFORMANCE OF HIGH MACH NUMBER INLETS	5. Report Date August 1977
	6. Performing Organization Code
7. Author(s) Edward Lumsdaine, Lorenzo R. Clark, Jenn G. Cherng, and Ismail Tag	8. Performing Organization Report No. L-11388
9. Performing Organization Name and Address NASA Langley Research Center Hampton, VA 23665	10. Work Unit No. 505-03-11-04
	11. Contract or Grant No.
12. Sponsoring Agency Name and Address National Aeronautics and Space Administration Washington, DC 20546	13. Type of Report and Period Covered Technical Note
	14. Sponsoring Agency Code

15. Supplementary Notes
Edward Lumsdaine, Jenn G. Cherng, and Ismail Tag: University of Tennessee, Knoxville, Tennessee.
Lorenzo R. Clark: Langley Research Center, Hampton, Virginia.

16. Abstract

Experimental results have been obtained for two types of high Mach number inlets, one with a translating centerbody and one with a fixed geometry (collapsing cowl) without centerbody. A study was made of the aerodynamic and acoustic performance of these inlets. The effects of several parameters such as area ratio and length-diameter ratio were investigated. The translating centerbody inlet was found to be superior to the collapsing cowl inlet both acoustically and aerodynamically, particularly for area ratios greater than 1.5. Comparison of length-diameter ratio and area ratio effects on performance near choked flow showed the latter parameter to be more significant. Also, greater high frequency noise attenuation was achieved by increasing Mach number from low to high subsonic values.

17. Key Words (Suggested by Author(s)) High Mach number inlets Area ratio Length-diameter ratio	18. Distribution Statement Unclassified - Unlimited Subject Category 71

19. Security Classif. (of this report)	20. Security Classif. (of this page)	21. No. of Pages	22. Price*
Unclassified	Unclassified	75	$4.50

* For sale by the National Technical Information Service, Springfield, Virginia 22161

AERODYNAMIC AND ACOUSTIC PERFORMANCE OF HIGH MACH NUMBER INLETS

Edward Lumsdaine,* Lorenzo R. Clark,
Jenn G. Cherng,* and Ismail Tag*
Langley Research Center

SUMMARY

Experimental results have been obtained for two types of high Mach number inlets, one with a translating centerbody and one with a fixed geometry (collapsing cowl) without centerbody. A study was made of the aerodynamic and acoustic performance of these inlets. The effects of several parameters such as area ratio and length-diameter ratio were investigated. The translating centerbody inlet was found to be superior to the collapsing cowl inlet both acoustically and aerodynamically, particularly for area ratios greater than 1.5. Comparison of length-diameter ratio and area ratio effects on performance near choked flow showed the latter parameter to be more significant. Also, greater high frequency noise attenuation was achieved by increasing Mach number from low to high subsonic values.

INTRODUCTION

Feasibility demonstrations of sonic and near-sonic inlets are numerous. The bibliography lists studies that have been conducted during the past few years. A large number of these studies were conducted by aircraft and engine manufacturers with applications directed toward specific engines. Despite this continual effort, and although most demonstration-of-concept studies yield impressive amounts of noise attenuation, this method of noise reduction has not achieved the status of acceptability as have other methods of noise reduction (such as acoustic liners).

At present, results from laboratory and full-scale (static) demonstrations of the noise benefits obtainable with sonic and near-sonic inlets have not yet been converted to practical applications on an aircraft. A detailed understanding of the interaction of the acoustic and aerodynamic fields has been hampered by the fact that the flow is near sonic at the throat; this hindrance makes both analytical description and careful experimental measurements difficult because of the dominance of nonlinear effects. However, a compilation of pertinent data can provide some general information which can be used to indicate certain design limits or show whether some form of boundary-layer control is required.

The purpose of this research project is to obtain some fundamental aerodynamic and acoustic information on sonic and near-sonic inlets. Specifically, this research program attempts to provide aerodynamic and acoustic data of a sufficiently general nature to keep open the options of various configurations in choked inlet design. The experimental test results reported here are comple-

*University of Tennessee, Knoxville, Tennessee.

mented by a continuing theoretical study. This inlet noise study emphasizes the translating centerbody inlet, although comparisons are made with a fixed-geometry (collapsing cowl) inlet. The collapsing cowl configuration was fixed because, unlike the translating centerbody inlet, it could not be varied mechanically.

An investigation of the influence of lip effects was also conducted with the inlets discussed here. Results from these tests have been reported in reference 1.

SYMBOLS

A	diffuser open cross-sectional area, cm^2
A_e	open area at diffuser exit, cm^2
A_{th}	open area at diffuser throat, cm^2
D	diffuser exit flow diameter without centerbody, cm
D_c	diffuser exit flow diameter with centerbody, cm
l	diffuser length from throat to exit, cm
M	flow Mach number
M_A	Mach number on diffuser axis
$\bar{M}_{th}$	average Mach number at geometric diffuser throat
M_w	Mach number at diffuser wall
$\dot{m}$	corrected mass flow, kg/sec
$\dot{m}_{max}$	maximum corrected mass flow, kg/sec
OASPL	overall sound pressure level, dB
p_{dis}	inlet pressure distortion, $\left[(p_{t2,d})_{max} - (p_{t2,d})_{min}\right] / \bar{p}_{t2,d}$, percent
$p_{t1,d}$	diffuser inlet total pressure, N/m^2
$p_{t2,d}$	diffuser exit total pressure, N/m^2
$\bar{p}_{t2,d}$	average total pressure at diffuser exit, N/m^2
$(p_{t2,d})_{max}$	maximum total pressure at diffuser exit, N/m^2
$(p_{t2,d})_{min}$	minimum total pressure at diffuser exit, N/m^2
$p_{t1,fan}$	fan inlet total pressure, N/m^2

$p_{t2,fan}$ fan discharge total pressure, N/m^2

SPL sound pressure level, dB

θ flow diffusion angle, deg

APPARATUS AND PROCEDURE

Description of Inlet Configurations

Two types of inlets, one with a translating centerbody and one with a collapsed cowl, were tested in this study. Table I summarizes the inlet configurations tested. Figures 1 to 7 show schematics of these inlets. These figures include the area distributions at the various centerbody positions.

In addition to being distinguished by one of the two basic geometries (variable and fixed), each configuration can be recognized in one of the following ways for test identification: (1) sonic inlet for use at subsonic and supersonic rotor tip speeds; and (2) accelerating (near-sonic) inlet for use at subsonic and supersonic rotor tip speeds.

Configuration 1 was used to determine the effect of sonic and near-sonic flows on noise at both subsonic and supersonic tip speeds. Configurations 2, 3, and 4 were used to determine the effects of area ratio on the performance of sonic inlets at subsonic tip speeds. Configurations 5 and 6 were fixed-geometry inlets, with which acoustic and aerodynamic data were taken principally for comparison purposes. The remaining configurations (configurations 7 to 9) were low area ratio inlets used primarily for studying the influence of high subsonic Mach numbers on noise associated with supersonic rotor tip speeds. As indicated by table I, three basic types of lips were used with the inlets tested. These lips were the short bellmouth lip, the simulated landing lip for simulating forward speed at a Mach number of 0.2, and the flight (take-off) lip. The diffuser sections for configurations 2 to 4 and 7 to 9 were nearly identical.

Procedure for Inlet Design

Inlets with and without centerbodies were designed for these tests. The translating centerbody inlets were designed to produce a high pressure gradient near the throat; the inlets without centerbodies were designed with a more gradual pressure gradient for the same overall area ratio. The sharp pressure gradient was placed near the throat (where for transonic flow, the streamlines are very stiff) because earlier tests showed that for a given overall pressure ratio, sound attenuation at near-sonic conditions was increased when the pressure gradient was high. This effect was recently confirmed by the results reported in reference 2. Because a high constant Mach number section (constant area) is also effective in reducing the source noise, particularly for supersonic tip speeds, a rapid diffusion near the throat was followed by a constant area section in the design.

The length-diameter ratio for the area ratios in the preliminary design was selected based on earlier work (see ref. 3) which showed that an optimum length-diameter ratio existed for a given area ratio. Figure 8 shows some results from these earlier tests obtained with six annular-configured inlets of different diffuser lengths having an area ratio of 3.2. Although parameters such as throat blockage caused by boundary-layer development and increasing Mach number have a considerable effect on decreasing the pressure recovery, this effect does not seem to have a significant influence on the optimum point. Also a literature search uncovered a large number of tests with circular and square diffusers. (See refs. 4 to 8.) These tests show the approximate relationship between area ratio and optimum length-diameter ratio. Some of the important results are compiled in figure 9. Only a relatively small amount of data pertaining to annular diffusers could be used for a similar graph. The limited data that could be found (refs. 9 and 10) are brought together in figure 10. The term "exit flow diameter," used for an annular diffuser, indicates the inner diffuser diameter minus the centerbody diameter at the exit. These data show that the centerbody inlet requires a smaller length-diameter ratio for the same area ratio than that required by an inlet without centerbody.

From an initial estimate of the length-diameter ratio for a given area ratio requirement, the inlet was designed on the basis of a smooth area progression for both the choked and unchoked positions. After the contour was laid out, a transonic potential flow computer program was used to calculate the flow field. The results were then substituted into a boundary-layer program to determine the corrections for the contour. In most of these calculations, some flow separation was predicted by the boundary-layer analysis because of the wide range of operating conditions occurring in the inlet and because of efforts to keep the inlet to a reasonable length for a given area ratio.

Figures 11 to 15 give the streamlines and Mach number distributions along the wall and centerbody for configuration 1 (take-off configuration with flight lip) for five of the centerbody positions tested. These results were used in the boundary-layer program to determine boundary-layer growth. Because of the high adverse pressure gradient when the centerbody is translated to 12.7 cm and beyond, some flow separation had been predicted from boundary-layer calculations. However, for this particular configuration, the actual separation was more severe as indicated by the surface pressure distributions measured in the inlet experimentally.

The fixed-geometry inlets were designed with straight diffuser walls since the contour of the wall does not have a significant influence on the aerodynamic performance. These inlets were designed with a slightly shorter length than the optimum length (if fig. 9 is followed) for the purpose of maintaining the same area ratio and approximately the same length-diameter ratio as the translating centerbody inlets in order to compare the effectiveness of the two types of inlets.

Description of Research Compressor

The test vehicle used for the present study was a single-stage transonic compressor. The compressor is installed in a 7.6-m by 7.6-m by 7.0-m high

anechoic chamber and is driven from the rear by an electric motor located directly behind the chamber wall. A photograph showing one of the test inlets installed on the compressor is presented in figure 16.

The compressor has a design speed of 24 850 rpm. At this speed, the fan has an airflow of 11.9 kg/sec and a pressure ratio of 1.325. The vehicle has 19 rotor blades, 26 stator vanes, and no inlet guide vanes. The rotor-to-stator spacing is 1.02 true rotor pitch chords.

Instrumentation and Data Acquisition Procedure

Both acoustic and aerodynamic instrumentation were used for data collection in this study. Schematics of some of the acoustic and aerodynamic instrumentation and the approximate locations in which the instruments were used are shown in figures 16 to 18. The acoustic instrumentation consisted of the following items:

(1) A traversable boom with one 0.635-cm condenser microphone located 4.57 m from the inlet entrance plane at the same elevation as the inlet center line

(2) Two stationary 0.635-cm condenser microphones also located 4.57 m from the inlet entrance plane

(3) One traversable acoustic probe situated at the exit plane of the inlet

(4) Four (or six depending on the inlet) flush-mounted 0.635-cm wall microphones located as shown in figures 1 to 7.

Each microphone was calibrated at the beginning and end of each test day with a discrete frequency calibrator. The boom microphone measured far-field noise at 15° intervals from 0° (on the inlet center line) to 90°. The two stationary microphones measured far-field noise continuously at 0° and 15° and were monitored on a 1/3-octave-band real-time analyzer. This analyzer was also used to monitor the speed at which inlet choking occurred and to help regulate the compressor operating conditions. Acoustic probe traverses were made near the choke point only, and traverse data were recorded for a minimum of 10 sec (for stabilization) at each point. The probe was immersed to five radial positions for data acquisition. Acoustic data at inlet walls and in the far field were recorded for a minimum of 1 min at each test condition.

The following instrumentation was used for collecting aerodynamic data:

(1) Four static pressure taps located circumferentially downstream of the cowl highlight (cowl leading edge)

(2) Sixty static pressure taps located at two circumferential stations (12 taps along one line and 48 on the other) for configuration 1, 45 pressure taps on each of the other configurations, and 12 static pressure taps on each centerbody

(3) One traversable Kiel head total pressure probe and two 20-element total pressure rakes located at the exit plane of the inlet

(4) One combination Kiel head total pressure and thermocouple probe fixed at the inlet exit plane.

The aerodynamic data were obtained with the aid of three scanivalves and recorded on computer cards with a card punch machine. Data from the total pressure Kiel probes were also recorded on an X-Y plotter. These data were taken at fixed immersion points and during continuous traverses. Data records were obtained for 10 sec at each fixed probe immersion.

Figure 19 shows the data acquisition room where the test operations were performed. The following operations used to test a translating centerbody configuration involved a typical sequence: with the centerbody completely retracted, the compressor rotor was gradually accelerated to some prescribed maximum rotational speed and stabilized; acoustic and aerodynamic data were recorded at prescribed intervals during this acceleration, and the centerbody was then translated to the next test position. The online 1/3-octave-band real-time analyzer monitored the sound levels until the acoustic choking speed point was reached. The fan pressure ratio was then adjusted to near maximum (blade stall) and also to minimum (pressure discharge valve fully open) with one intermediate point to give different blade loadings for the same speed. Other inlets were run with the back pressure valve wide open only.

RESULTS AND DISCUSSION

Sonic inlets are defined as those where the flow is accelerated until a sonic barrier exists near the throat of the inlet at which time the inlet is aerodynamically choked (or nearly so) with a corresponding large noise reduction. These inlets are known to be very effective acoustically since the only noise that can propagate upstream in this case is the noise escaping through the boundary layer. The problems associated with the sonic inlet are primarily aerodynamic, that is, the problems of achieving a sonic surface with the shortest inlet, with low distortion, with negligible instability, and with minimum pressure loss.

In the near-sonic (or accelerating) inlet, the flow near the throat is at a velocity which results in noise reduction but has not yet reached the aerodynamic choking point. For one-dimensional flow, such a differentiation would not be necessary since the two types of inlets need only be separated by an arbitrary throat Mach number, for example, 0.8. This oversimplification, however, can cause problems when data from different tests are compared, because for inlets of practical length and for near-sonic velocities, the flow deviates greatly from the one-dimensional potential flow approximation. As can be seen in figure 20 (taken from ref. 4), the center-line throat Mach number is a very inadequate parameter, since it remains nearly constant for the three very different flow conditions (a, b, and c) with differing amounts of mass flow. This inadequacy can also lead to the mistaken notion that near-sonic inlets are effective when the center-line throat Mach number indicates subsonic flow, even though supersonic conditions exist downstream of the throat.

Inlet noise attenuation characteristics constitute another area which must be considered. As reported in reference 3, tests were conducted by use of an ejector with inlets of different length-diameter ratio but with the same area ratio and noise source. The attenuations obtained had different values for the same average maximum axial Mach number. These tests, including those from reference 11 (see fig. 21), showed that the shorter diffusers tended to be more effective in terms of noise reduction at subsonic speeds whereas the longer diffusers produced little or no noise reduction until the flow was close to being aerodynamically choked. This result can be attributed either to a supersonic pocket near the throat for the shorter diffusers (caused by the smaller radius of curvature at the throat) which is effective in reducing some of the noise propagated or to the larger axial pressure gradient for the same overall pressure difference. In any case, figure 21 points out the inadequacy of plotting noise reduction against a single parameter (in this case, the average maximum axial Mach number) since extrapolation or comparison of data is not reliable because conditions downstream of the throat influence the noise attenuation. The percentage of maximum mass flow is a better parameter for plotting noise reduction. However, mass flow is very sensitive near choked flow; a change of about 4 percent in mass flow changes the Mach number from 0.8 to 1.0.

Translating Centerbody Results

Noise attenuation for inlets under near-sonic conditions seems to depend on the source (tip speed, peak frequency) as well as on the flow conditions (axial velocity gradient, radial gradient, peak Mach number); thus, the choice of parameters to represent the acoustic and aerodynamic conditions should be made very carefully. Five parameters were found to largely define the performance of the various inlets tested. These parameters are noise attenuation, mass flow, average maximum Mach number (cowl and centerbody), pressure recovery, and pressure distortion. The effects of these parameters on the performance of configuration 1 are shown in figures 22 to 26. The detailed Mach number distributions along the cowl and centerbody for each test condition indicated are expected to be compiled at a later date. The constant noise attenuation lines (broken lines) seen in figures 23 and 25 are interpolations which show the amounts of noise reduction obtained for the mass flow and pressure recovery changes indicated. Noise attenuation values presented for configuration 1 were taken with respect to the fully retracted centerbody position. For all other configurations, the values were taken with respect to a baseline, normally without the centerbody.

Figure 22 shows that the noise attenuation obtained with configuration 1 changes gradually with corrected speed (compressor rotational speed corrected for ambient temperature variations) so that the noise does not drop rapidly as the choke point is approached. This behavior is typical of high area ratio short inlets and agrees with results presented in figure 21. Because of a long constant area section downstream of the throat, configuration 1 also has a very low distortion level. (See fig. 26).

Figure 27 shows the influence of changes in compressor pressure ratio on noise at the 0^{o} microphone for configuration 1. As can be seen from this figure, there is very little change in noise at this far-field microphone as a

result of changing the compressor back pressure for the same mass flow. The influence of compressor blade loading on far-field noise with the inlet is an important problem, and further tests are necessary to gain more precise and useful information in this area.

Figures 28 to 42 give performance results for inlet configurations 2, 3, and 4. These configurations differ only in the shape of their respective lips; the centerbody and the diffusers are the same. For these inlets with relatively low area ratios, noise attenuation is quite sudden and occurs primarily within 5 to 10 percent of maximum mass flow. (See figs. 43 to 45 where the far-field noise is plotted as a function of percentage of maximum mass flow.) Most of the noise reduction for each configuration occurs in the interval of 90 to 100 percent of maximum mass flow. It should be further noted that the major noise drop is within a narrow 5-percent range of mass flow. On a one-dimensional basis, this means a move from very little noise reduction to almost full choke for a 5-percent change in area. Near Mach 1.0, a 5-percent change in area causes the average Mach number to change from 0.75 to 1.0. In addition, when the centerbody was translated, there was an increase in the noise level radiated from the individual inlets. This increase can be readily seen in figures 29, 34, and 39.

As a result of mechanical problems in the design, a slightly higher pressure loss than expected was encountered with the translating centerbody inlets because there was a discontinuity between the centerbody and the cylinder over which it slides. Also, a groove in the cylinder was exposed when the centerbody was translated forward. This groove was necessary to keep the centerbody from rotating, but when a configuration was tested with the centerbody, the pressure of the groove may have contributed to the increase in far-field noise. The noise level rose as the centerbody was translated further, exposing a larger segment of the groove. (See fig. 45.) Furthermore, with the centerbody translated, the existence of a higher pressure gradient in the inlet caused some flow separation which contributed to the increased noise level.

Figure 46 shows frequency spectra for inlet configuration 2 at approximately 17 500 rpm and at various centerbody positions. The amount of noise reduction at the blade passing frequency is much higher than the overall noise reduction and noise is attenuated much more at the higher frequencies than at the lower frequencies for this speed setting. At fully choked conditions, however, the amount of noise reduction at the various spectral frequencies is more uniform, as shown in figure 47.

Collapsing Cowl Results

Figures 48 to 52 show the performance results for configurations 5 and 6, two fixed-geometry inlets simulating a collapsing cowl inlet without centerbody. Although the area ratios are not very high (see table I), both inlets performed very poorly. The flow was so unstable, and the monitor for the far-field noise showed such large variations, that the average noise reduction shown in figure 48 is very approximate. It appeared that even under choked conditions, the amount of noise reduction was very small. Because of severe pressure and acoustic fluctuations, the testing of configurations 5 and 6 was discontinued at 17 000 and 19 000 rpm, respectively. The distortion levels associated with

these inlets, as indicated by figure 50, were quite high. The Mach number data given in figure 52 are represented by wall Mach number and not by the average maximum Mach number which was used in previous graphs. The average values in the present case are lower than the peak wall Mach numbers. Figure 53 is a graph of noise reduction as a function of percentage mass flow for configurations 5 and 6. These poor results were quite unexpected since the guidelines followed for the present designs were the same as those used to design configurations 1, 2, 3, and 4.

Baseline Configurations

The remaining configurations (7, 8, and 9) were tested to obtain baseline data for configurations 2, 3, and 4 and to provide noise attenuation information at high throat Mach numbers with the fan at supersonic tip speeds. Figures 54 to 57 show the basic flow characteristics of configurations 7, 8, and 9. Note that here, too, the Mach number plot (fig. 55) shows wall Mach number instead of average values. Figure 58 compares the far-field acoustic characteristics of these inlets with configuration 1 at 0-cm centerbody displacement. At the lower speeds (lower Mach numbers), the inlet with the centerbody gives a few decibels more attenuation than the same inlet without centerbody (configuration 9). However, this is only true when comparisons are made with the centerbody fully retracted (0-cm displacement). Although configuration 9 has a consistently higher noise level at lower speeds, a reversal of this trend is observed at higher rpm values. This result is more clearly evidenced by the blade-passing-frequency data presented in figure 59.

CONCLUSIONS

An investigation has been conducted to determine the aerodynamic and acoustic performance of high Mach number inlets. Extensive data were obtained for both a translating centerbody (variable-geometry) inlet and a collapsing cowl (fixed-geometry) inlet. Tests of these configurations lead to the following conclusions:

1. Collapsing cowl inlets with low area ratios (less than 1.5) perform poorly with regard to noise reduction and the crucial aerodynamic parameters, such as pressure recovery and flow distortion.

2. When a high area ratio centerbody inlet is compared to a collapsing cowl with identical area and length-diameter ratios, the centerbody inlet gives superior performance.

3. Most of the noise reduction obtainable with high Mach translating centerbody inlets takes place at values between 90 and 100 percent of maximum mass flow.

4. With the translating centerbody inlet, blade-passing-frequency noise is much better attenuated than overall noise. Additionally, high frequency noise is better attenuated than low frequency noise.

Langley Research Center
National Aeronautics and Space Administration
Hampton, VA 23665
May 26, 1977

REFERENCES

1. Lumsdaine, Edward; Cherng, Jenn G.; and Tag, Ismail: Noise Suppression With High Mach Number Inlets. NASA CR-2708, 1976.

2. Wilson, J. M.; and Savell, C. T.: Inlet Flowpath Design To Attenuate Supersonic Noise. R73-AEG-412, Tech. Information Ser., Gen. Elec. Co., Sept. 20, 1973.

3. Lumsdaine, Edward; and Clark, Lorenzo R.: Noise Suppression With Sonic and Near-Sonic Inlets. Proceedings Second Interagency Symposium on University Research in Transportation Noise, Volume I, June 1974, pp. 432-447.

4. Emmons, Howard W.: The Theoretical Flow of Frictionless, Adiabatic, Perfect Gas Inside of a Two-Dimensional Hyperbolic Nozzle. NACA TN 1003, 1946.

5. Runstadler, P. W., Jr.; and Dean, R. C., Jr.: Straight Channel Diffuser Performance at High Inlet Mach Numbers. Trans. ASME, Ser. D: J. Basic Eng., vol. 91, no. 3, Sept. 1969, pp. 397-422.

6. Reneau, L. R.; Johnston, J. P.; and Kline, S. J.: Performance and Design of Straight, Two-Dimensional Diffusers. Trans. ASME, Ser. D: J. Basic Eng., vol. 89, no. 1, Mar. 1967, pp. 141-150.

7. Van Dewoestine, Robert V.; and Fox, Robert W.: An Experimental Investigation on the Effect of Subsonic Inlet Mach Number on the Performance of Conical Diffusers. Tech. Rep. FMTR-66-1, U.S. Army, Feb. 1966. (Available from DDC as AD 632 787.)

8. Rhoades, W. W.: A Semi-Empirical Method for Predicting Subsonic Diffuser Performance. AIAA Paper No. 73-1272, Nov. 1973.

9. Lumsdaine, Edward: Development of a Sonic Inlet for Jet Aircraft. Inter-Noise 72 Proceedings, Malcolm J. Crocker, ed., 1972, pp. 501-506.

10. Klujber, F.; Bosch, J. C.; Demetrick, R. W.; and Robb, W. L.: Investigation of Noise Suppression by Sonic Inlets for Turbofan Engines.
Volume I: Program Summary. NASA CR-121126, 1973.
Volume II: Appendixes. NASA CR-121127, 1973.

11. Chestnutt, David; and Clark, Lorenzo R.: Noise Reduction by Means of Variable-Geometry Inlet Guide Vanes in a Cascade Apparatus. NASA TM X-2392, 1971.

ANNOTATED BIBLIOGRAPHY ON SONIC AND NEAR-SONIC INLETS

Sobel, J. A., III; and Welliver, A. D.: Sonic Block Silencing for Axial and Screw-Type Compressors. Noise Centr. Shock Vib., vol. 7, no. 5, Sept.-Oct. 1961, pp. 9-11.

Sonic inlet tests with centerbody on compressor and Olympus-6 turbojet

McKaig, M. B.: J-75 Inlet Noise Suppression Test. Rep. T6-3173, Boeing Co., Oct. 27, 1964.

SST-type inlet on J-75 engine

Sawhill, R. H.: Investigation of Inlet Airflow Choking as a Means of Suppressing Compressor Noise - 5" Inlet Model. Doc. D6A 10155-1, Boeing Co., July 6, 1966.

Ejector tests with 12.7-cm SST-type inlet

Anderson, A. O.: An Acoustic Evaluation of the Effect of Choking Using a Model Supersonic Inlet. Doc. D6A 10378-1 TN, Boeing Co., Sept. 12, 1966.

Ejector tests with 12.7-cm SST-type inlet

Cawthorn, Jimmy M.; Morris, Garland J.; and Hayes, Clyde: Measurement of Performance, Inlet Flow Characteristics, and Radiated Noise for a Turbojet Engine Having Choked Inlet Flow. NASA TN D-3929, 1967.

SST-type inlet with Viper-8 jet engine

Study and Tests To Reduce Compressor Sounds of Jet Aircraft. FAA-DS-68-7, Feb. 1968.

Model cascade

Chestnutt, David: Noise Reduction by Means of Inlet-Guide-Vane Choking in an Axial-Flow Compressor. NASA TN D-4682, 1968.

Ejector tests with cambered and uncambered airfoils

Higgins, C. C.; Smith, J. N.; and Wise, W. H.: Sonic-Throat Inlets. Progress of NASA Research Relating to Noise Alleviation of Large Subsonic Jet Aircraft, NASA SP-189, 1968, pp. 197-215.

JT3D engine with contracting cowl

Smith, J. N.: Inlet and Engine Performance With Eight-Segment Adjustable Boilerplate Sonic Inlet - JT3D-3B Engine. Doc. D6-23469, Boeing Co., May 21, 1969.

JT3D engine

Putnam, Terrill W.; and Smith, Ronald H.: XB-70 Compressor-Noise Reduction and Propulsion-System Performance for Choked Inlet Flow. NASA TN D-5692, 1970.

Static test with XB-70 airplane

Chestnutt, David; and Clark, Lorenzo R.: Noise Reduction by Means of Variable-Geometry Inlet Guide Vanes in a Cascade Apparatus. NASA TM X-2392, 1971.

Variable geometry cascade inlet tests with ejector

Anderson, R.; DeStefannis, P.; Farquhar, B. W.; Giarda, G.; Schuehle, A. L.; and VanDuine, A. A.: Boeing/Aeritalia Sonic Inlet Feasibility Study. Doc. D6-40208, Boeing Co., Mar. 21, 1972.

Grid and radial type vane inlet with fan

Lumsdaine, Edward; and Fathy, Assem: Effect of Spanwise Circulation on Compressor Noise Generation. Inter-Noise 72 Proceedings, Malcolm J. Crocker, ed., 1972, pp. 482-487.

Model tests of several inlets with ejector

Lumsdaine, Edward: Development of a Sonic Inlet for Jet Aircraft. Inter-Noise 72 Proceedings, Malcolm J. Crocker, ed., 1972, pp. 501-506.

Model tests of several inlets with ejector

Klujber, F.; Bosch, J. C.; Demetrick, R. W.; and Robb, W. L.: Investigation of Noise Suppression by Sonic Inlets for Turbofan Engines.
Volume I - Program Summary. NASA CR-121126, 1973.
Volume II - Appendixes. NASA CR-121127, 1973.

Transonic 0.35-m diam fan using inlets with low area ratio (max. $A_e/A_{th} = 1.6$)

Miller, Brent A.; and Abbott, John M.: Low-Speed Wind-Tunnel Investigation of the Aerodynamic and Acoustic Performance of a Translating-Centerbody Choked-Flow Inlet. NASA TM X-2773, 1973.

Small fan with cross flow at various angles with translating centerbody (two positions only)

Wilson, J. M.; and Savell, C. T.: Inlet Flowpath Design To Attenuate Supersonic Rotor Noise. R73-AEG-412, Tech. Information Ser., Gen. Elec. Co., Sept. 20, 1973.

Test with Langley transonic compressor with expanding centerbody (A_e/A_{th} = 2.6)

Compagnon, M. A.: A Study of Engine Variable Geometry Systems for an Advanced High Subsonic Long Range Commercial Aircraft. NASA CR-134495, 1973.

Study of engine variable geometry systems with high Mach number inlets - collapsing cowl inlet recommended

Groth, Harold W.: Sonic Inlet Noise Attenuation and Performance With a J-85 Turbojet Engine as a Noise Source. AIAA Paper No. 74-91, Jan.-Feb. 1974.

Translating centerbody with radial vanes tested with a J-85 engine

Lumsdaine, Edward; and Clark, Lorenzo R.: Noise Suppression With Sonic and Near-Sonic Inlets. Proceedings Second Interagency Symposium on University Research in Transportation Noise, Volume I, June 1974.

Results of choked inlets tested with 30.5-cm fan

Koch, R. L.; Ciskowski, T. M.; and Garzon, J. R.: Turbofan Noise Reduction Using a Near Sonic Inlet. AIAA Paper No. 74-1098, Oct. 1974.

Fixed geometry inlet tested with model fan (1/5 scale of advanced fan)

Lumsdaine, Edward: Fan Noise Reduction at Subsonic and Supersonic Tip Speeds With High Mach Number Inlets. Inter-Noise 75 Proceedings, Ken'iti Kido, ed., 1975, pp. 283-290.

Sonic and near-sonic inlet tests with NASA Langley transonic compressor

Miller, Brent A.; Dastoli, Benjamin J.; and Wesoky, Howard L.: Effect of Entry-Lip Design on Aerodynamics and Acoustics of High-Throat-Mach-Number Inlets for the Quiet, Clean, Short-Haul Experimental Engine. NASA TM X-3222, 1975.

Effect of lip design on acoustic and aerodynamic performance of high Mach number inlets, tests at different angles of attack in wind tunnel, siren source

Jibben, J. J.; and Lumsdaine, E.: An Automatic Control System for Sonic Inlets. Paper 75-WA/Aut-1, ASME Winter Annual Meeting (Houston, Texas), Nov.-Dec. 1975.

First test of an automatic control system designed for the choked inlet

Lumsdaine, Edward; Cherng, Jenn G.; and Tag, Ismail: Noise Suppression With High Mach Number Inlets. NASA CR-2708, 1976.

High Mach number inlet tests with NASA Langley transonic compressor

TABLE I.- LIST OF INLET CONFIGURATIONS TESTED

Inlet type	Type of lip	Maximum tip speed (maximum rpm)	Length-diameter ratio	Centerbody position, cm	Area ratio	Remarks	Designed maximum mass flow, kg/sec
			Configuration 1				
Translating centerbody	Flight lip	Supersonic (25 000)	1.90	0.0	----	Sonic (and near-sonic) inlet	19.00
				5.1	----		-----
				12.7	2.35		12.00
				17.8	2.90		9.75
				20.3	3.20		8.60
				25.4	3.50		7.90
			Configuration 2				
Translating centerbody	Short bellmouth	Subsonic (21 000)	1.68	0.0	1.40	Sonic (and near-sonic) inlet	10.00
				3.8	1.80		8.60
				7.6	2.20		7.50
				11.4	2.60		6.35
			Configuration 3				
Translating centerbody	Simulated landing	Subsonic (21 000)	1.68	0.0	1.40	Sonic (and near-sonic) inlet	10.00
				3.8	1.80		8.60
				7.6	2.20		7.50
				11.4	2.60		6.35
			Configuration 4				
Translating centerbody	Flight lip	Subsonic (21 000)	1.68	0.0	1.40	Sonic (and near-sonic) inlet	10.00
				3.8	1.80		8.60
				7.6	2.20		7.50
				11.4	2.60		6.35
			Configuration 5				
Fixed geometry	Simulated landing	Subsonic (20 000)	1.54		2.60	Sonic (and near-sonic) inlet	6.35
			Configuration 6				
Fixed geometry	Simulated landing	Subsonic (20 000)	1.54		2.30	Sonic (and near-sonic) inlet	7.50
			Configuration 7				
Fixed geometry	Short bellmouth	Supersonic (25 000)	1.68		1.20	Near-sonic inlet	15.20
			Configuration 8				
Fixed geometry	Simulated landing	Supersonic (25 000)	1.68		1.20	Near-sonic inlet	15.20
			Configuration 9				
Fixed geometry	Flight lip	Supersonic (25 000)	1.68		1.20	Near-sonic inlet	15.20

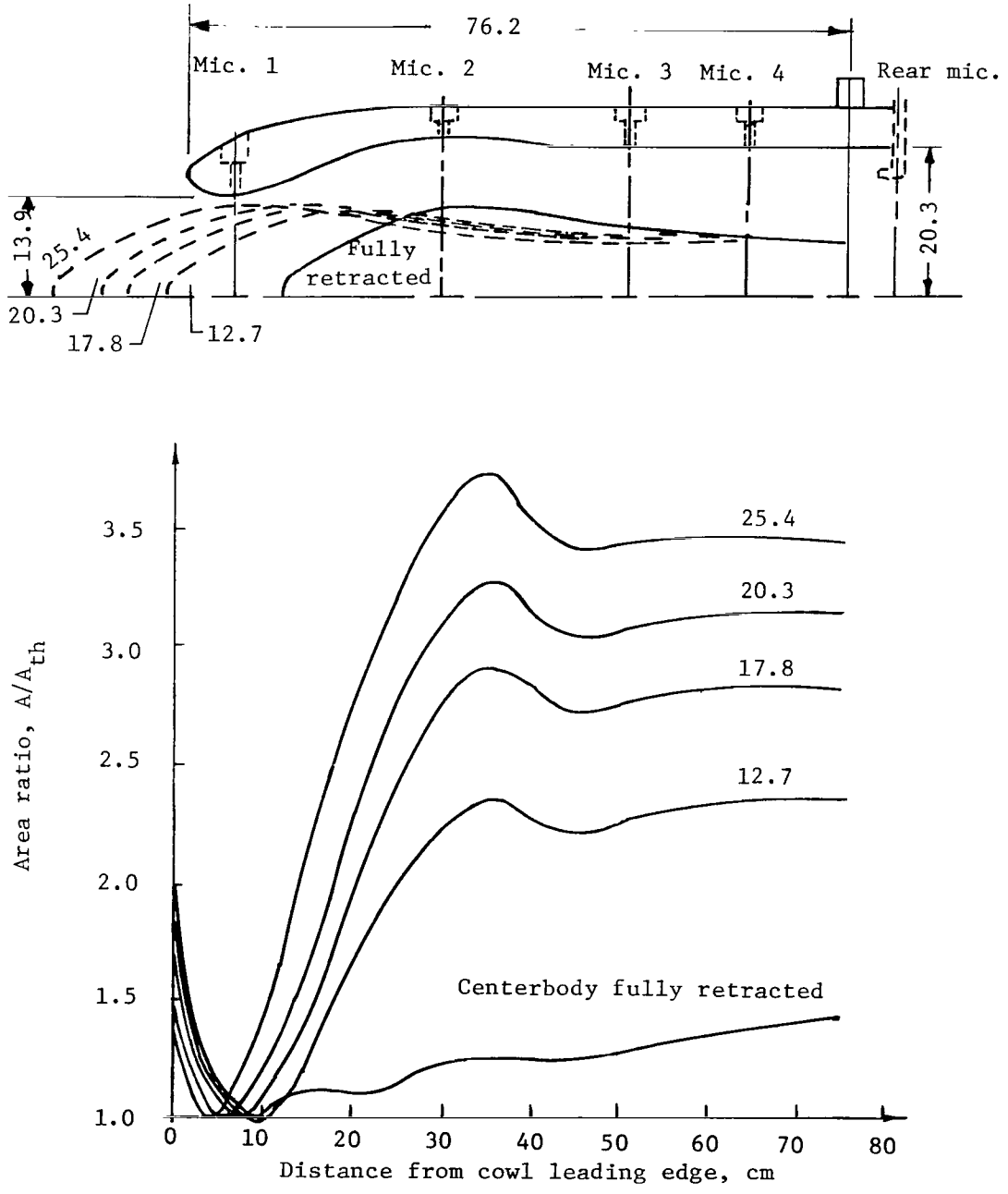

Figure 1.- Schematic and area distribution of translating centerbody inlet, configuration 1. All dimensions are in cm.

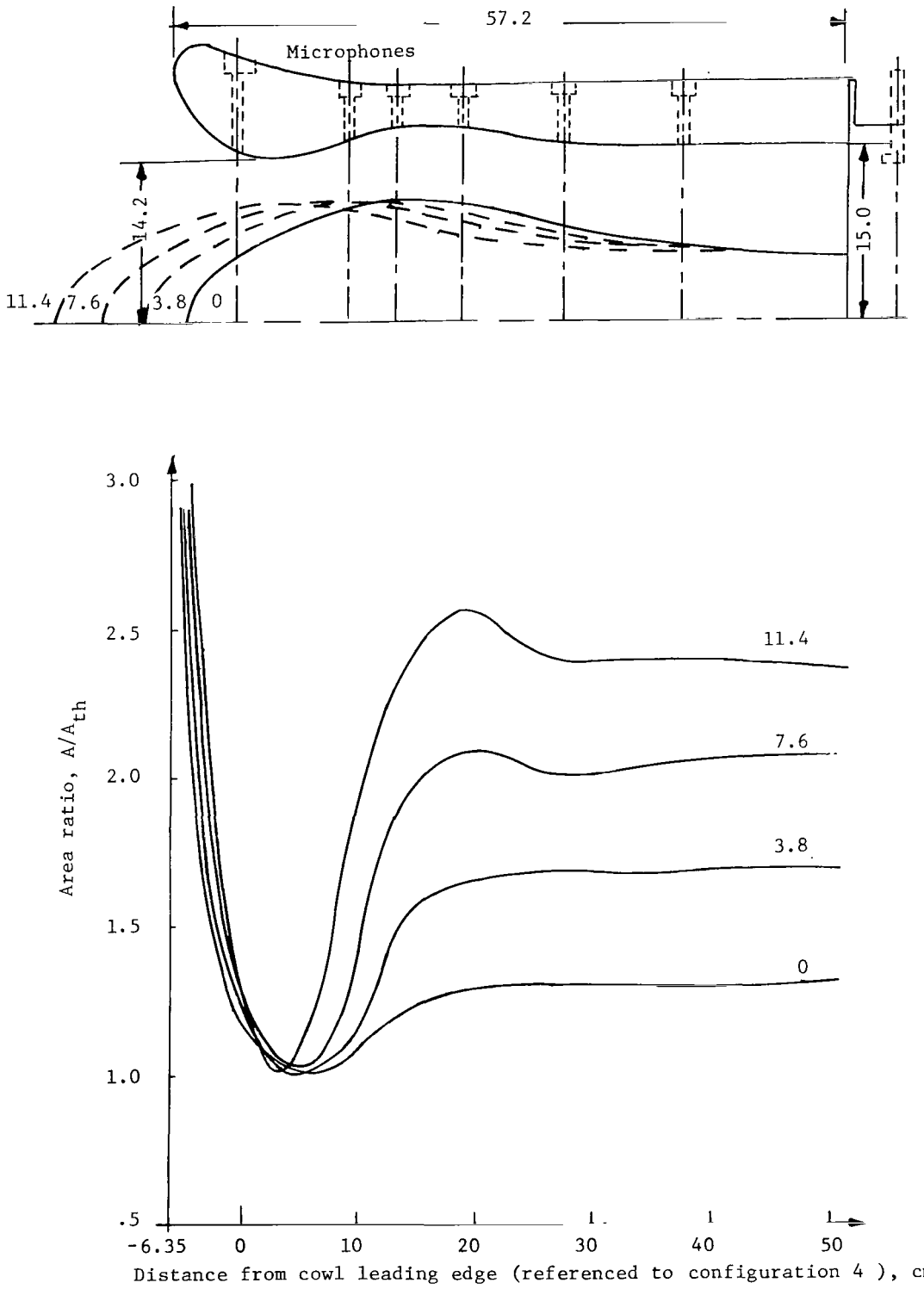

Figure 2.- Schematic and area distribution of translating centerbody inlet, configuration 2. All dimensions are in cm.

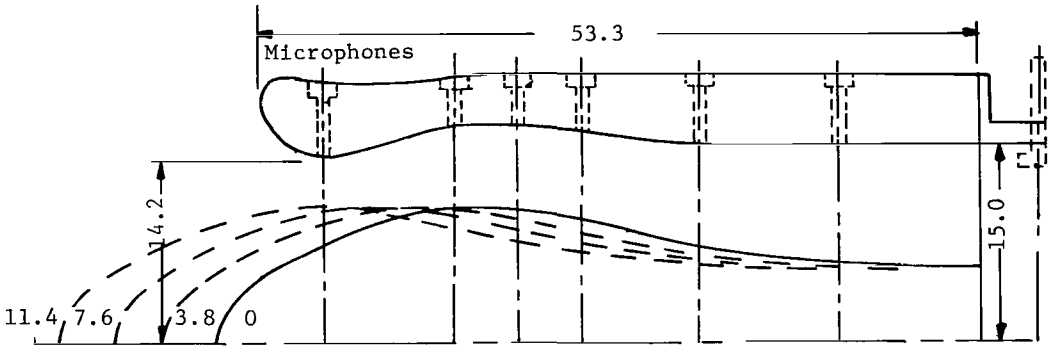

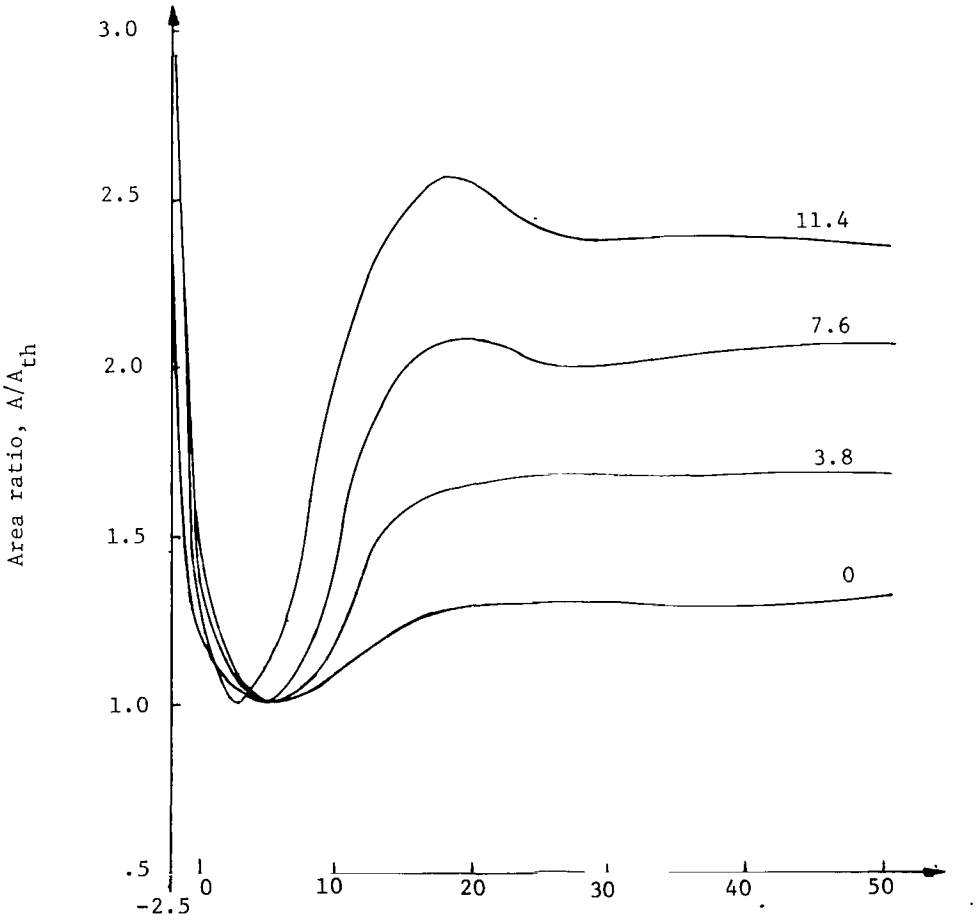

Figure 3.- Schematic and area distribution of translating centerbody inlet, configuration 3. All dimensions are in cm.

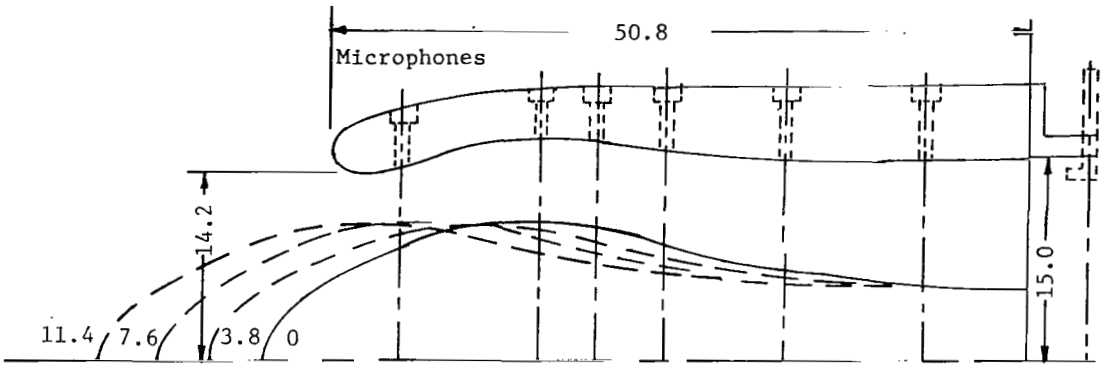

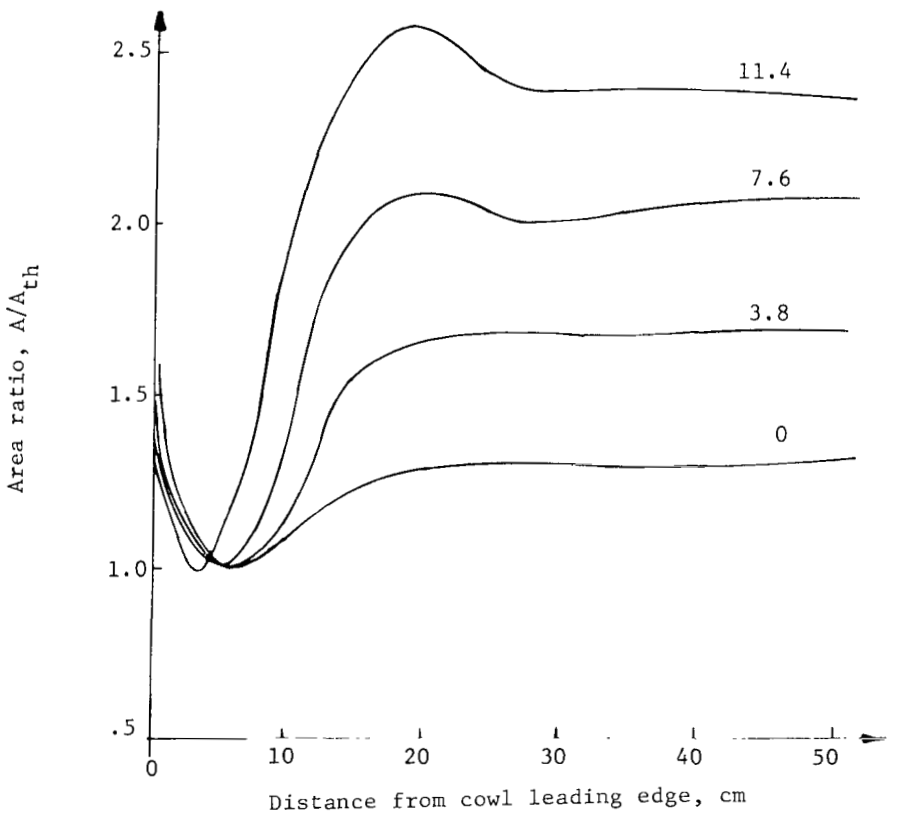

Figure 4.- Schematic and area distribution of translating centerbody inlet, configuration 4. All dimensions are in cm.

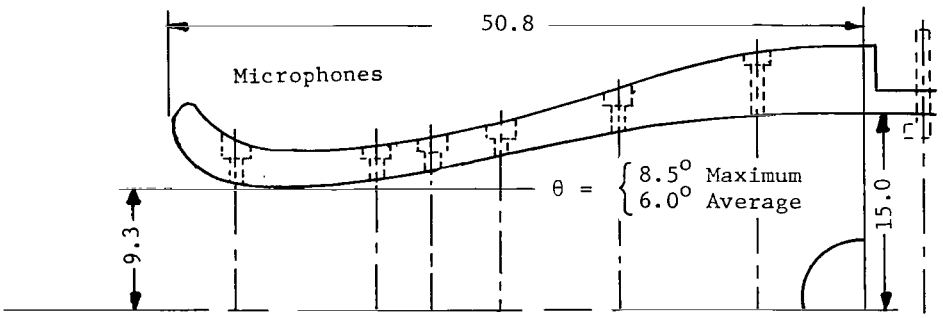

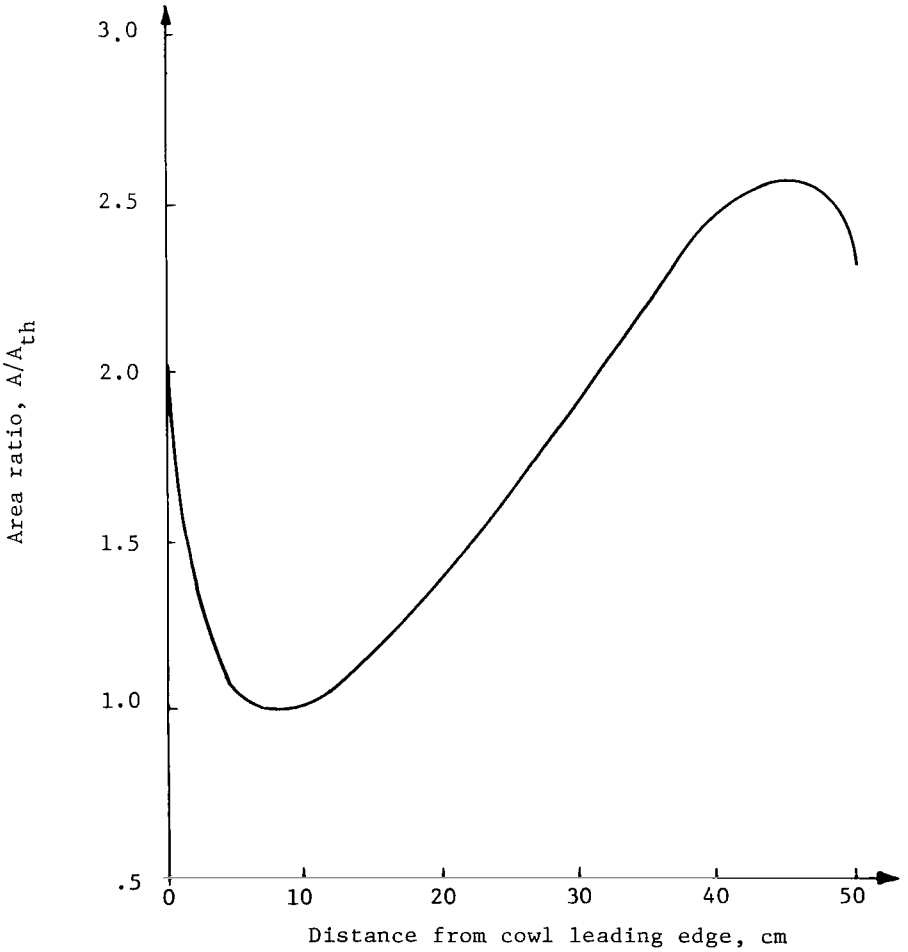

Figure 5.- Schematic and area distribution of fixed-geometry (collapsing cowl) inlet, configuration 5. All dimensions are in cm.

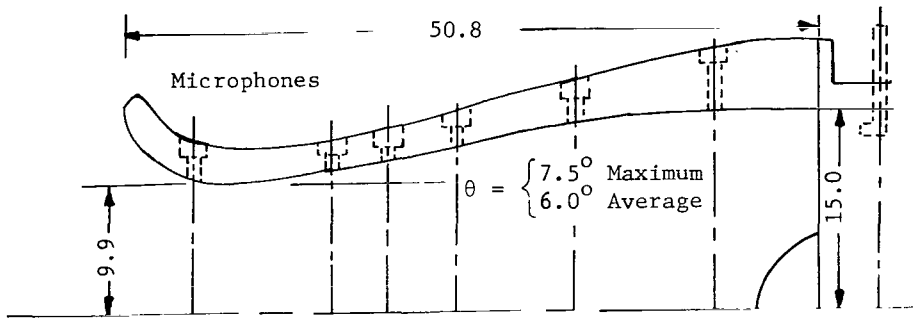

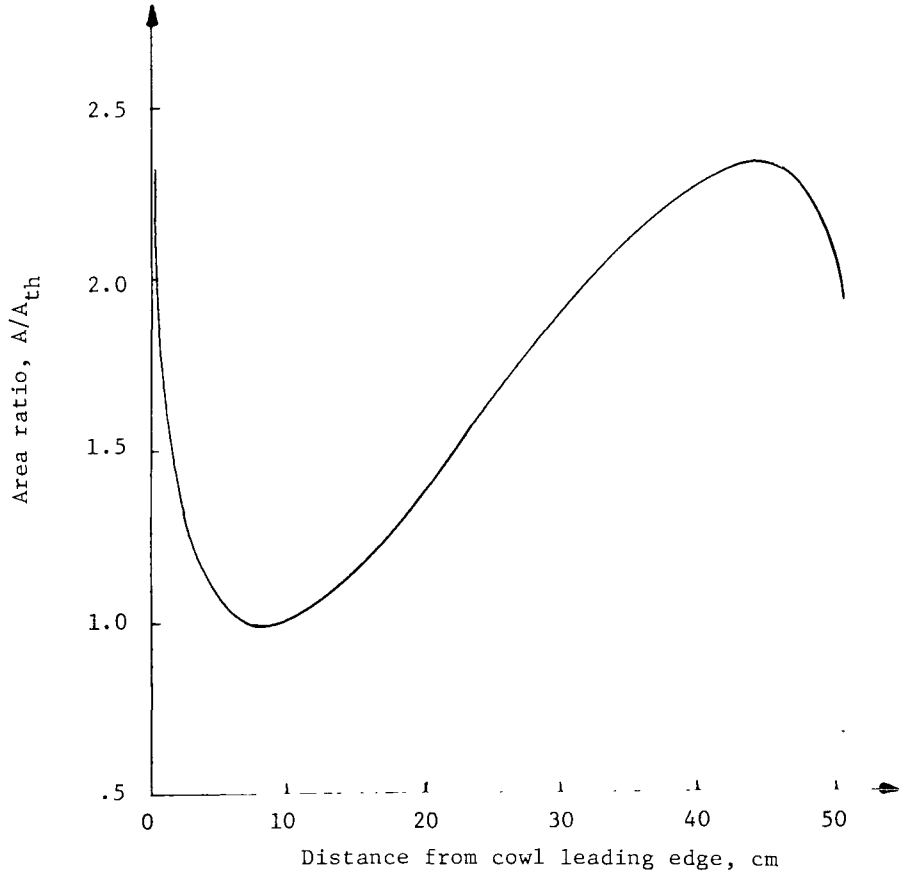

Figure 6.- Schematic and area distribution of fixed-geometry (collapsing cowl) inlet, configuration 6. All dimensions are in cm.

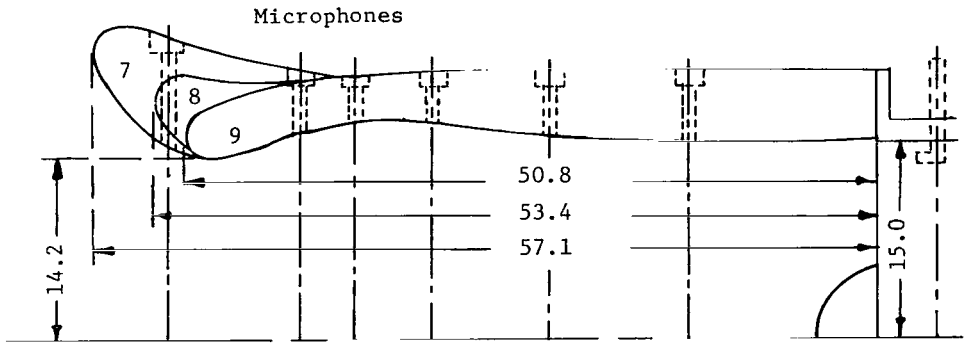

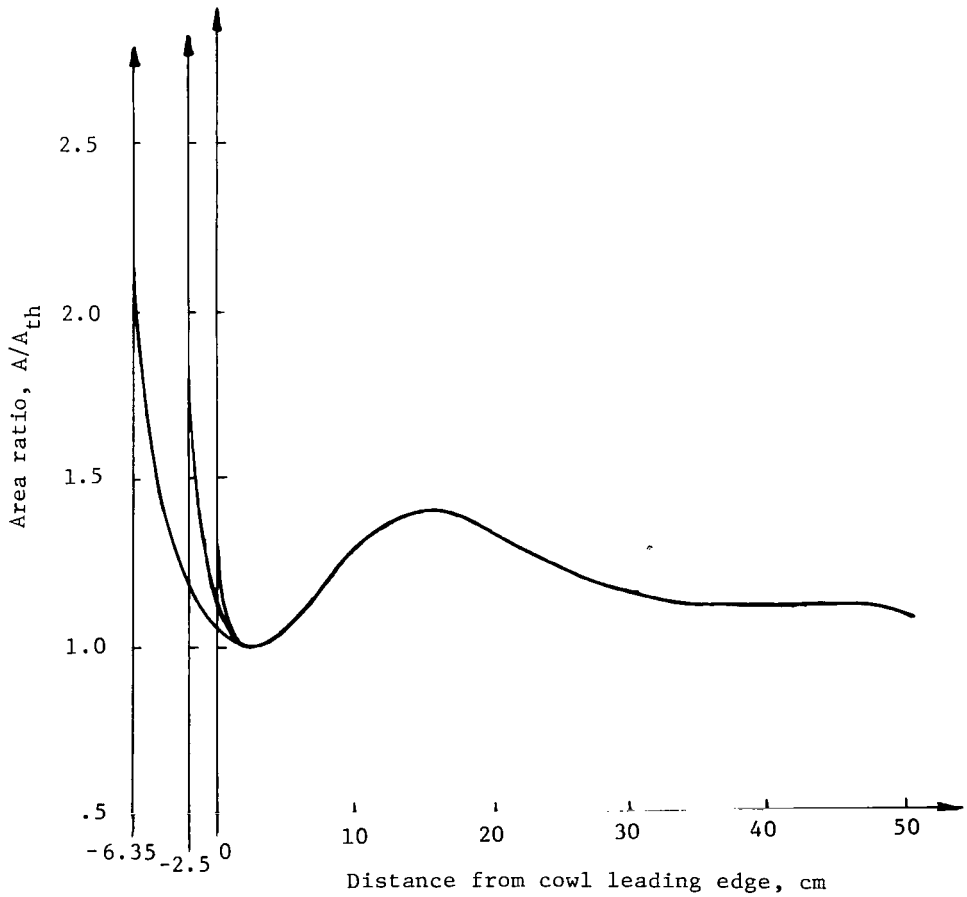

Figure 7.- Schematic and area distribution of fixed-geometry inlet, configurations 7, 8, and 9. All dimensions are in cm.

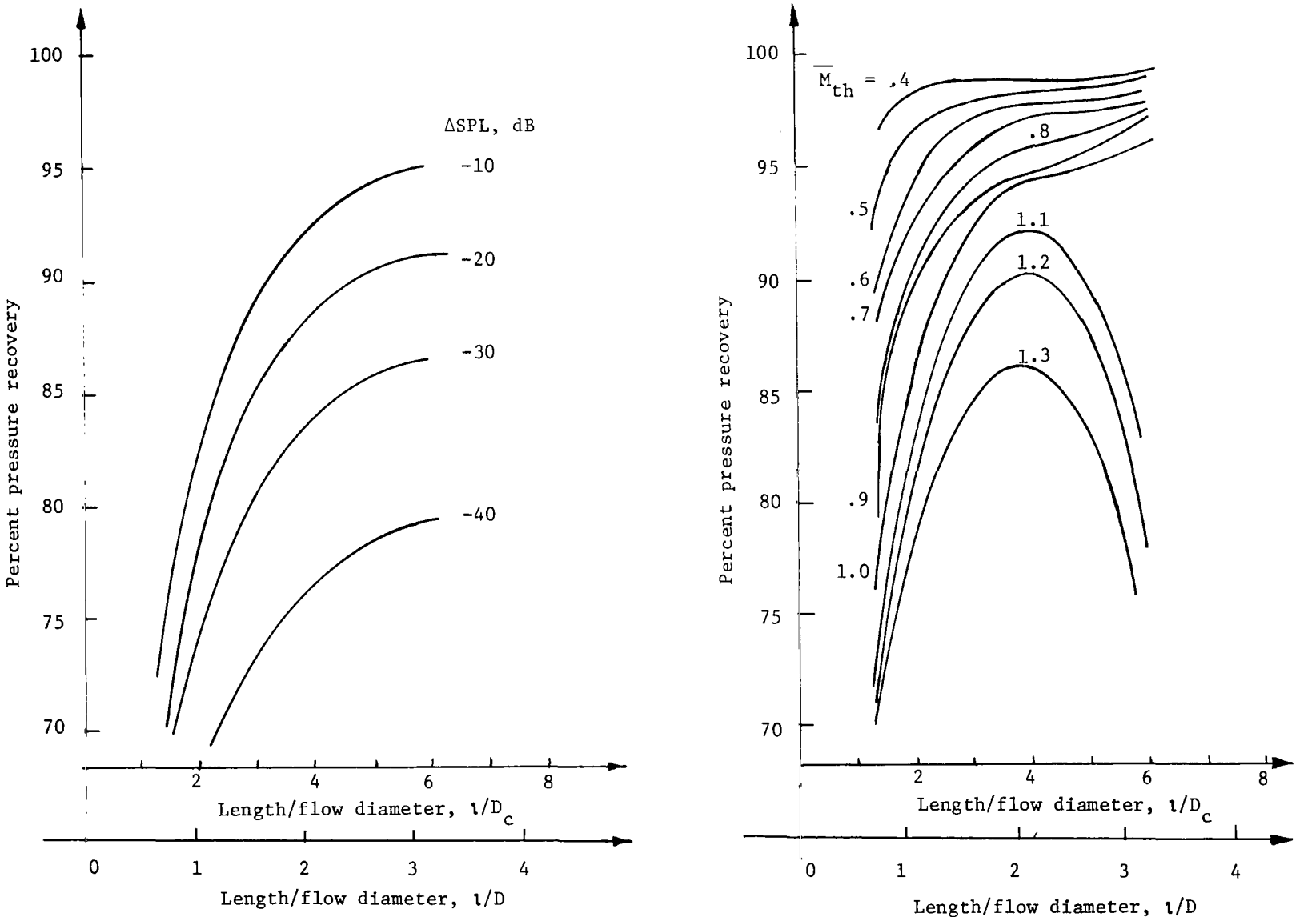

Figure 8.- Aerodynamic and acoustic performance of annular inlets with different length-diameter ratios (A/A_{th} = 3.2). Inlet pressure recovery, $p_{t2,d}/p_{t1,d}$.

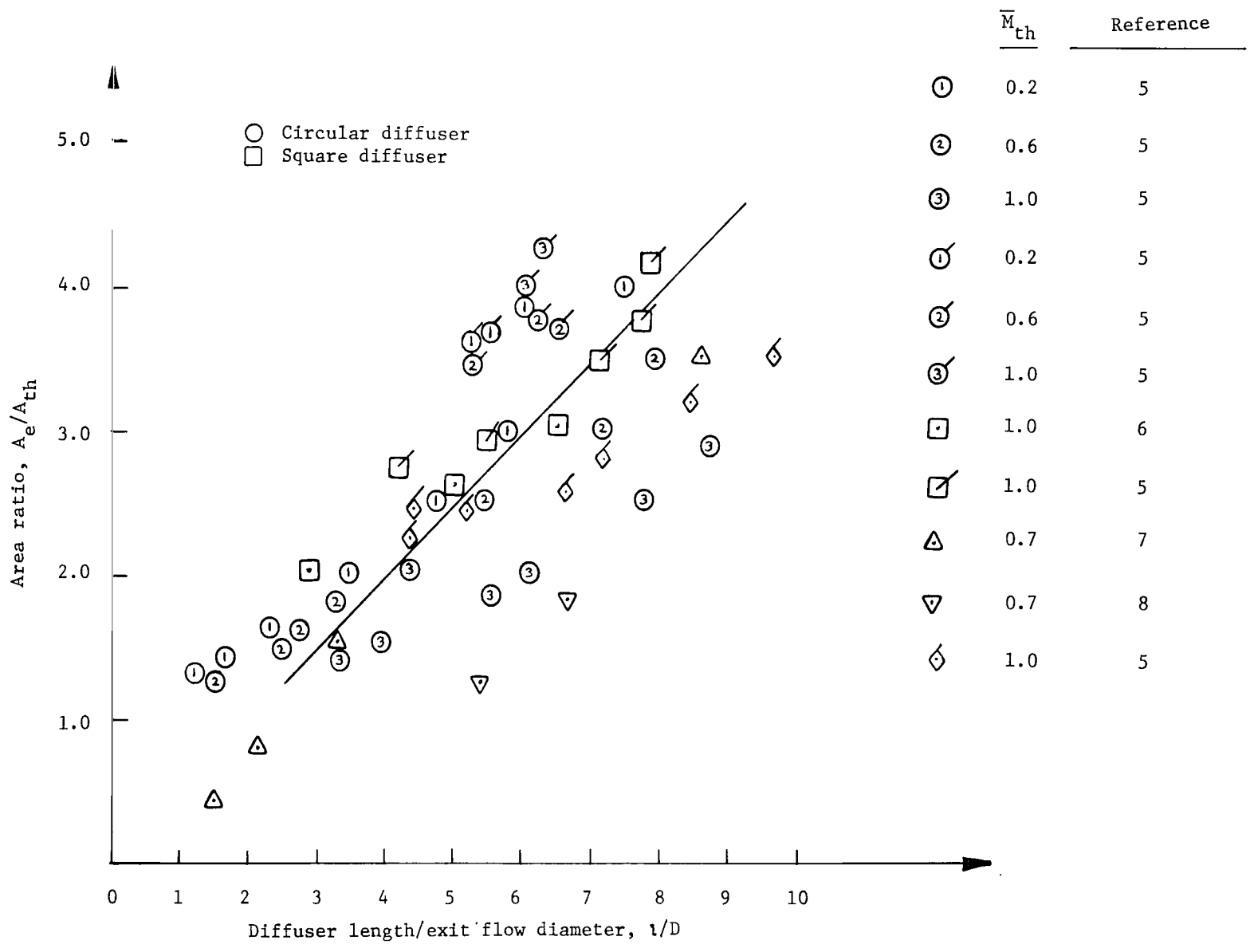

Figure 9.- Optimum l/D for given area ratio at different throat Mach numbers for circular and square diffusers.

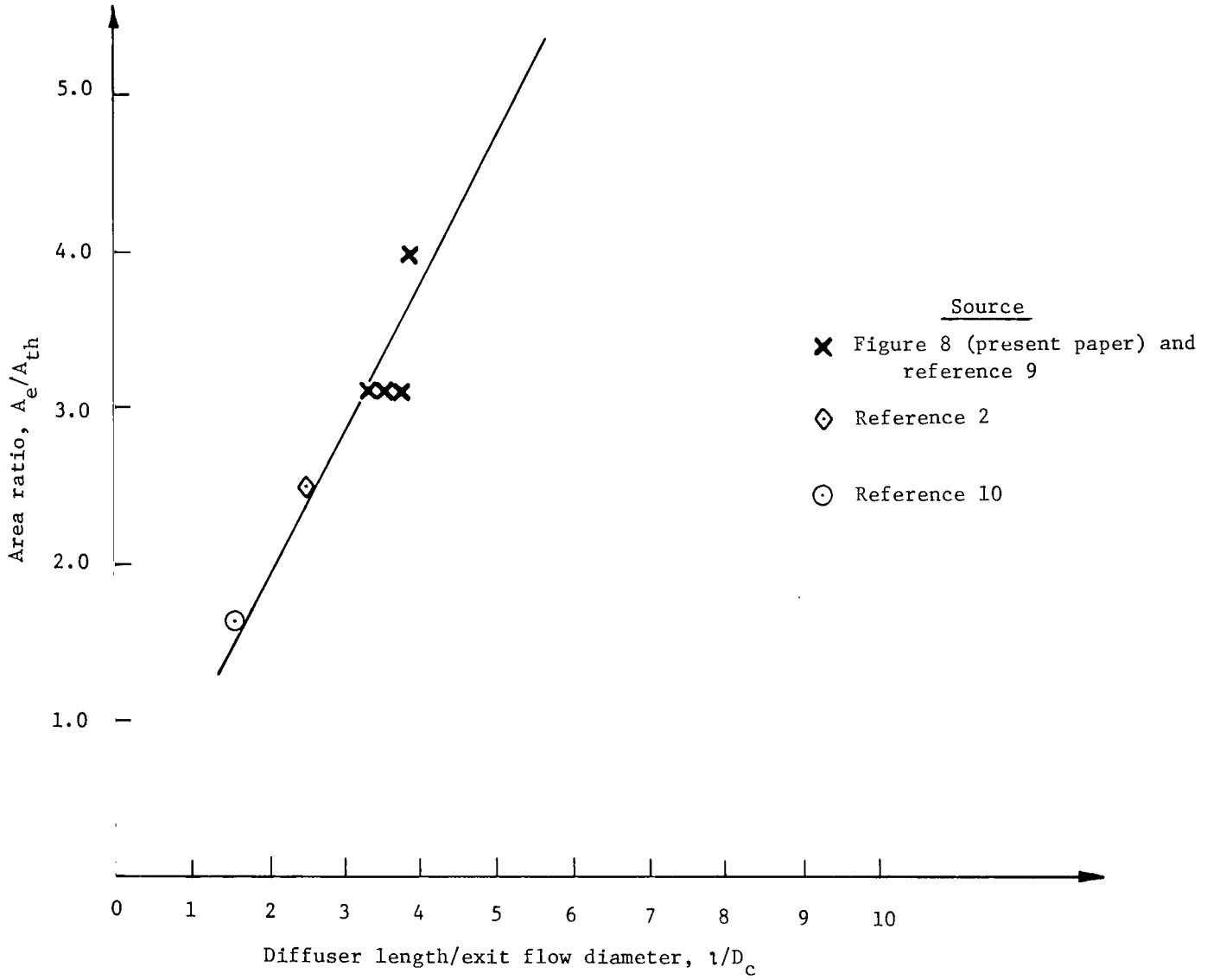

Figure 10.- Optimum ℓ/D_c for given area ratio at $\bar{M}_{th} = 1.0$ for annular diffusers.

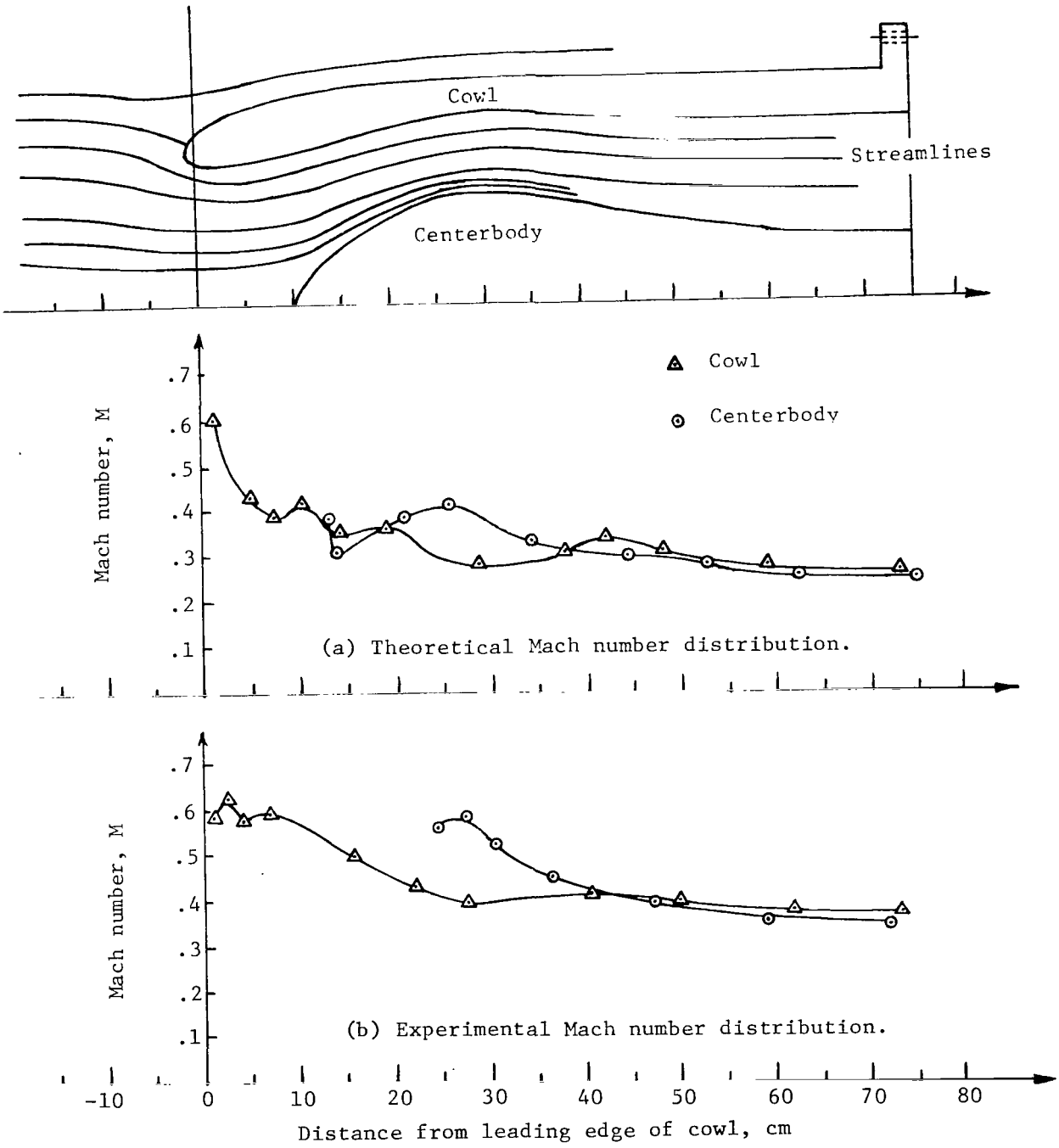

Figure 11.- Theoretical potential flow and experimental results for configuration 1 with centerbody at 0-cm displacement.

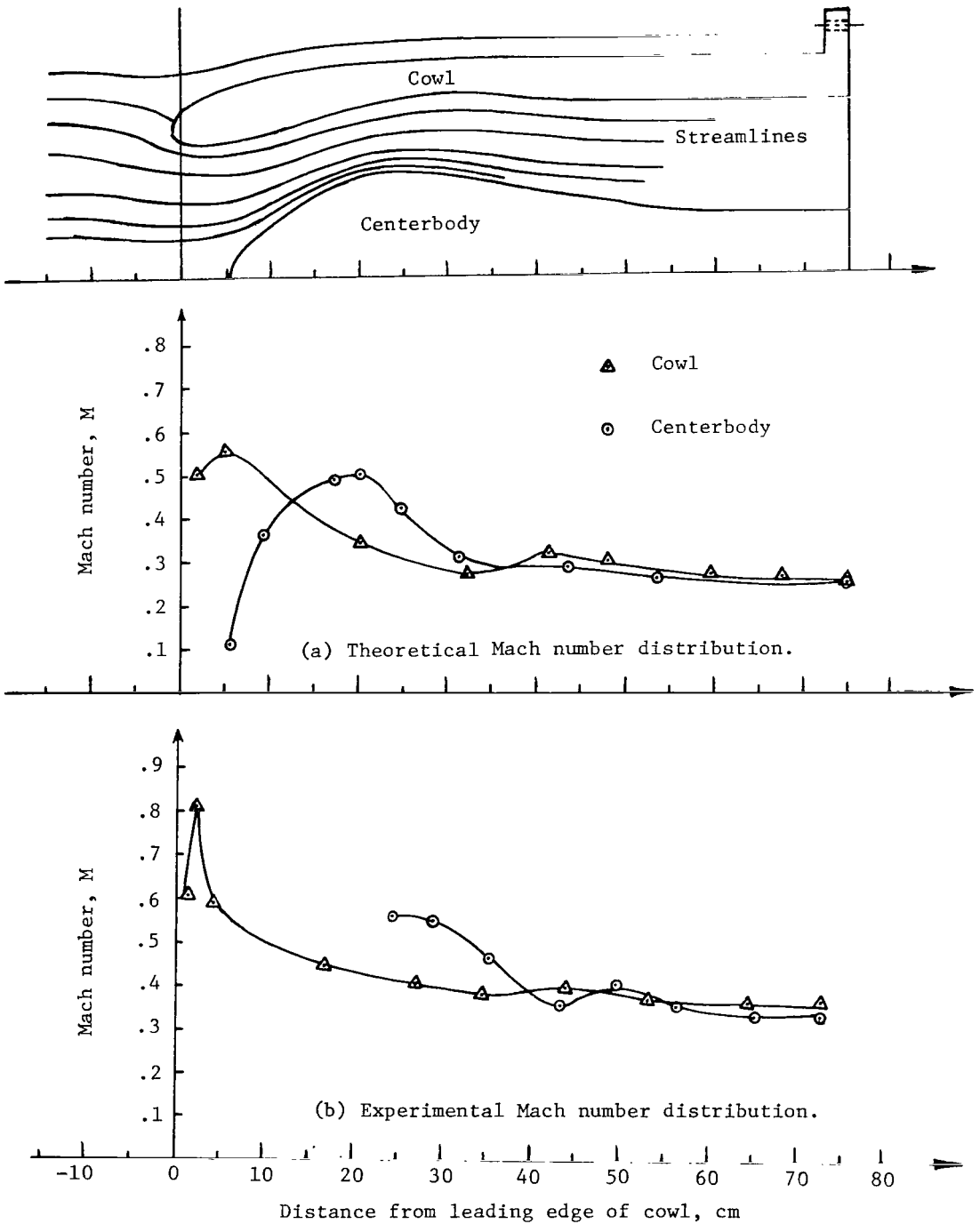

Figure 12.- Theoretical potential flow and experimental results for configuration 1 with centerbody at 5.1-cm displacement.

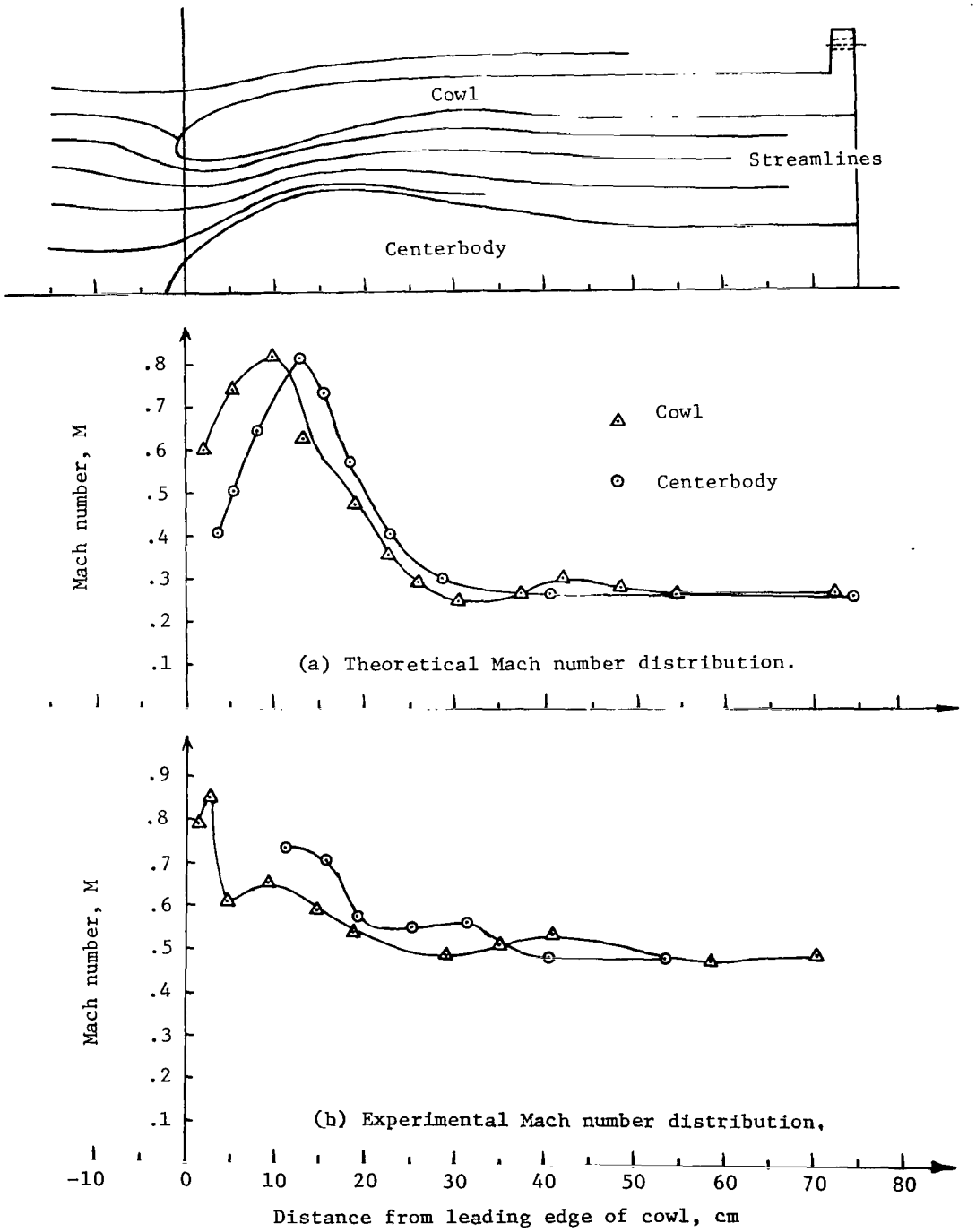

Figure 13.- Theoretical potential flow and experimental results for configuration 1 with centerbody at 12.7-cm displacement.

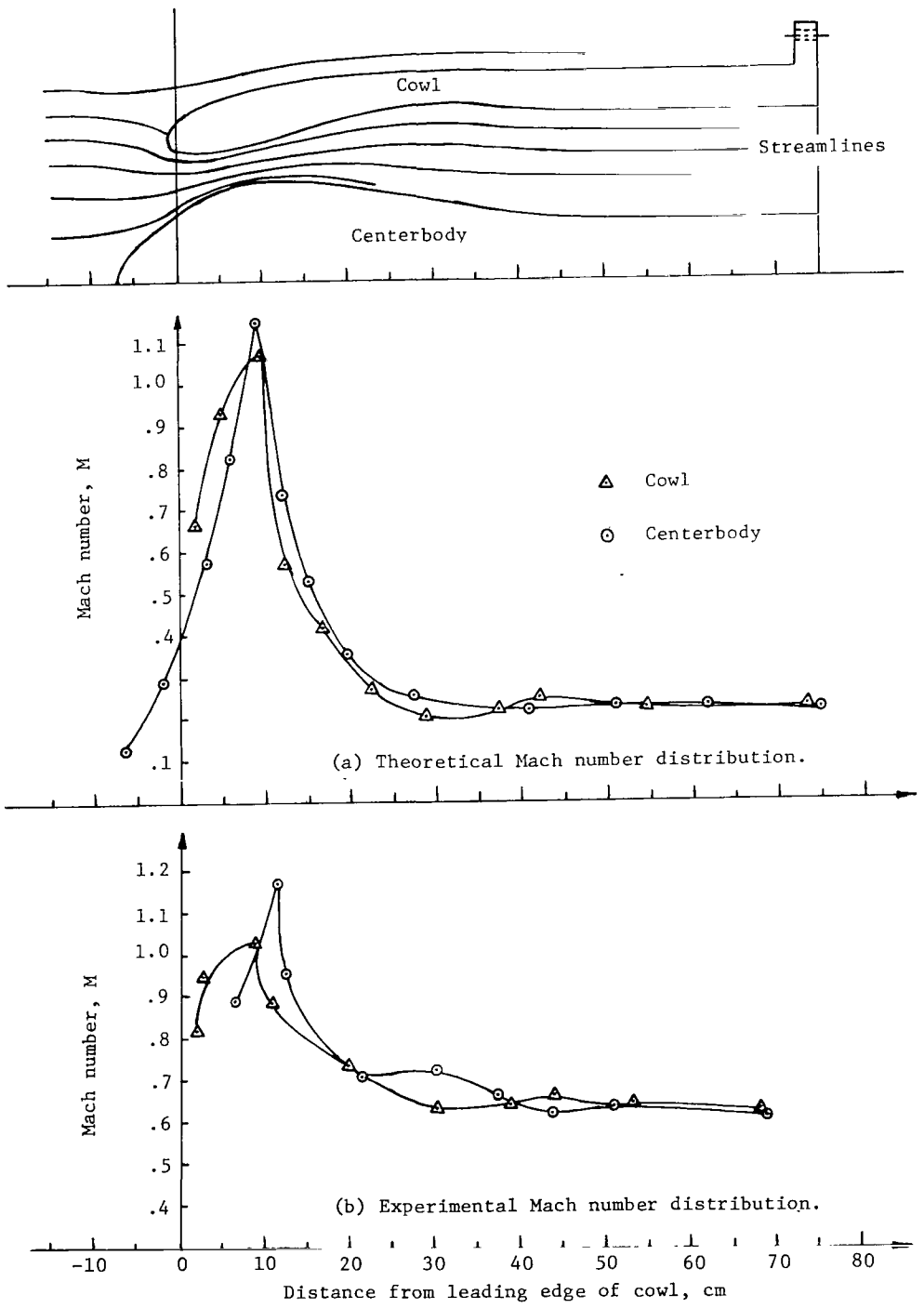

Figure 14.- Theoretical potential flow and experimental results for configuration 1 with centerbody at 17.8-cm displacement.

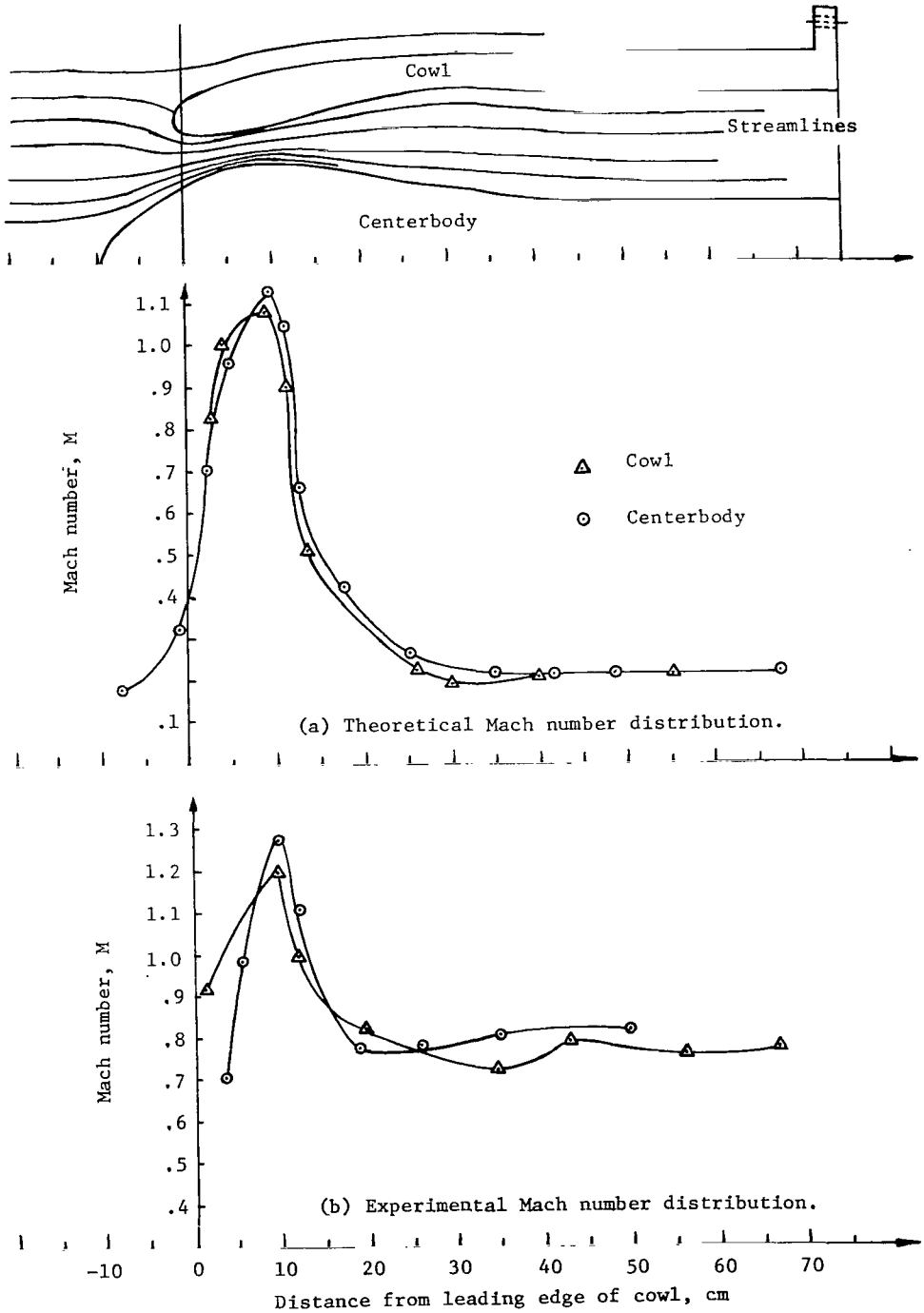

Figure 15.- Theoretical potential flow and experimental results for configuration 1 with centerbody at 20.3-cm displacement.

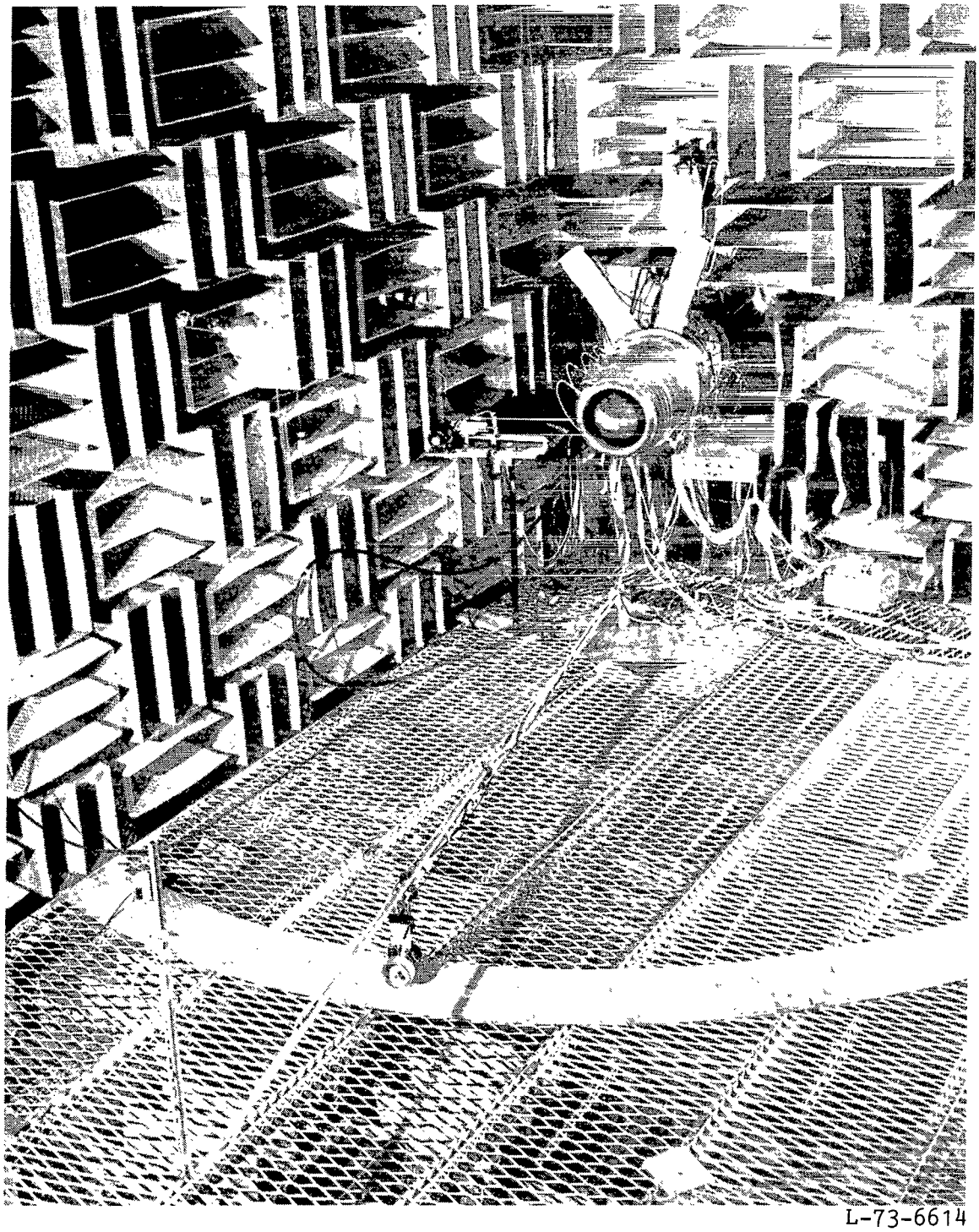

L-73-6614

Figure 16.- Photograph of compressor inlet and microphone boom installed in anechoic chamber.

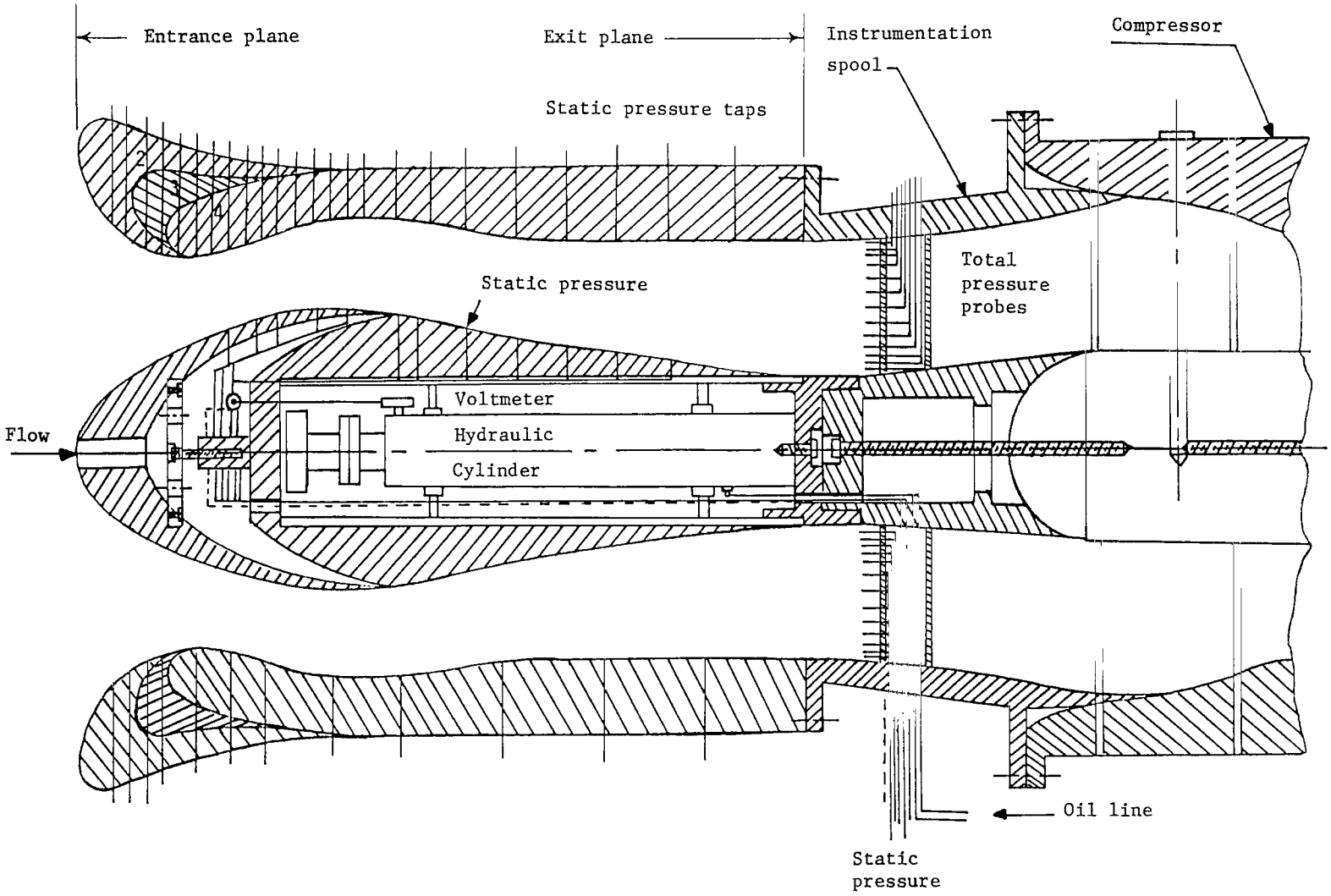

Figure 17.- Translating centerbody inlet (configurations 2, 3, and 4) with aerodynamic instrumentation.

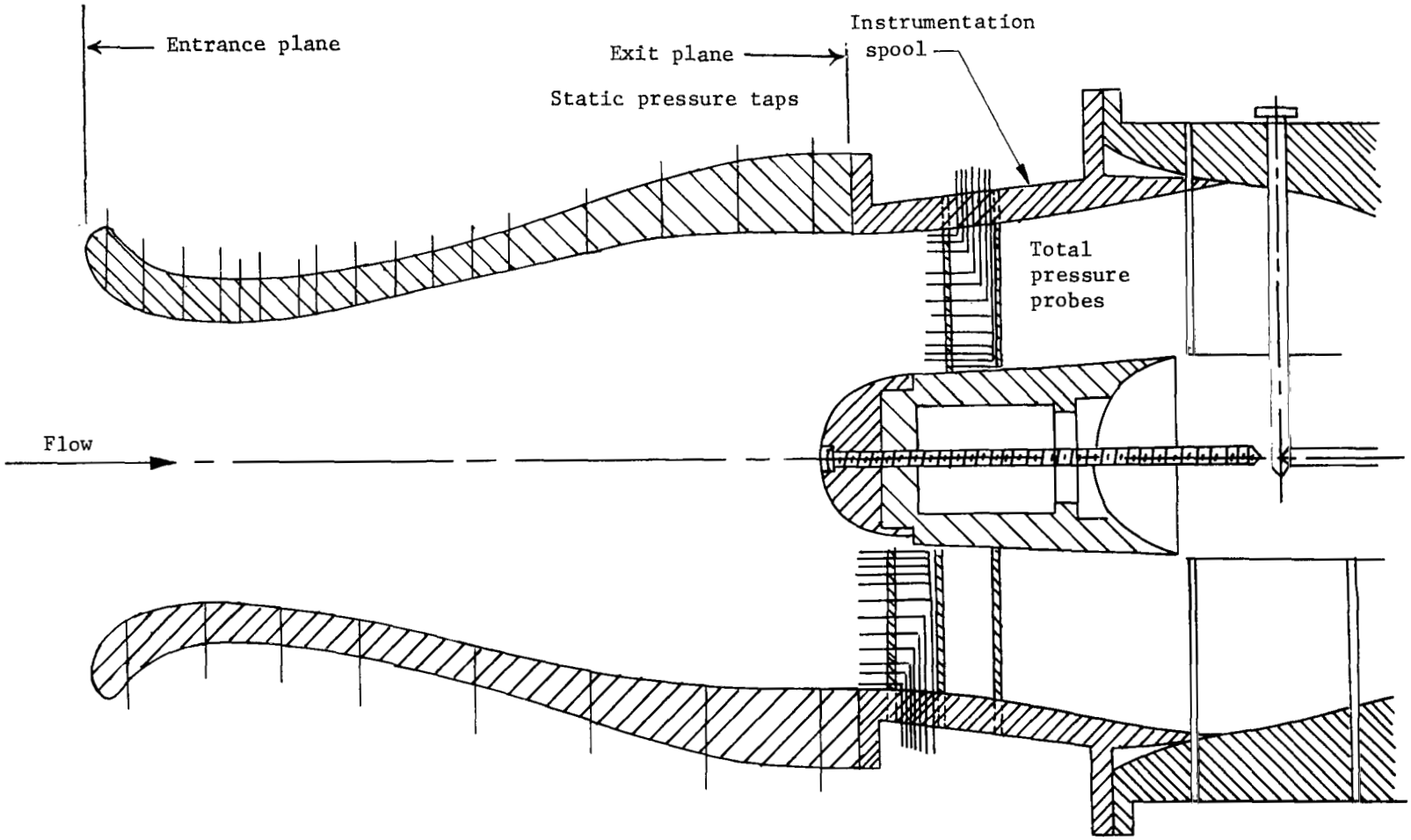

Figure 18.- Collapsing cowl (configuration 5) with aerodynamic instrumentation.

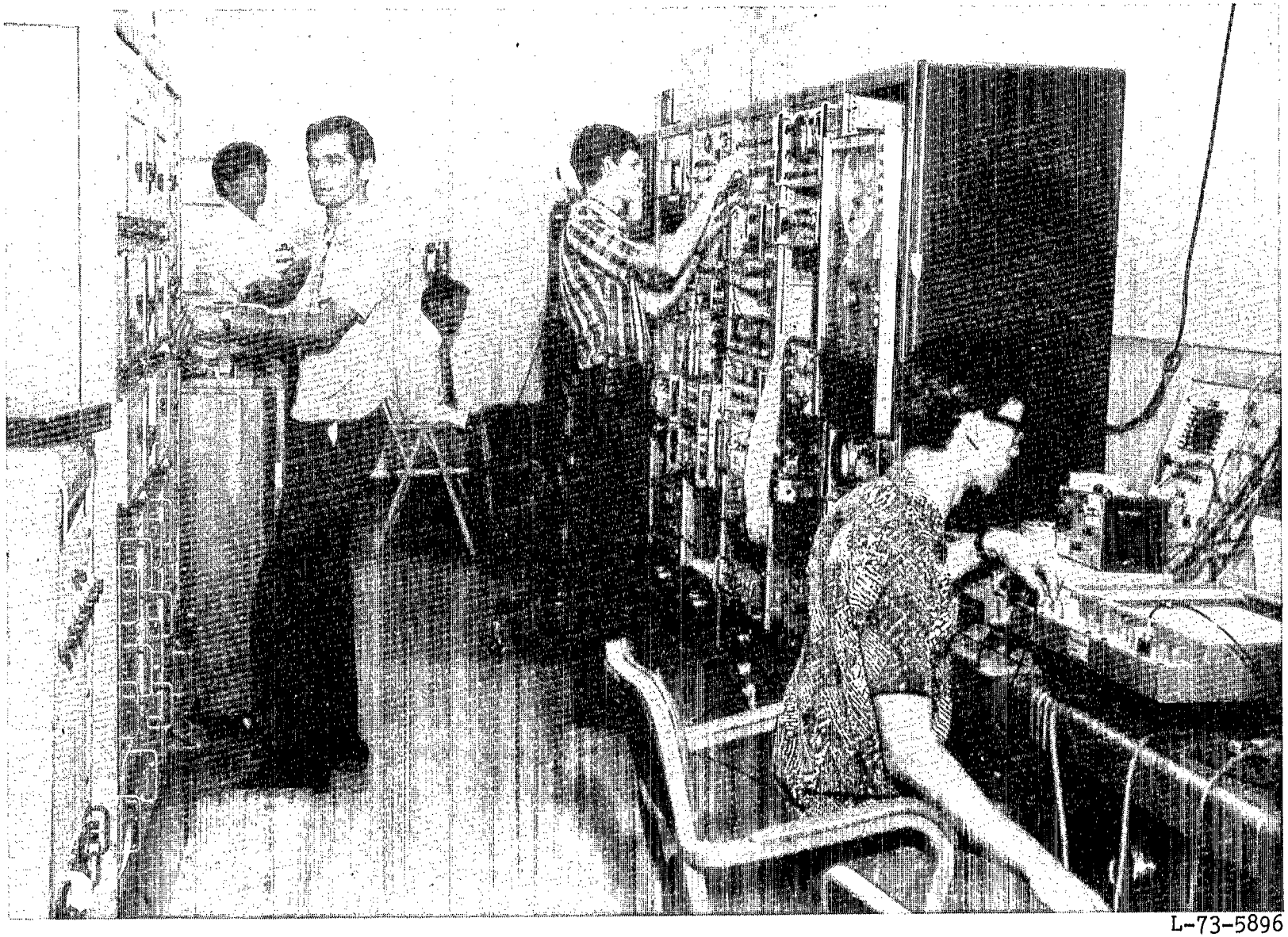

L-73-5896

Figure 19.- Instrumentation room used for acoustic and aerodynamic data acquisition.

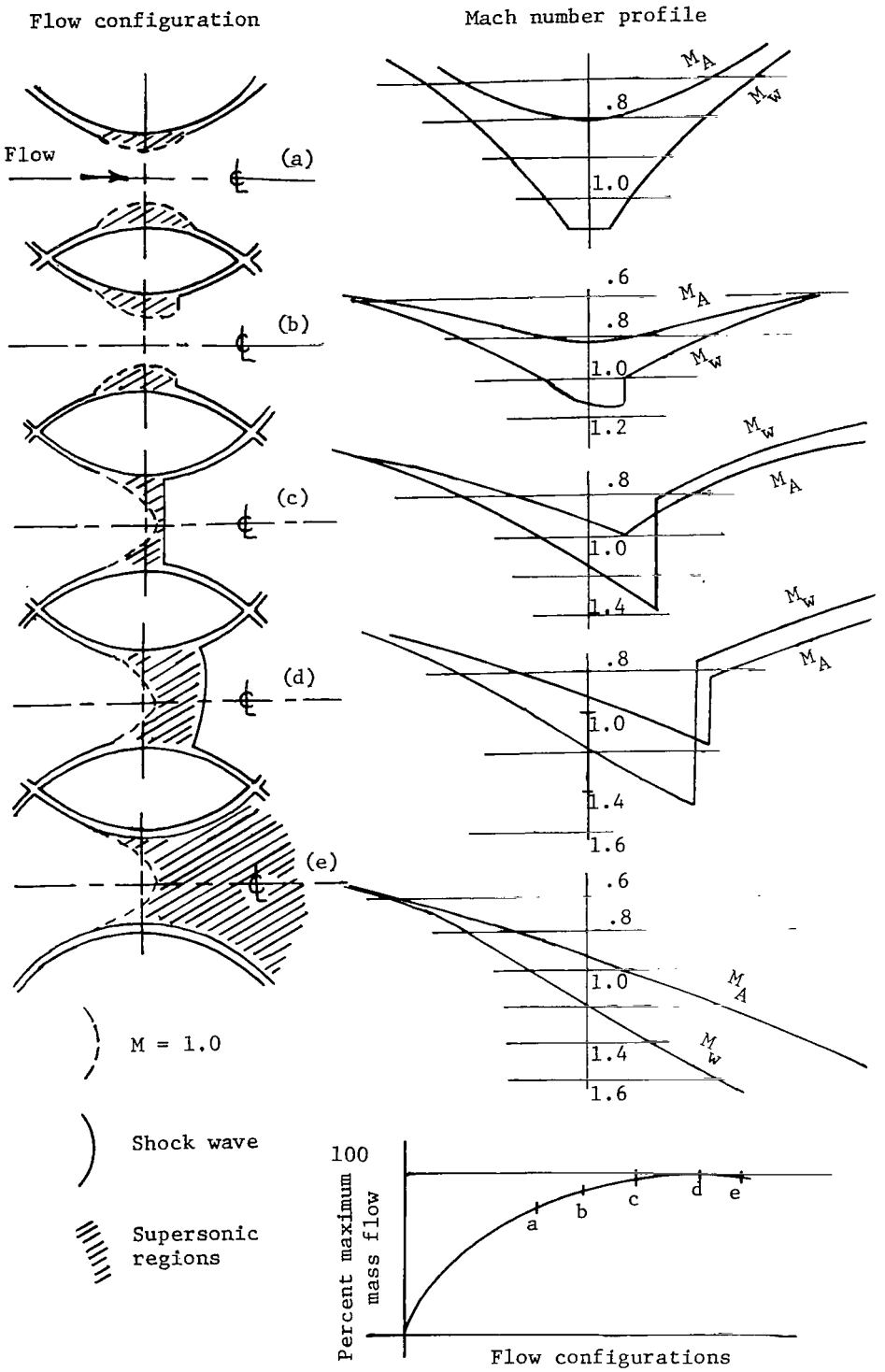

Figure 20.- Wall and center line Mach numbers for potential flow in two dimensions.

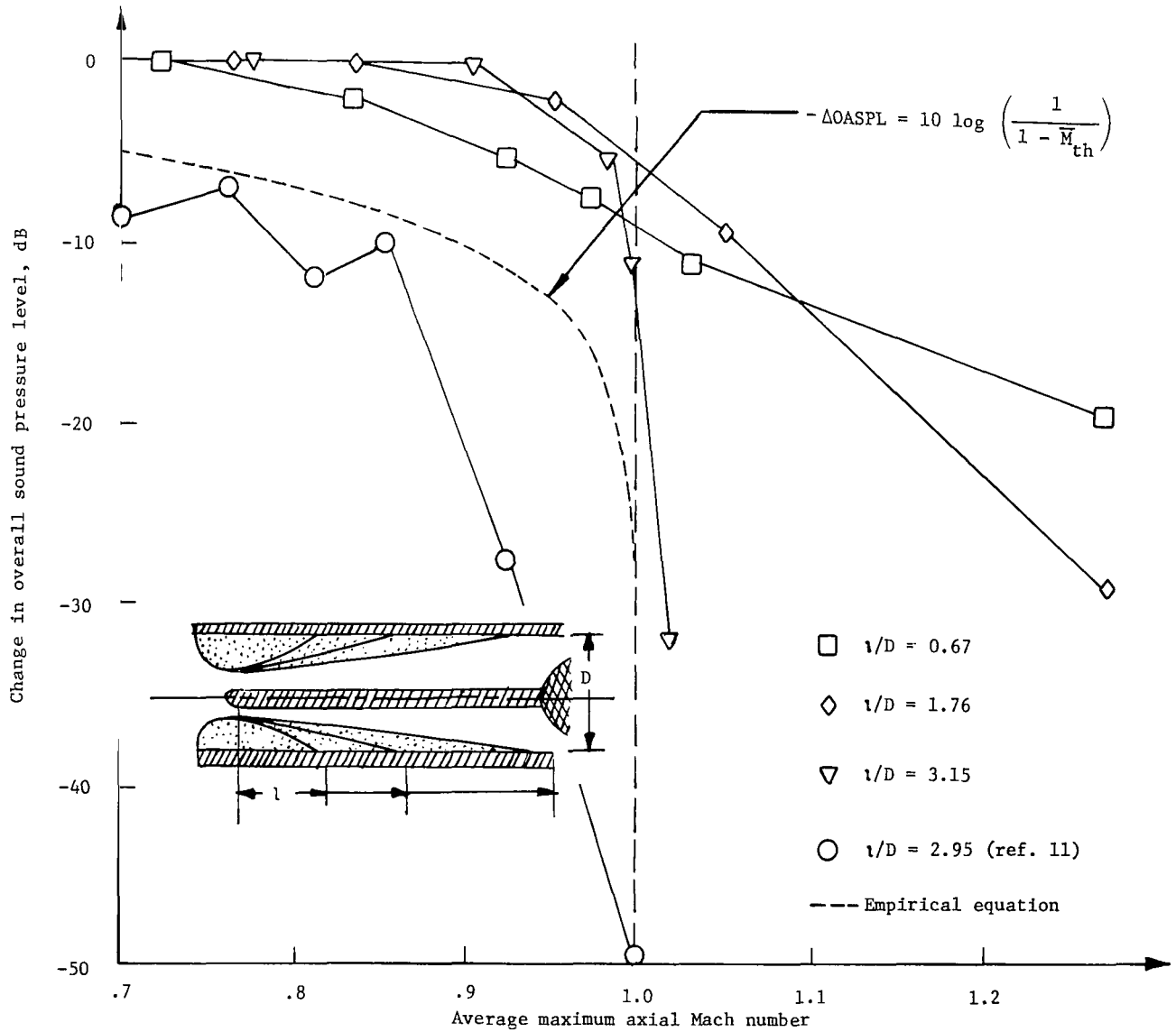

Figure 21.- Influence of length-diameter ratio on noise attenuation (ejector source).

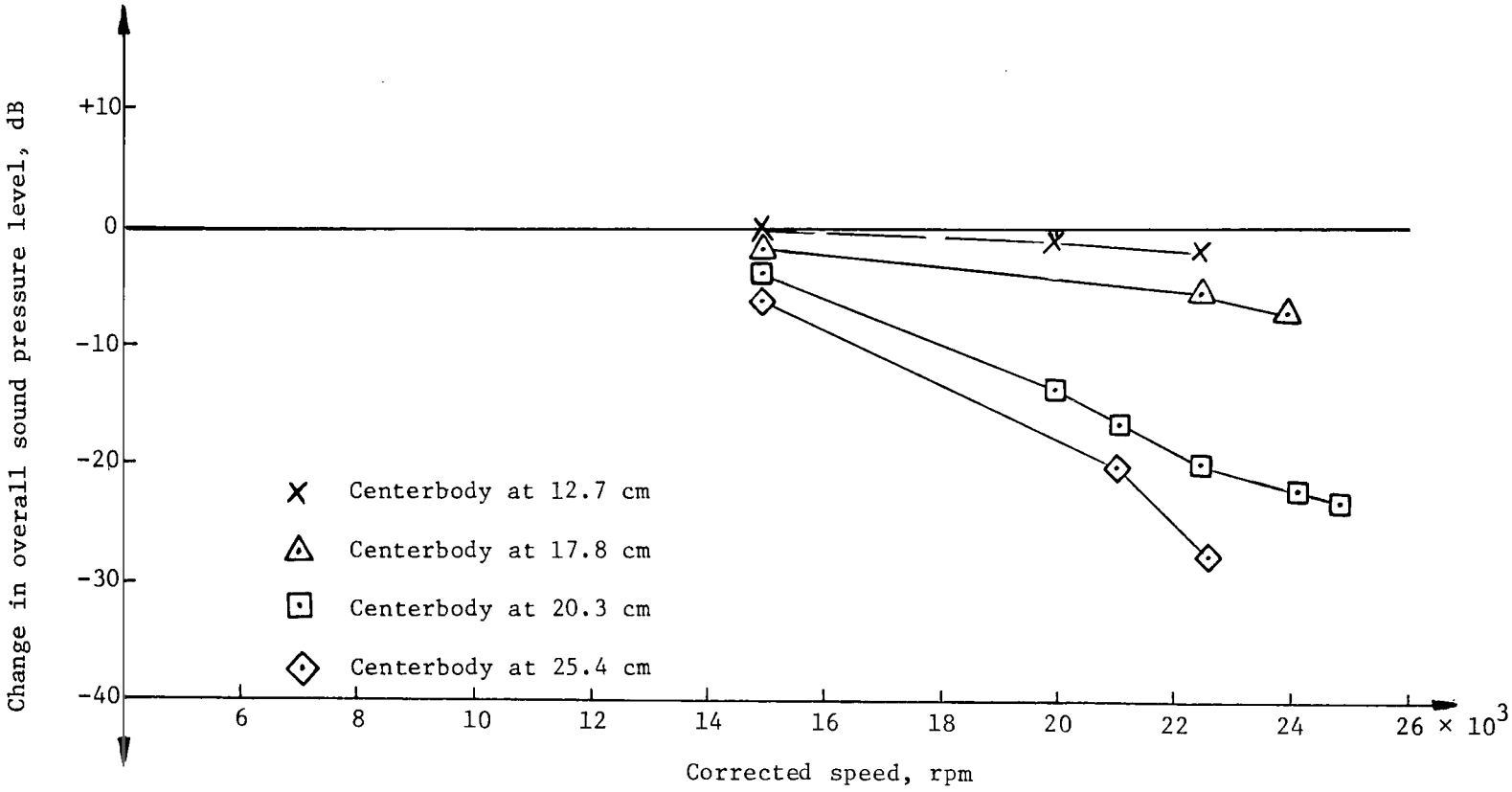

Figure 22.- Noise attenuation for inlet configuration 1; boom microphone at 0°.

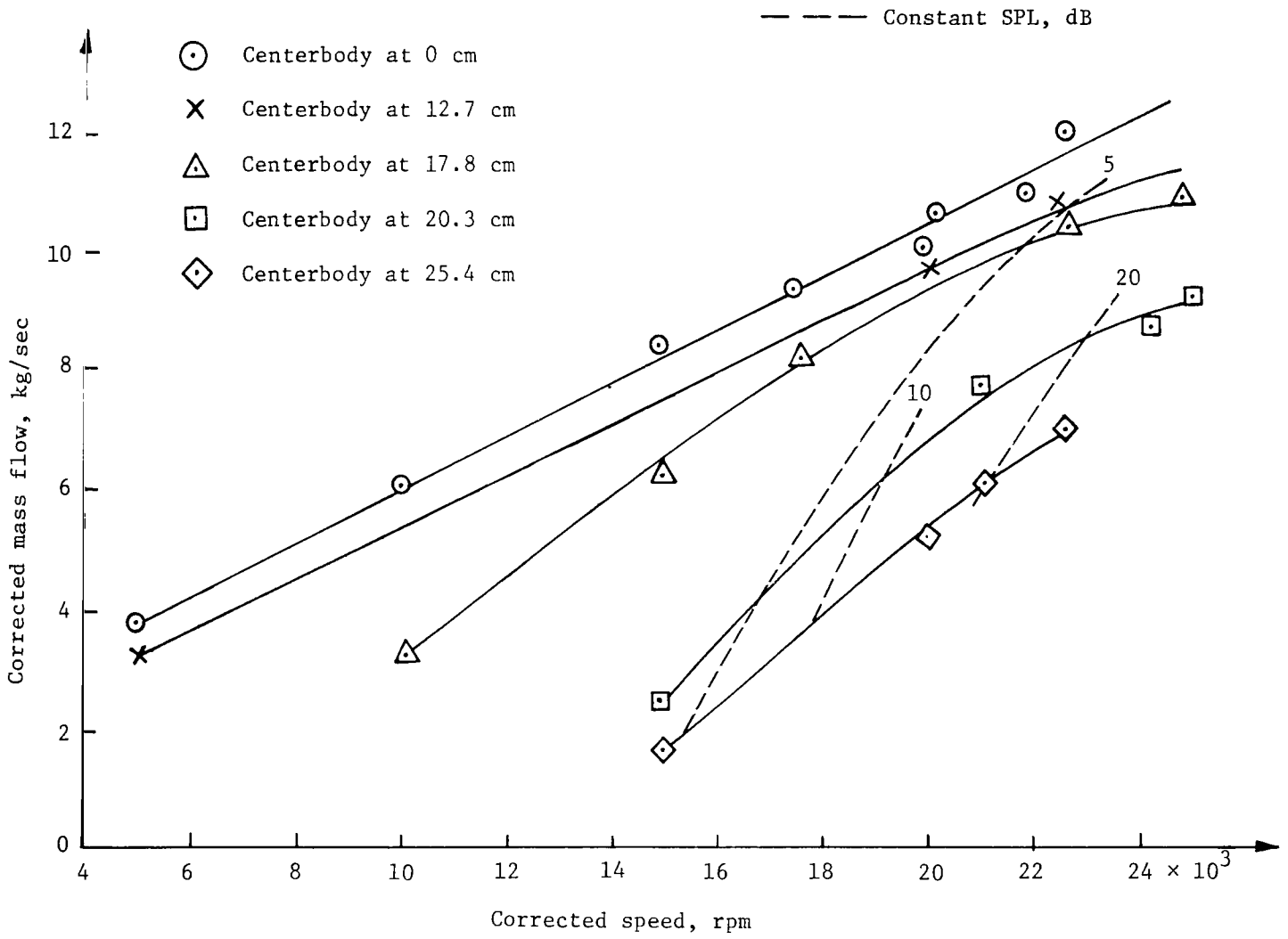

Figure 23.- Mass flow for inlet configuration 1.

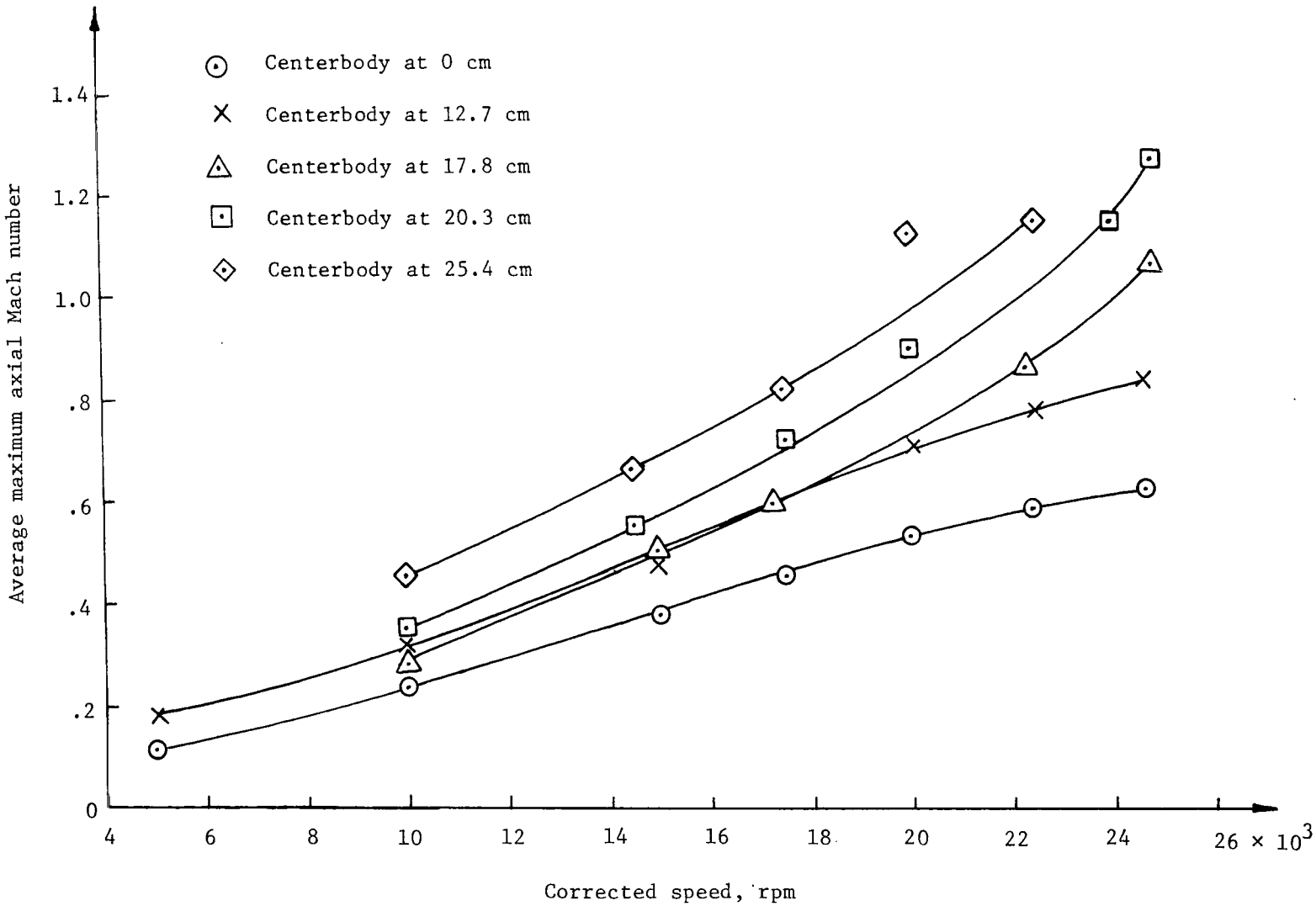

Figure 24.- Average maximum axial Mach number of inlet configuration 1.

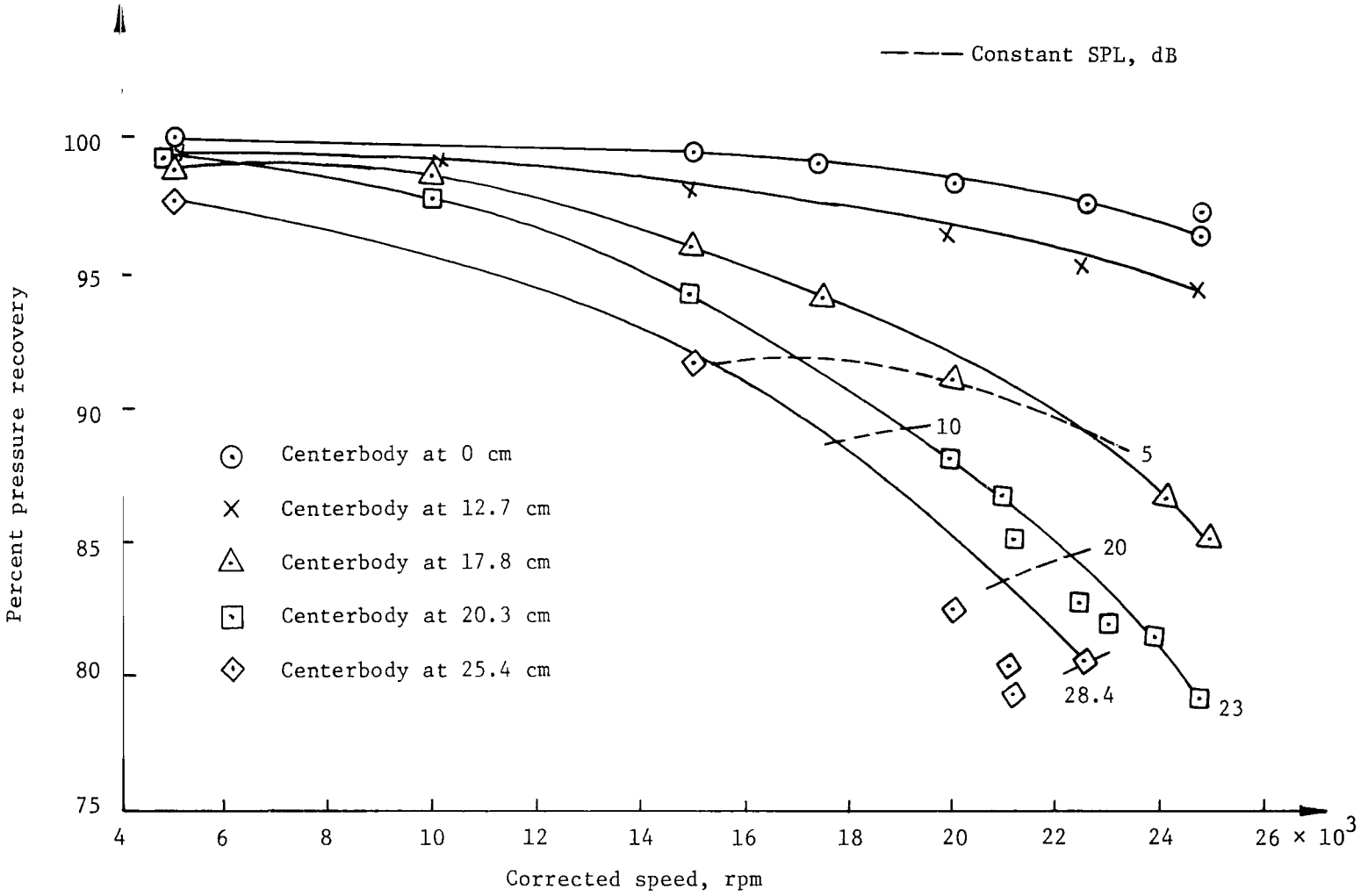

Figure 25.- Pressure recovery for inlet configuration 1. Inlet pressure recovery, $p_{t2,d}/p_{t1,d}$.

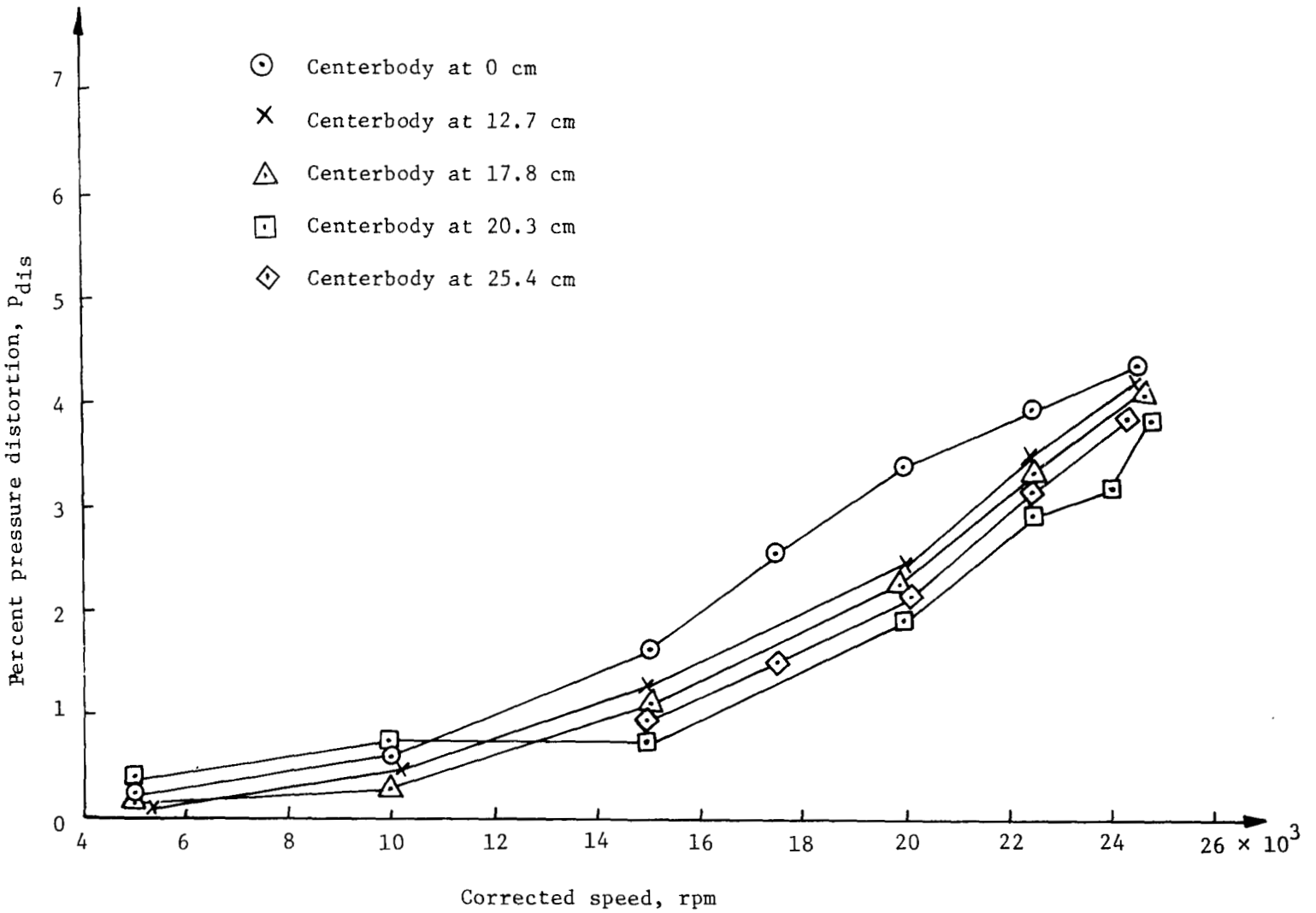

Figure 26.- Pressure distortion for inlet configuration 1.

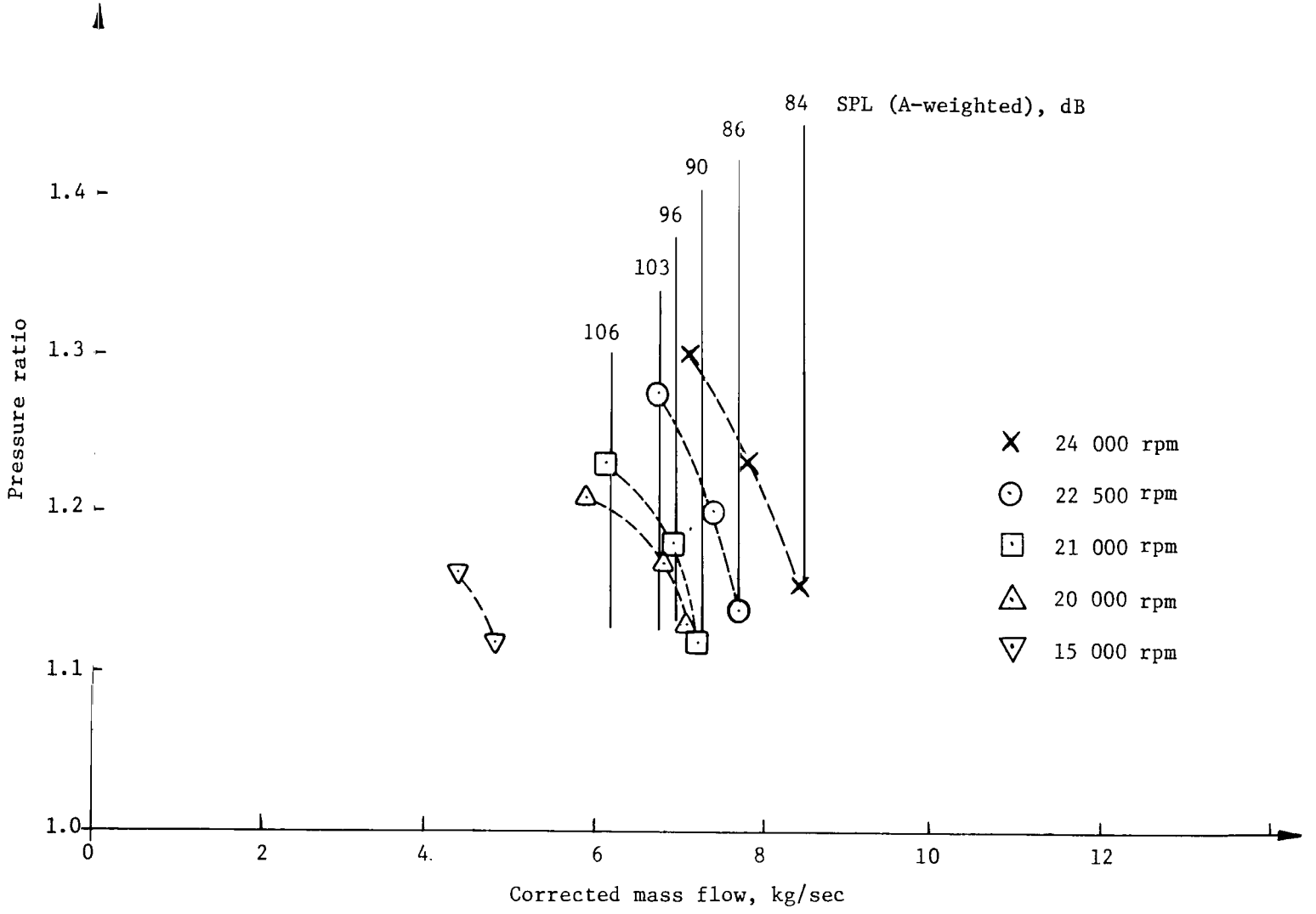

Figure 27.- Influence of compressor pressure ratio on noise; inlet configuration 1; 20.3-cm centerbody translation. Compressor pressure ratio, $p_{t1,fan}/p_{t2,fan}$.

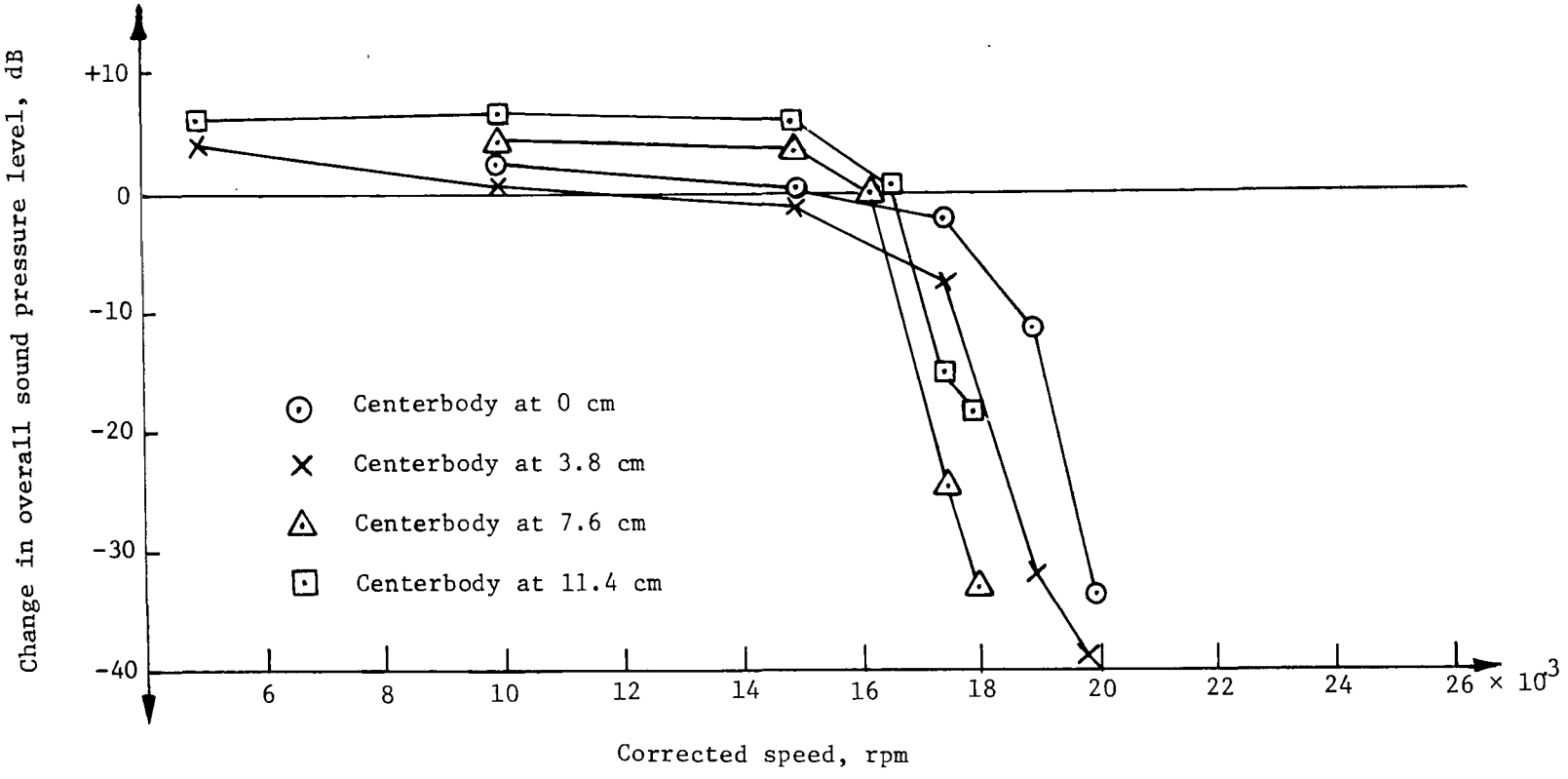

Figure 28.- Noise attenuation for inlet configuration 2; boom microphone at 0°.

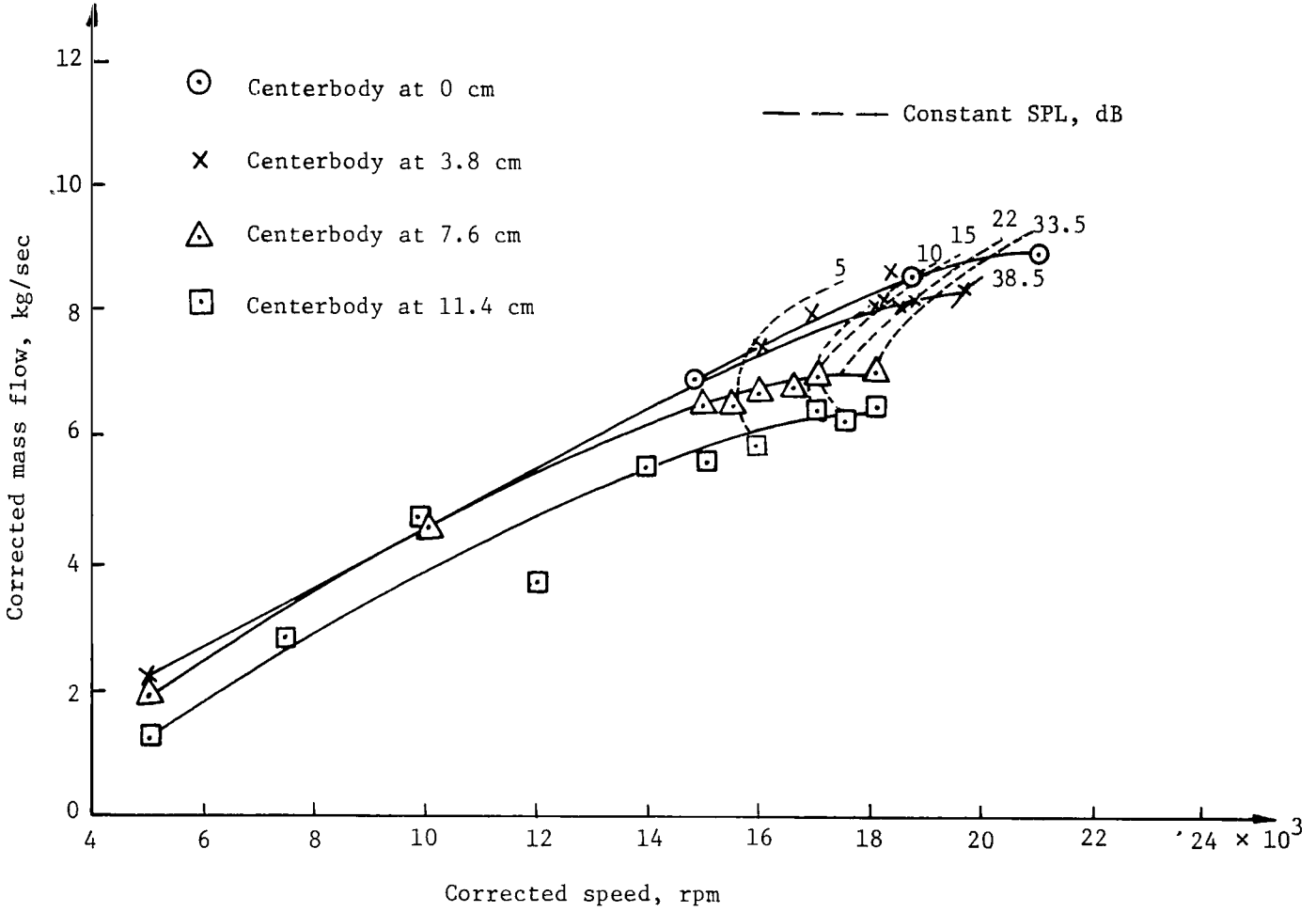

Figure 29.- Mass flow for inlet configuration 2.

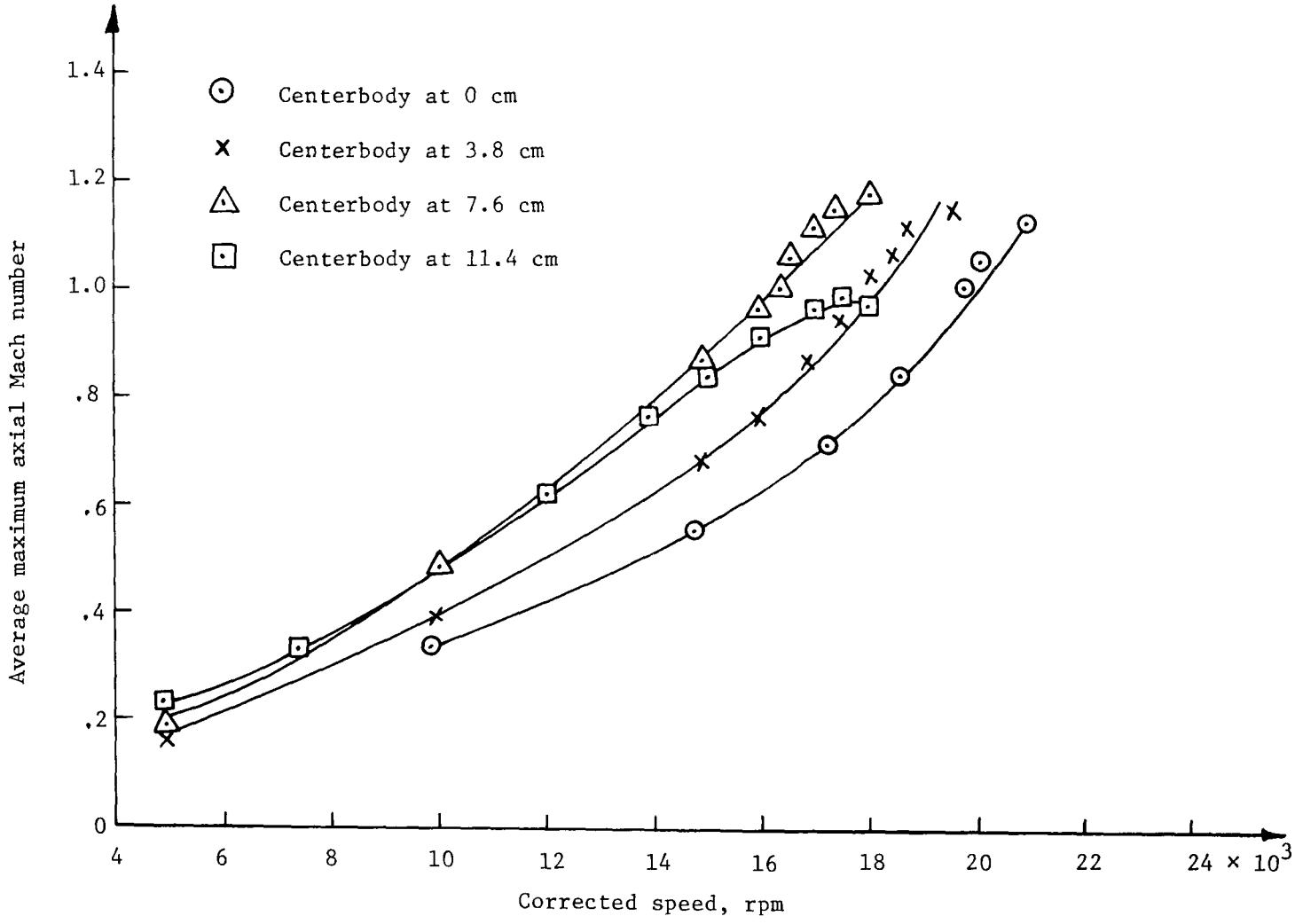

Figure 30.- Average maximum axial Mach number of inlet configuration 2.

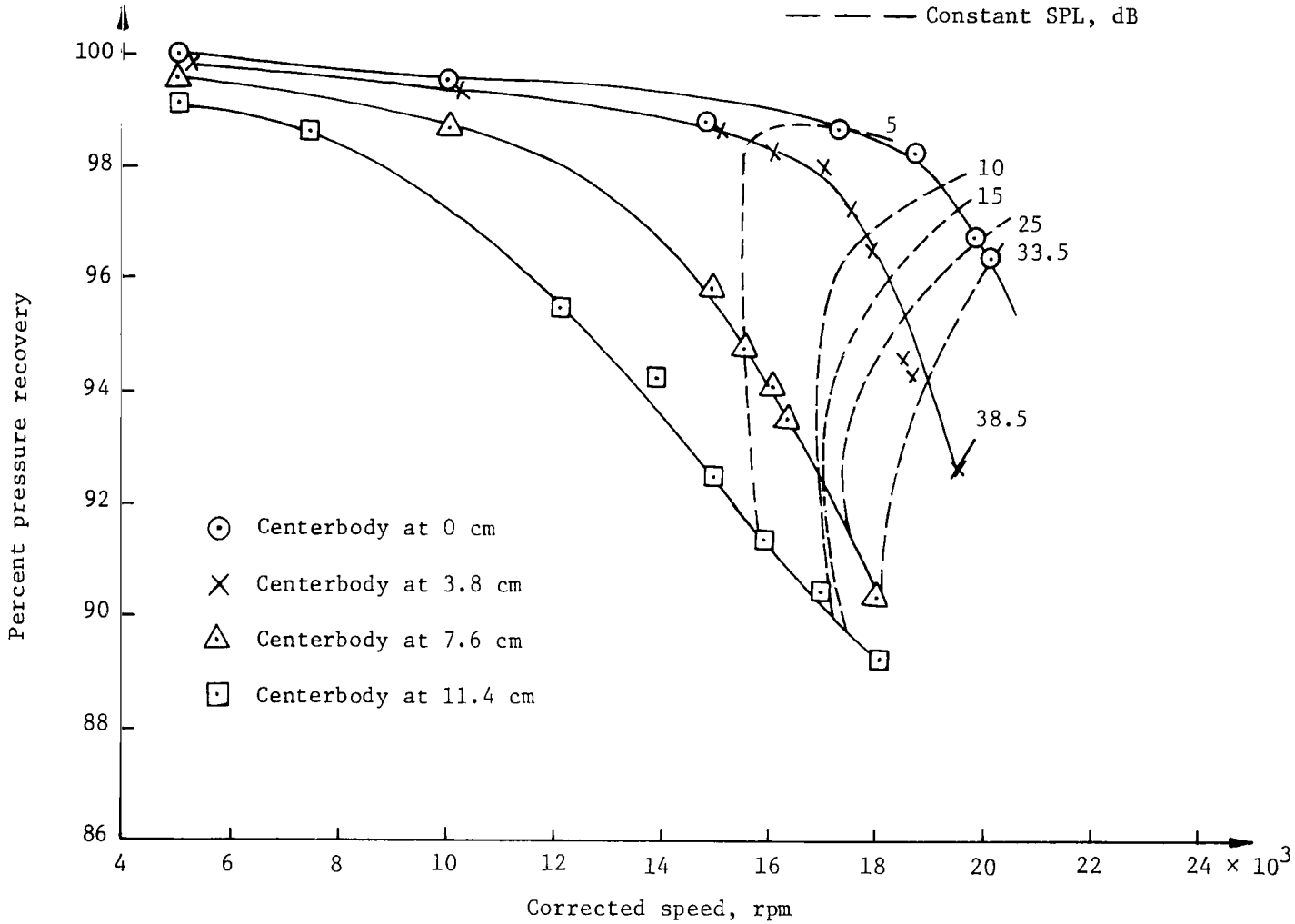

Figure 31.- Pressure recovery for inlet configuration 2. Inlet pressure recovery, $p_{t2,d}/p_{t1,d}$.

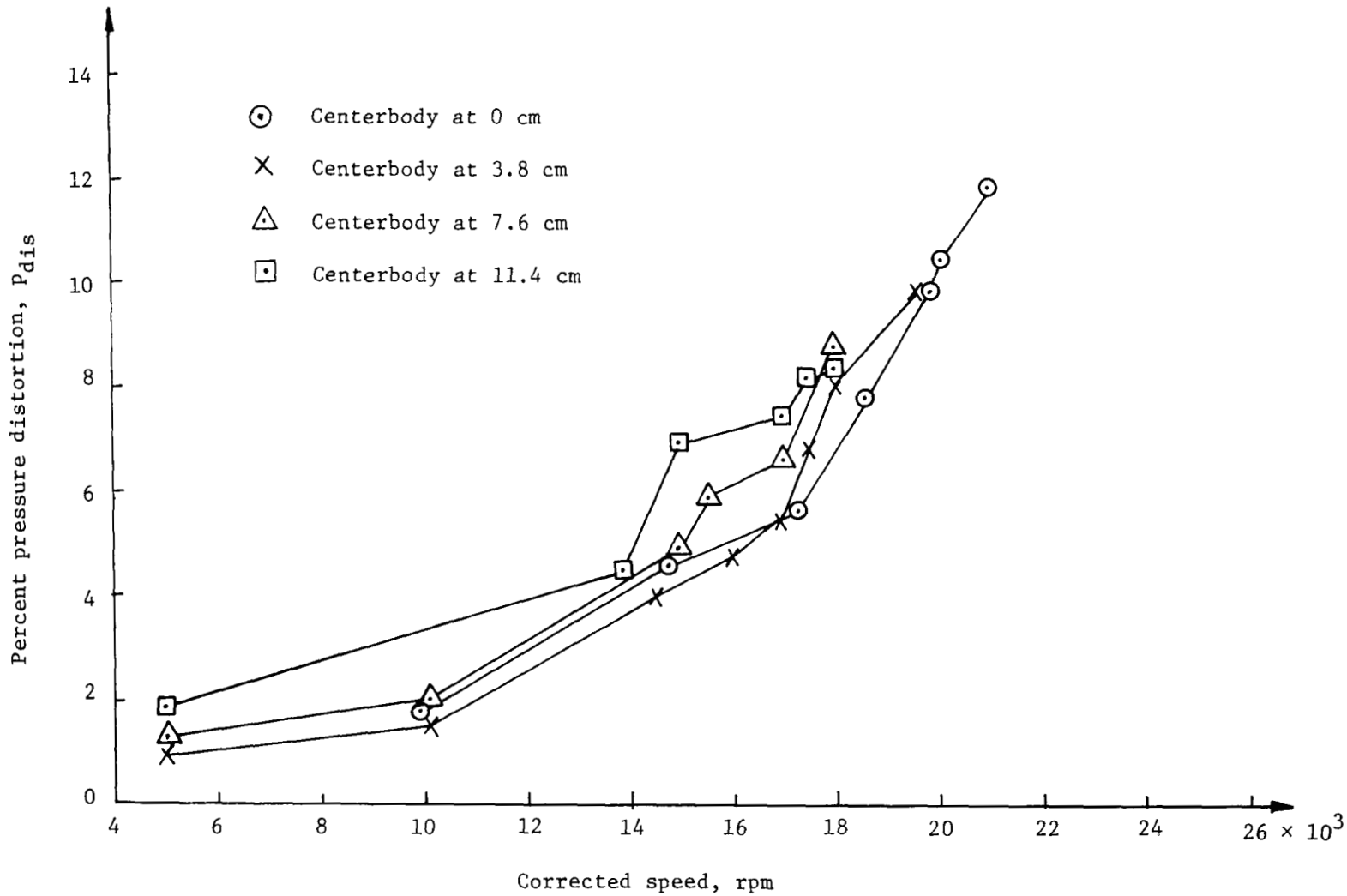

Figure 32.- Pressure distortion for inlet configuration 2.

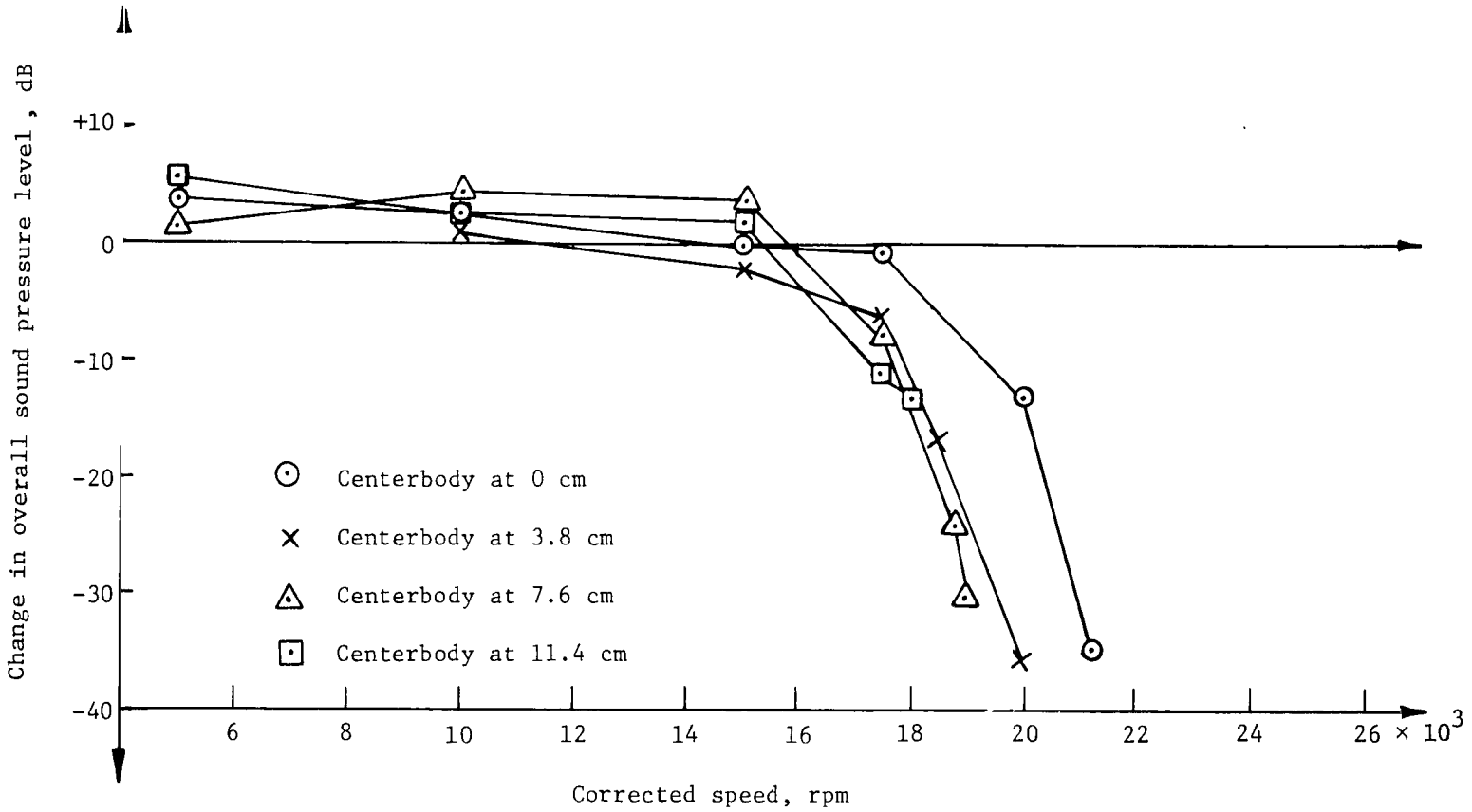

Figure 33.- Noise attenuation for inlet configuration 3; boom microphone at 0°.

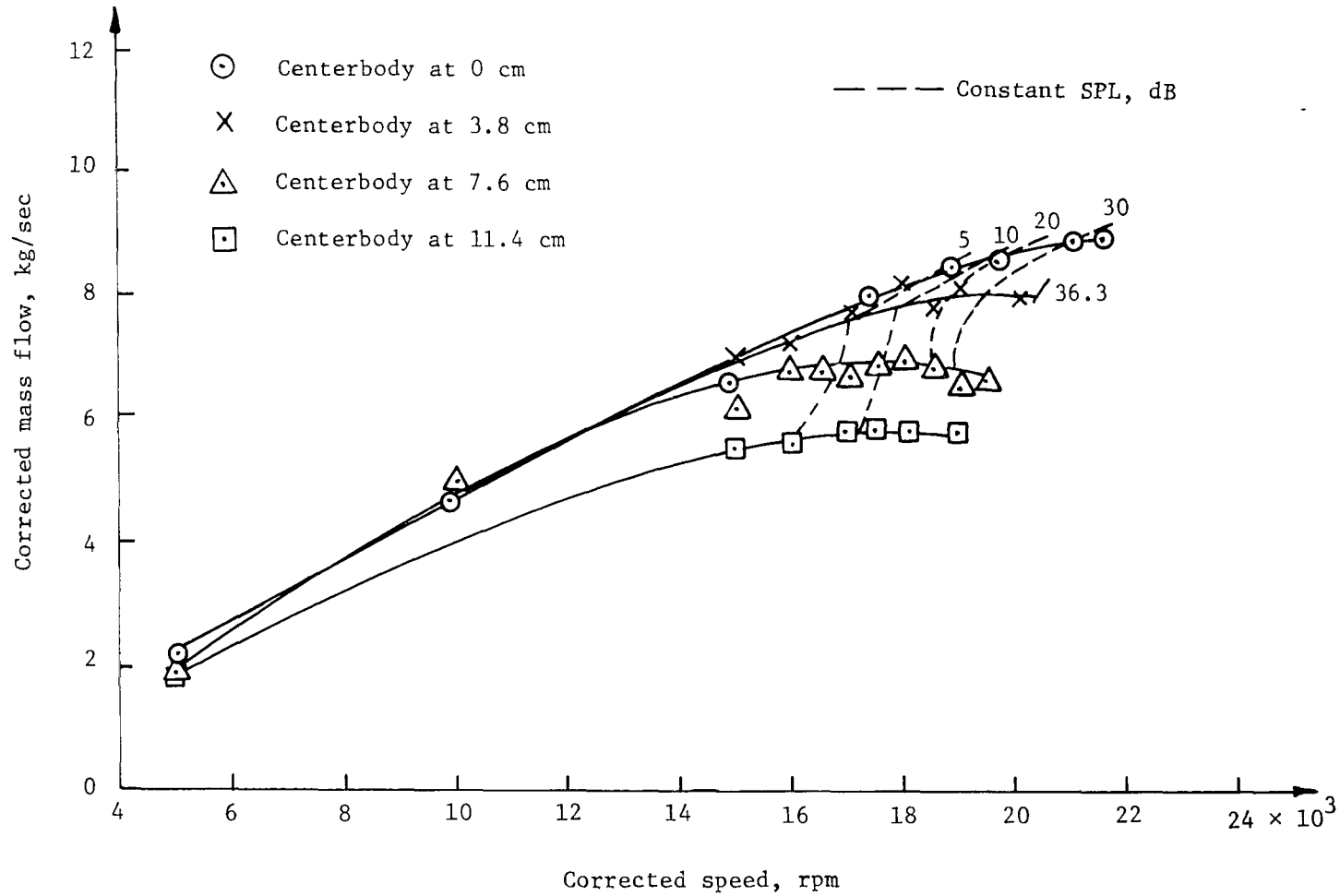

Figure 34.- Mass flow for inlet configuration 3.

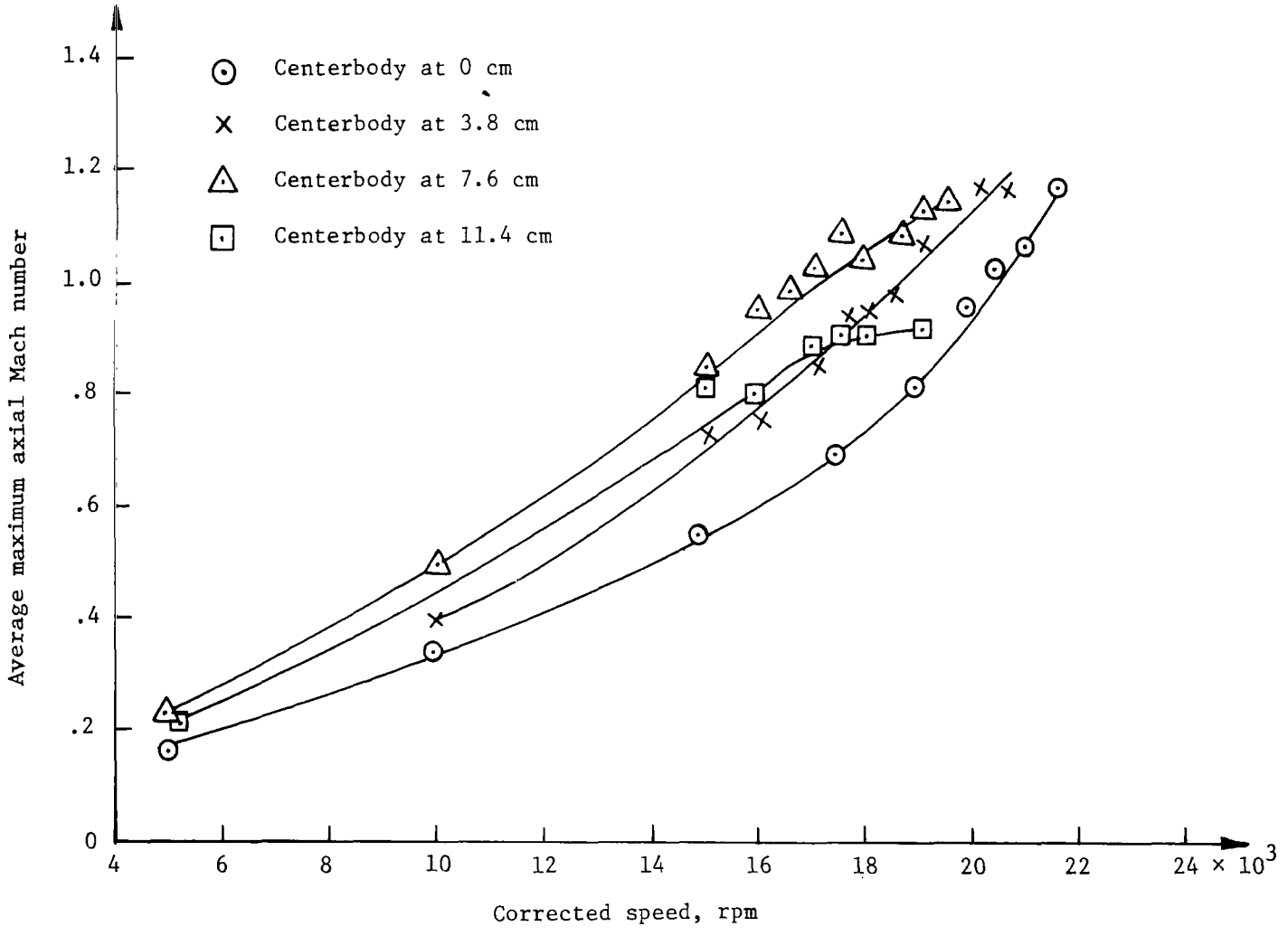

Figure 35.- Average maximum axial Mach number for inlet configuration 3.

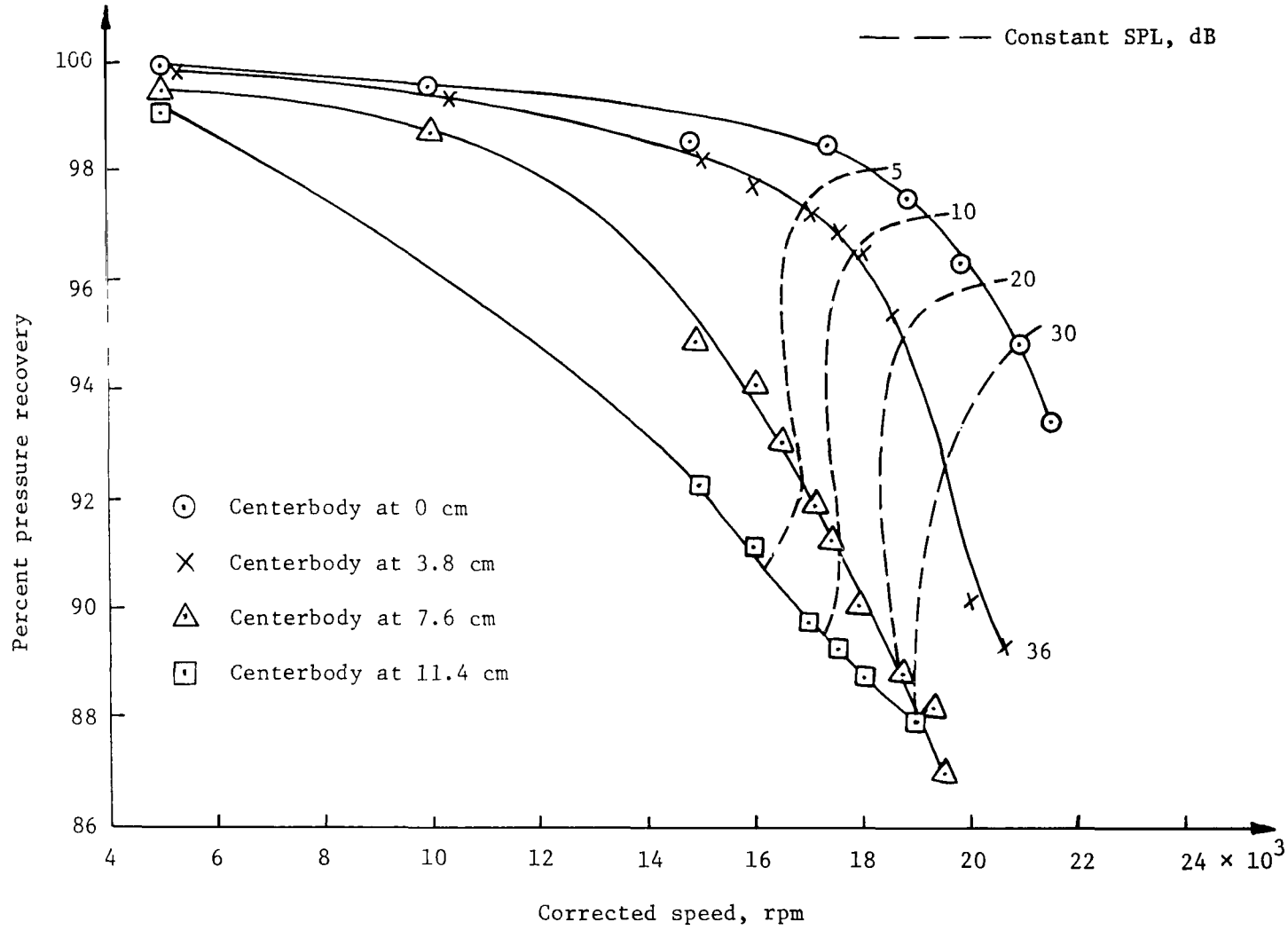

Figure 36.- Pressure recovery for inlet configuration 3. Inlet pressure recovery, $p_{t2,d}/p_{t1,d}$.

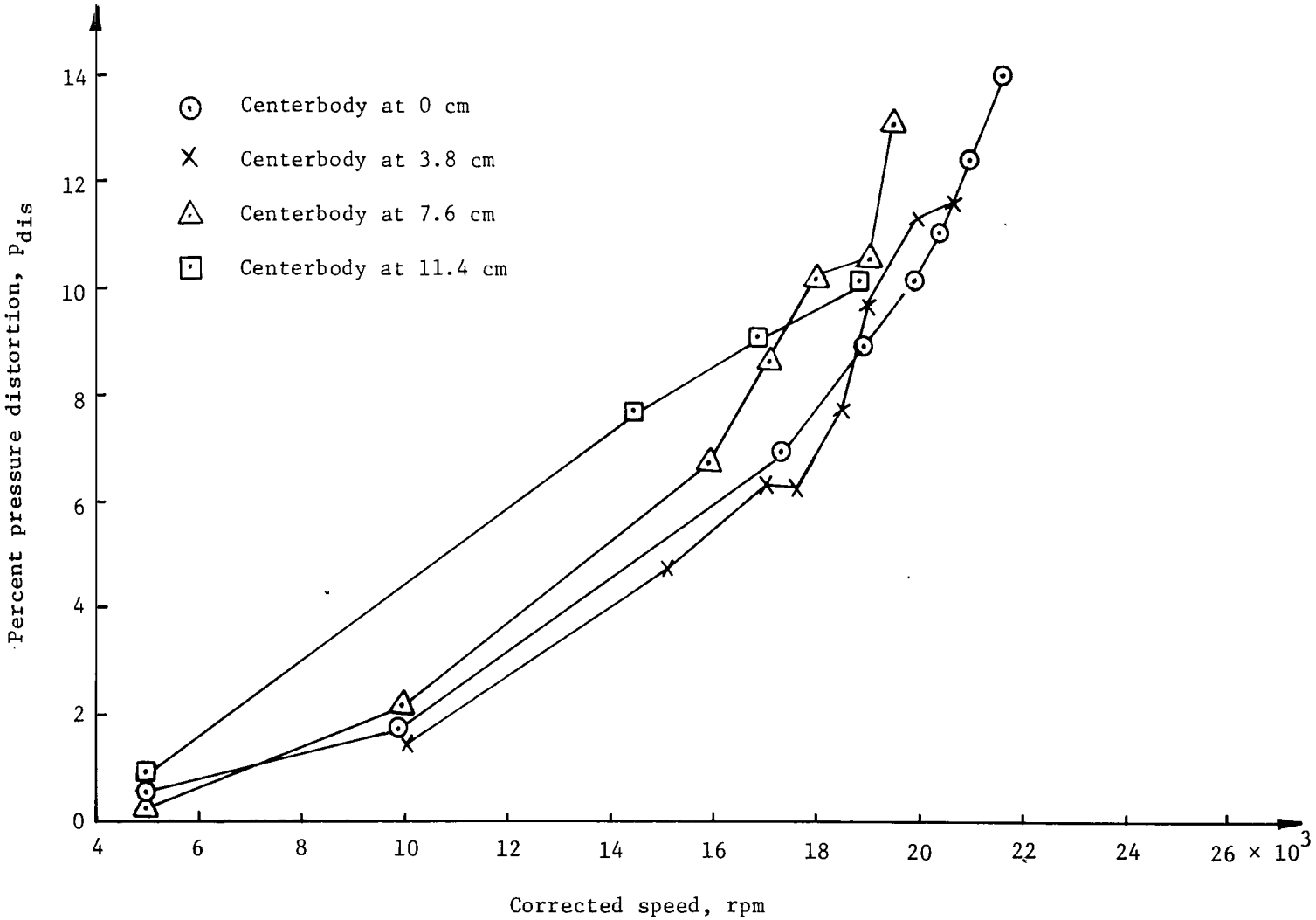

Figure 37.- Pressure distortion for inlet configuration 3.

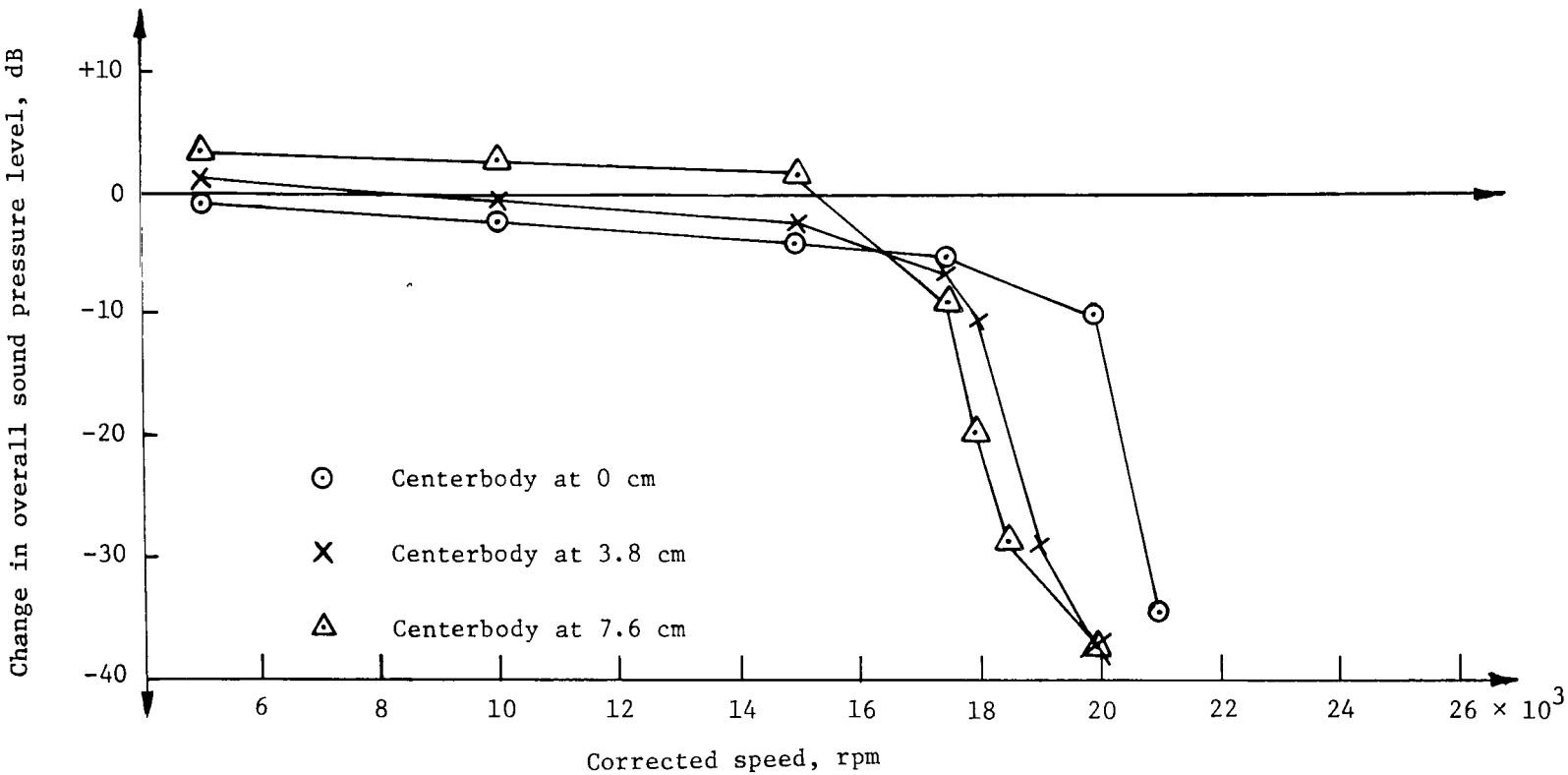

Figure 38.- Noise attenuation for inlet configuration 4; boom microphone at 0°.

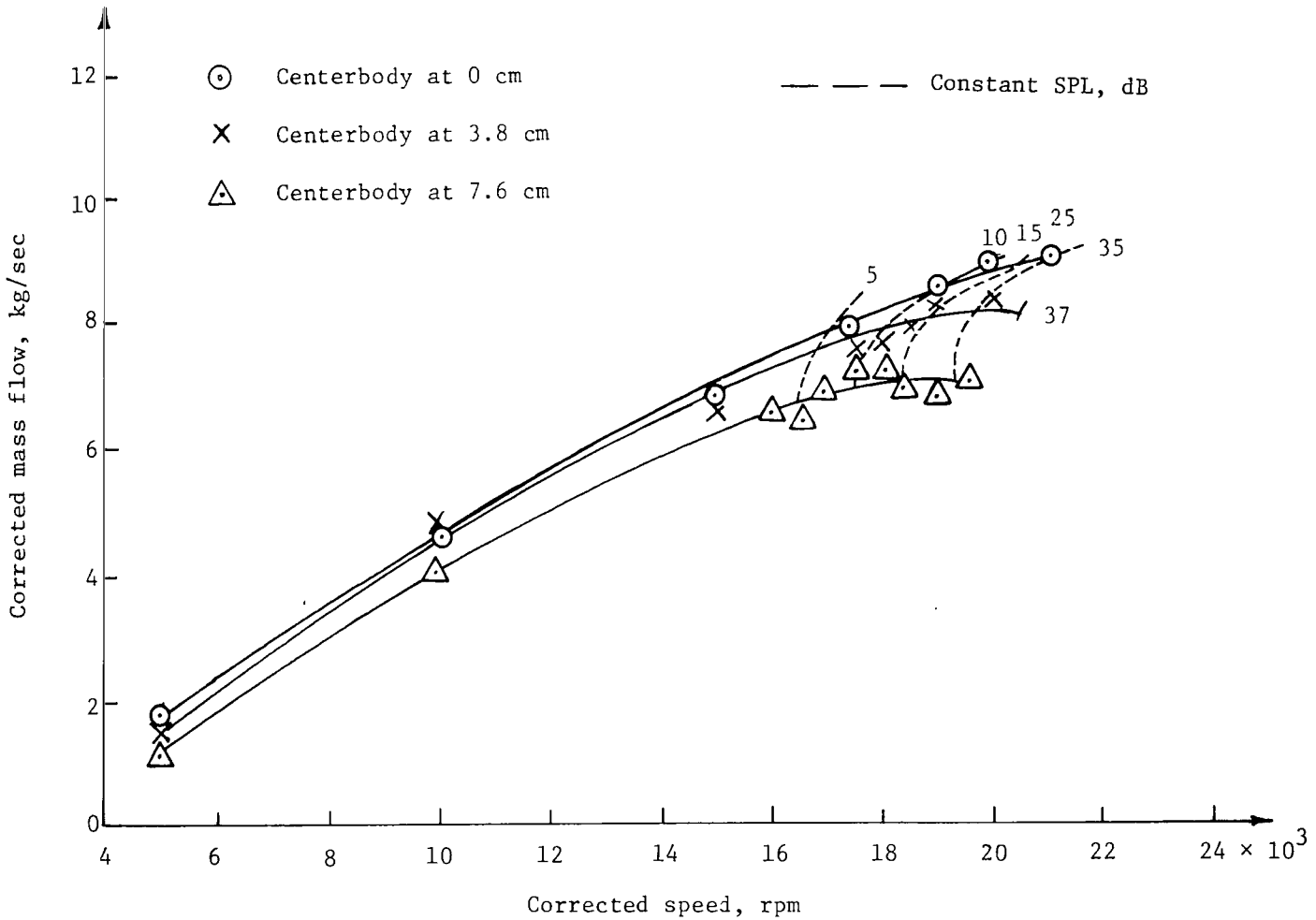

Figure 39.- Mass flow for inlet configuration 4.

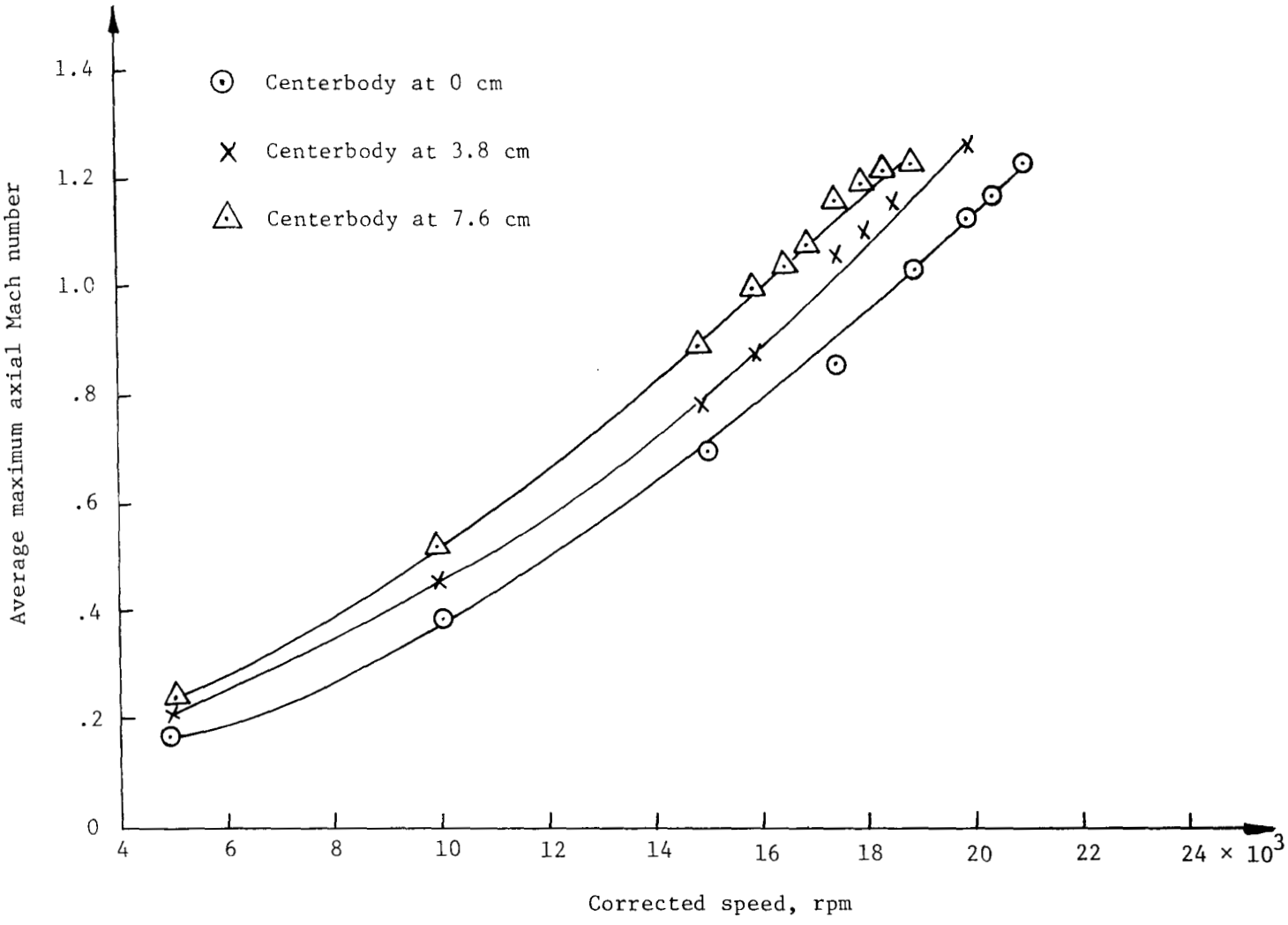

Figure 40.- Average maximum axial Mach number for inlet configuration 4.

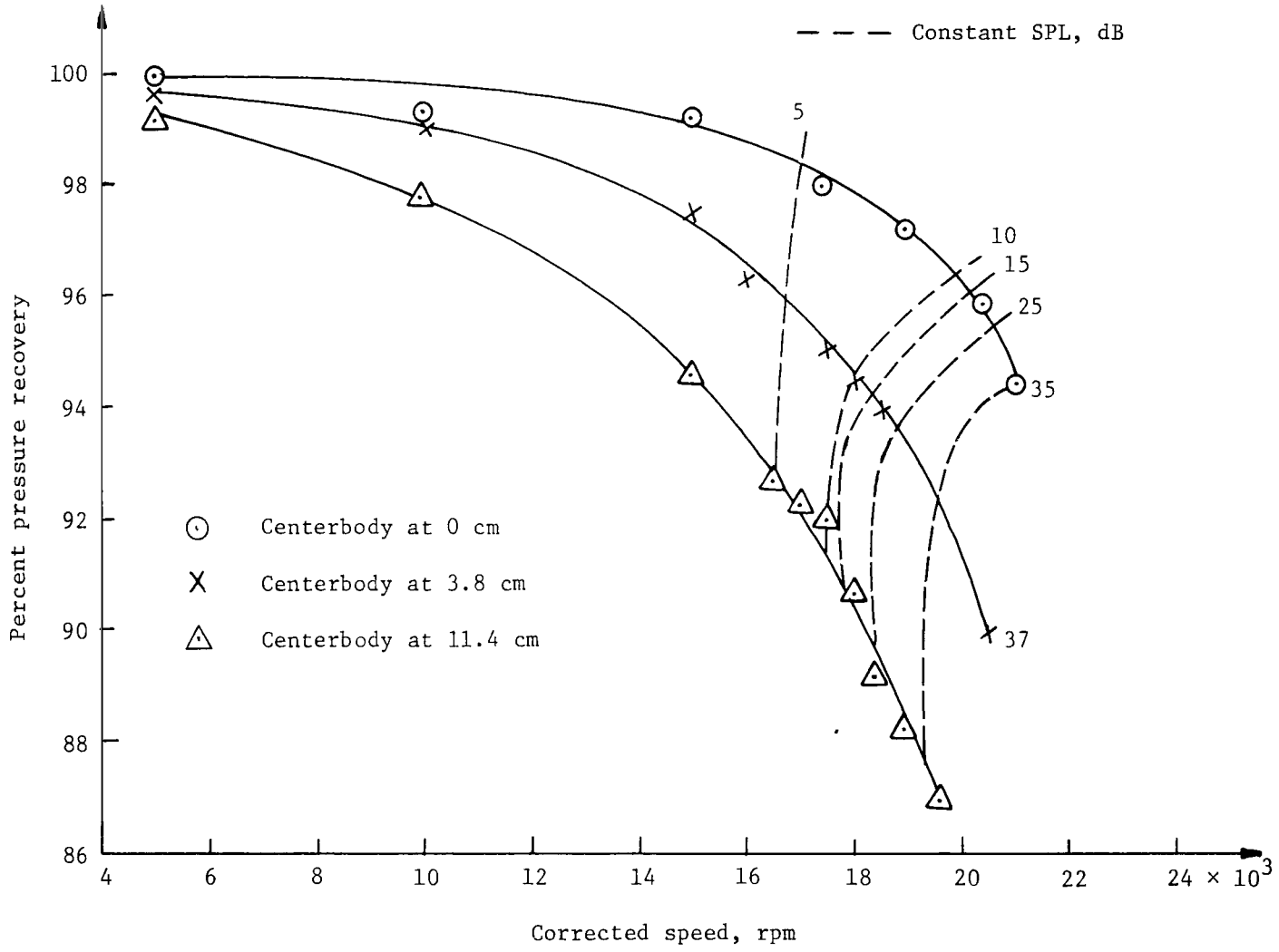

Figure 41.- Pressure recovery for inlet configuration 4. Inlet pressure recovery, $p_{t2,d}/p_{t1,d}$.

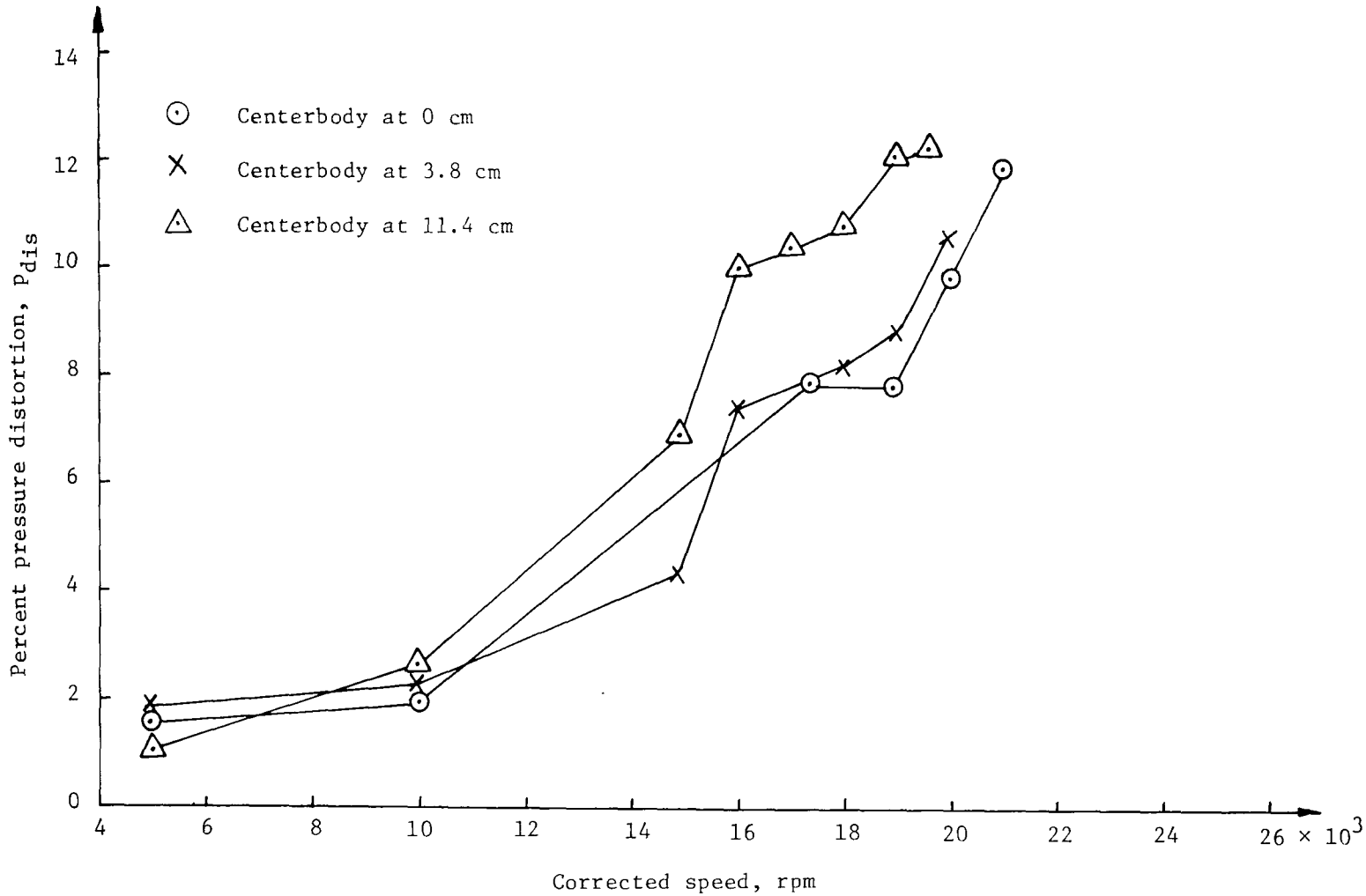

Figure 42.- Pressure distortion for inlet configuration 4.

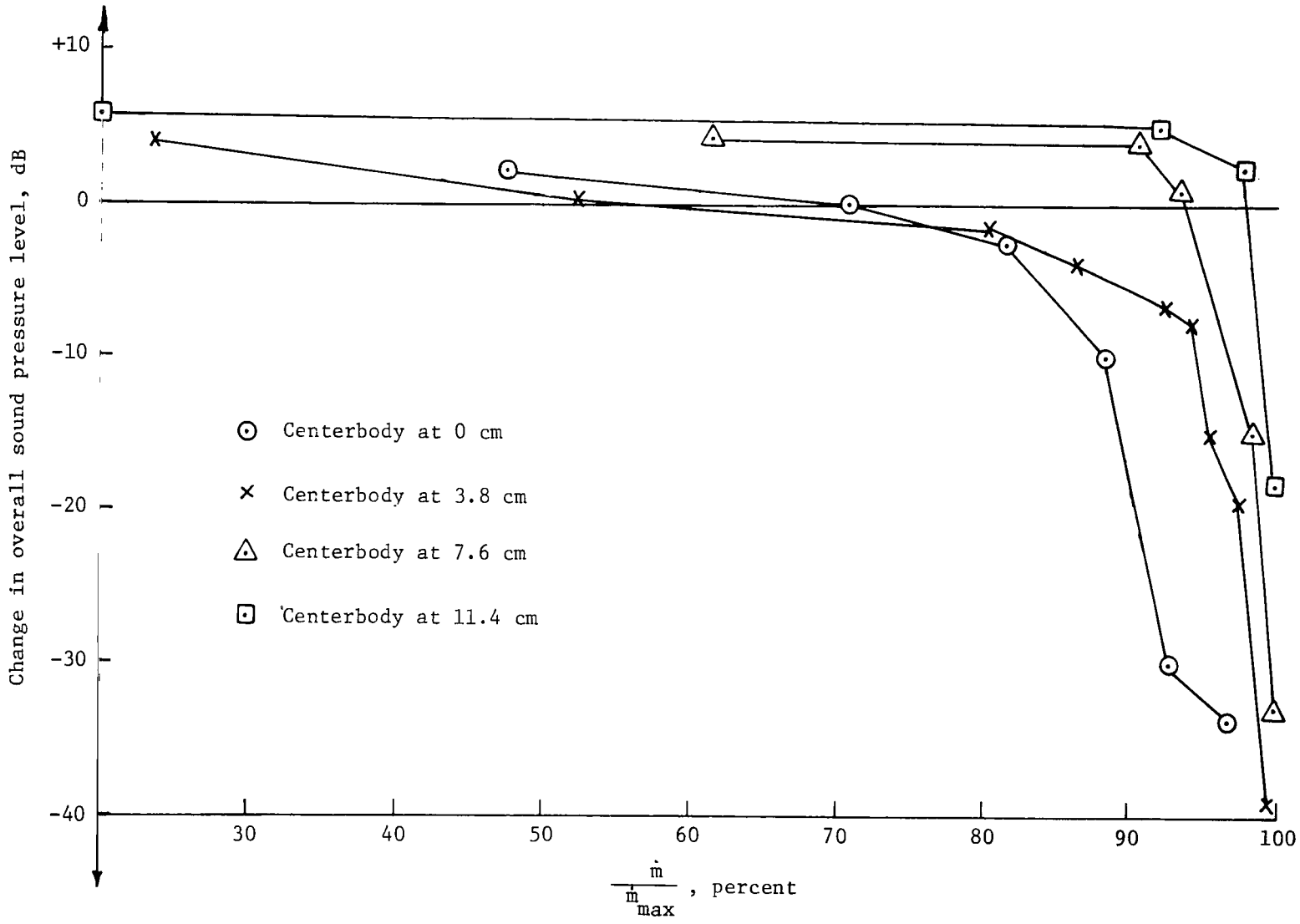

Figure 43.- Effect of percentage of maximum mass flow on noise attenuation for inlet configuration 2.

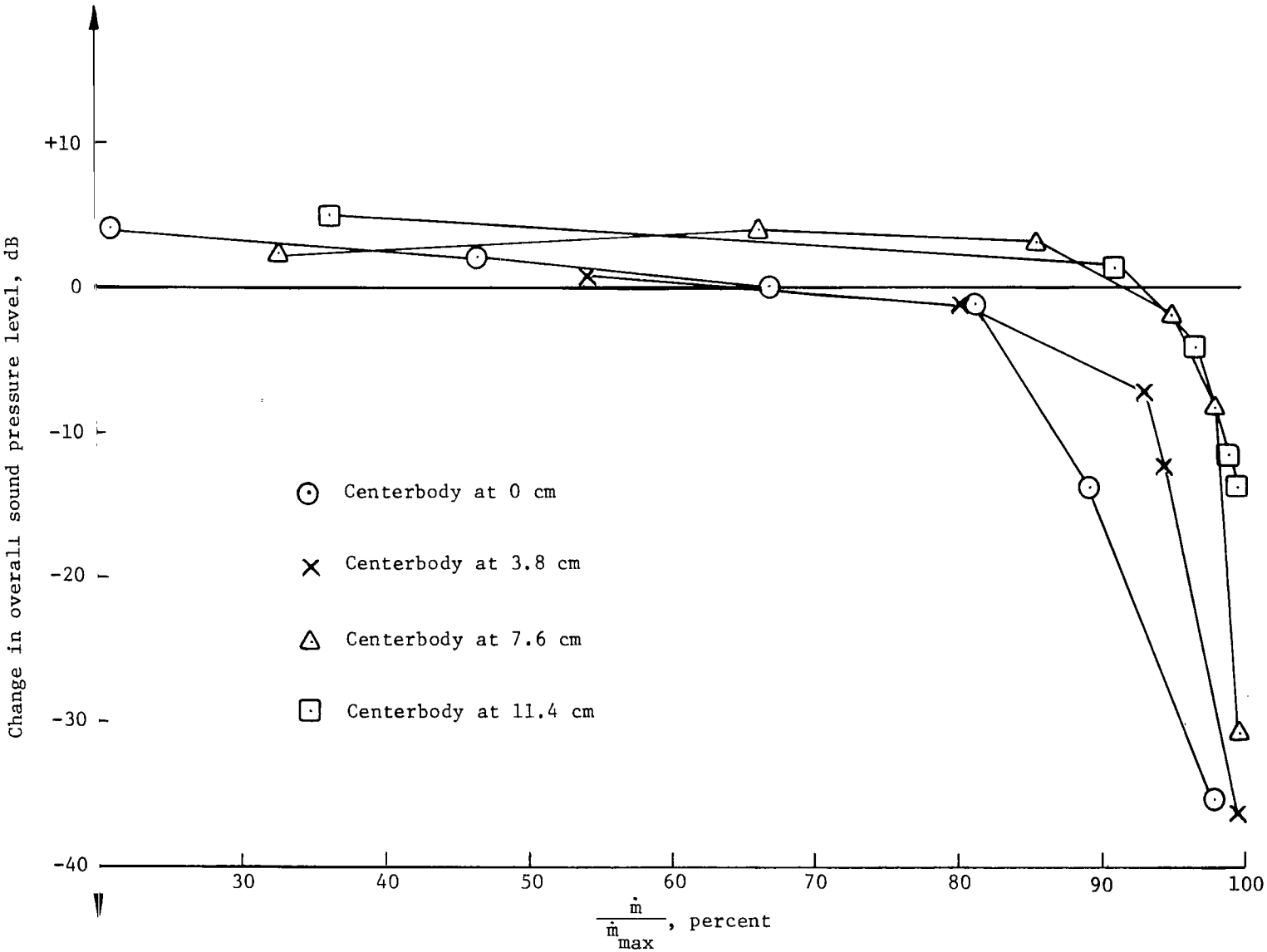

Figure 44.- Effect of percentage of maximum mass flow on noise attenuation for inlet configuration 3.

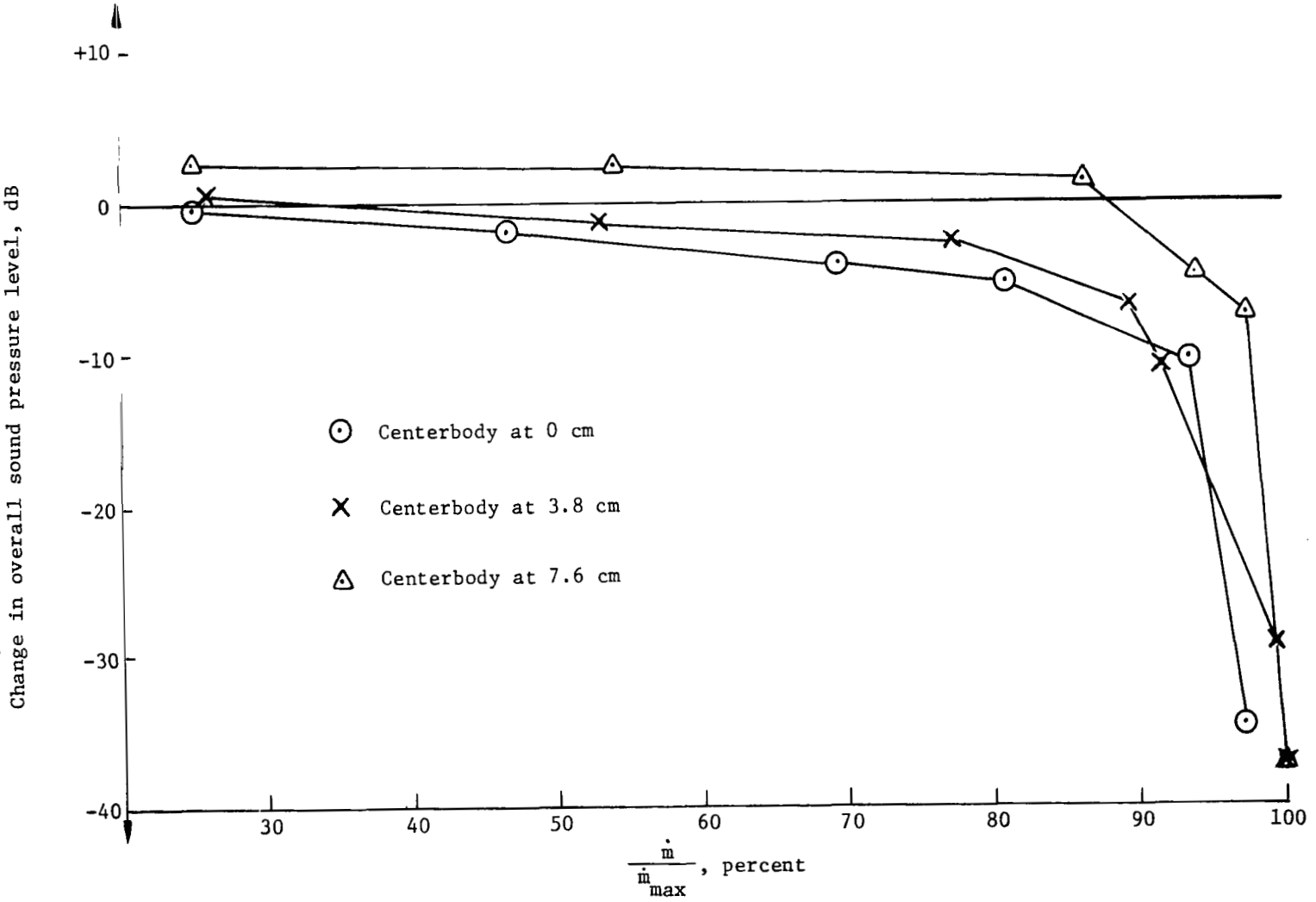

Figure 45.- Effect of percentage of maximum mass flow on noise attenuation for inlet configuration 4.

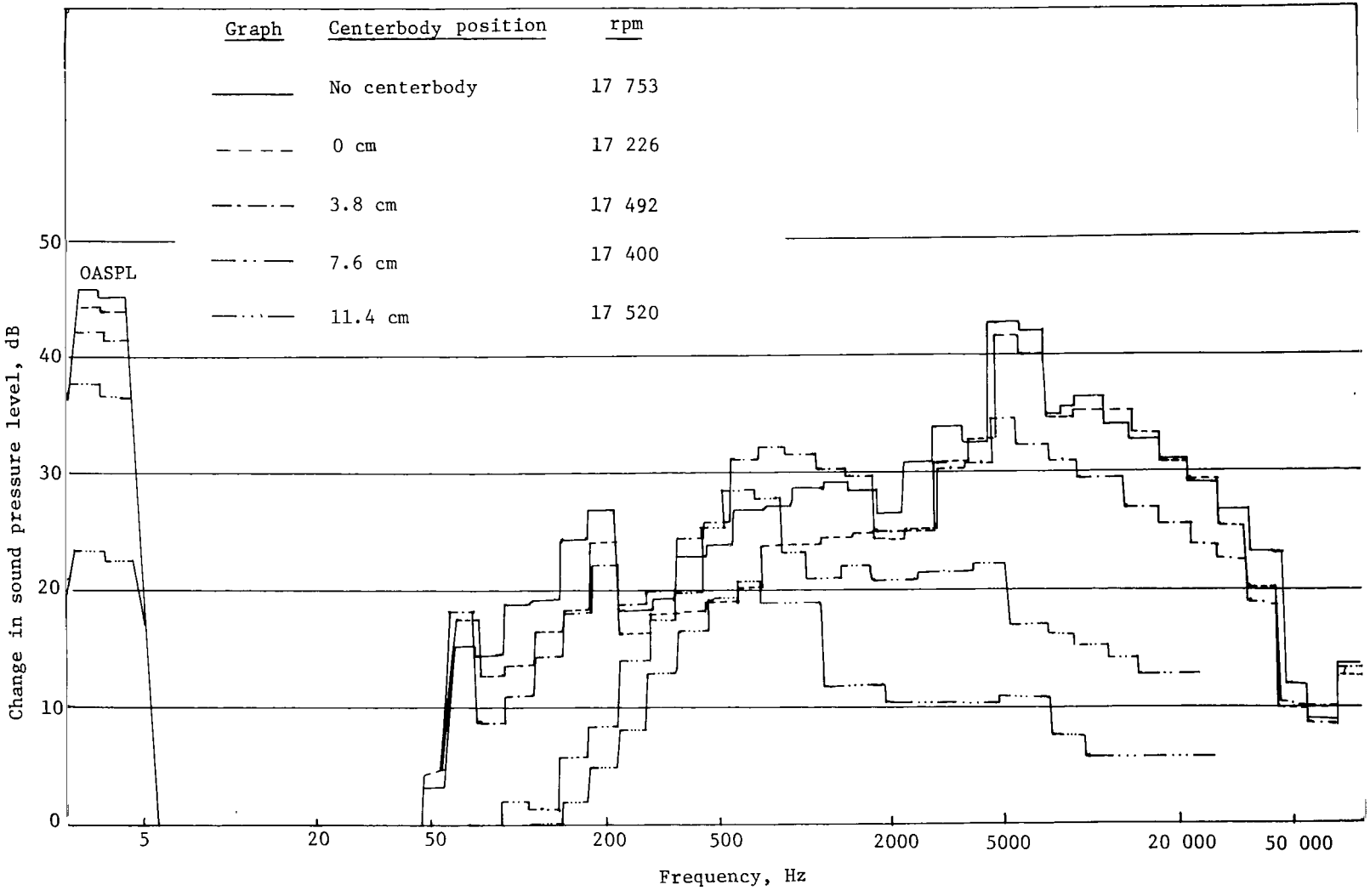

Figure 46.- Frequency spectra for configuration 2 at approximately 17 500 rpm; boom microphone at 45°.

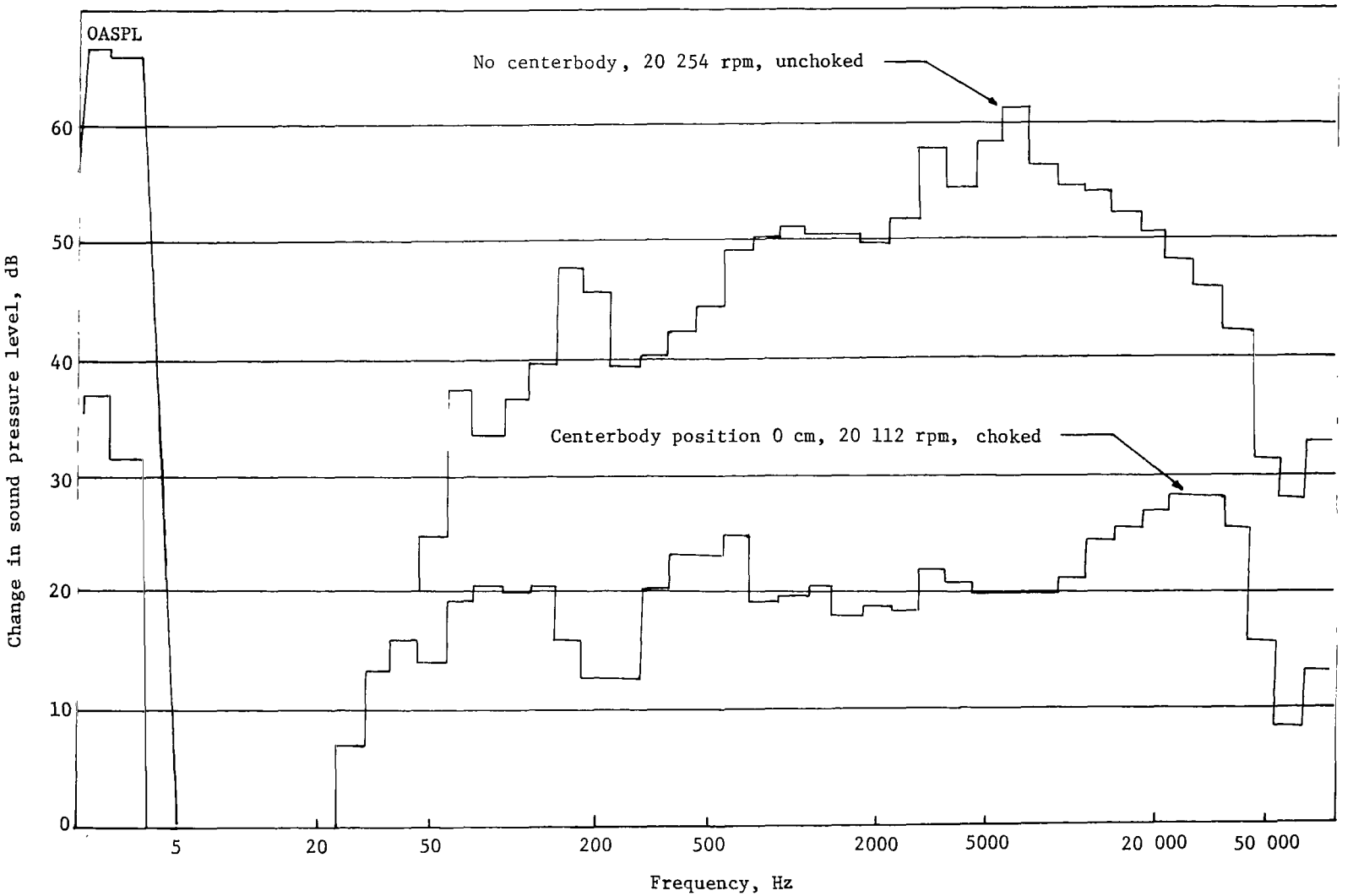

Figure 47.- Frequency spectra for configuration 2 at approximately 20 100 rpm; boom microphone at 45°.

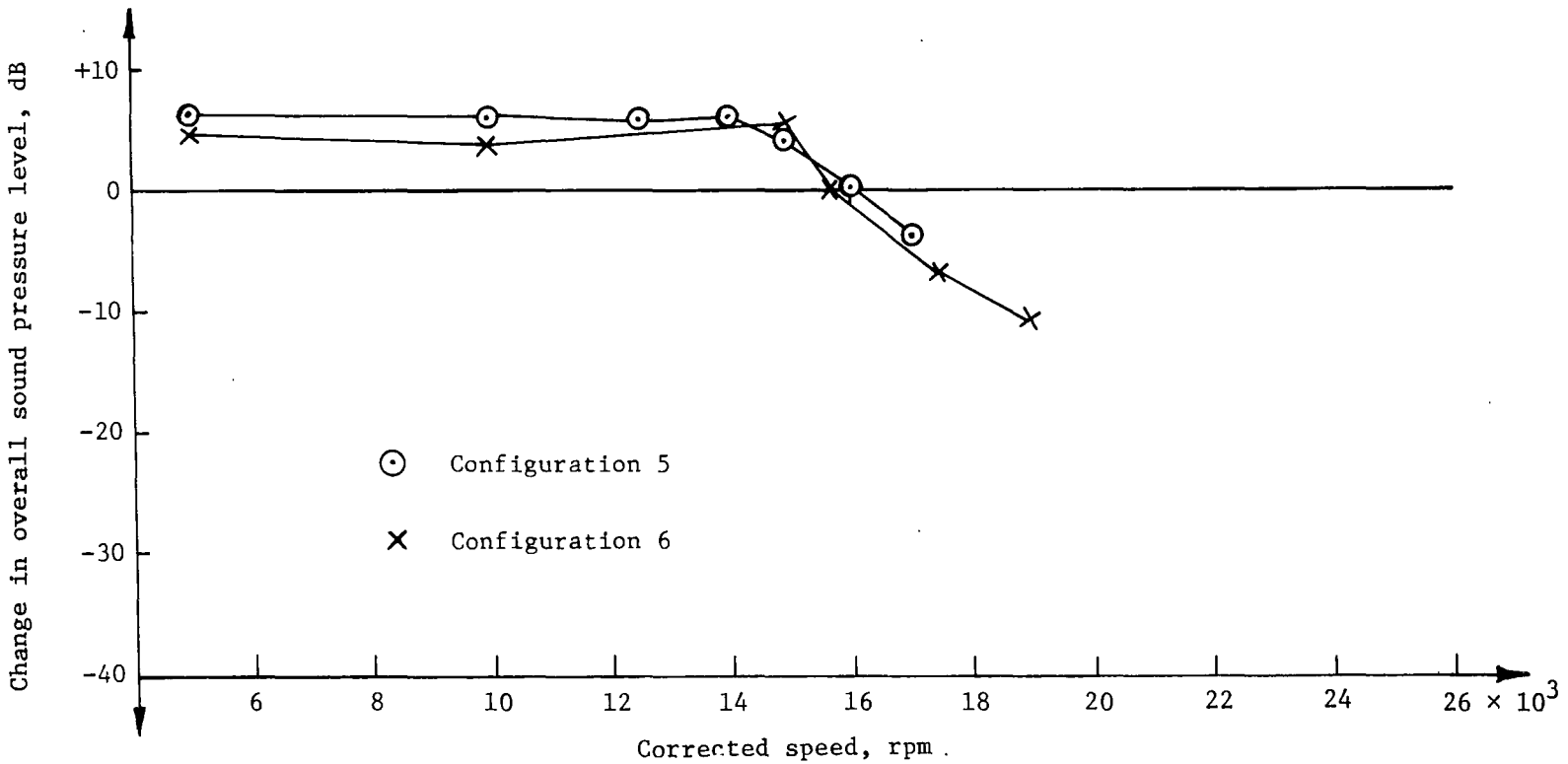

Figure 48.- Noise attenuation for inlet configurations 5 and 6; boom microphone at 0°.

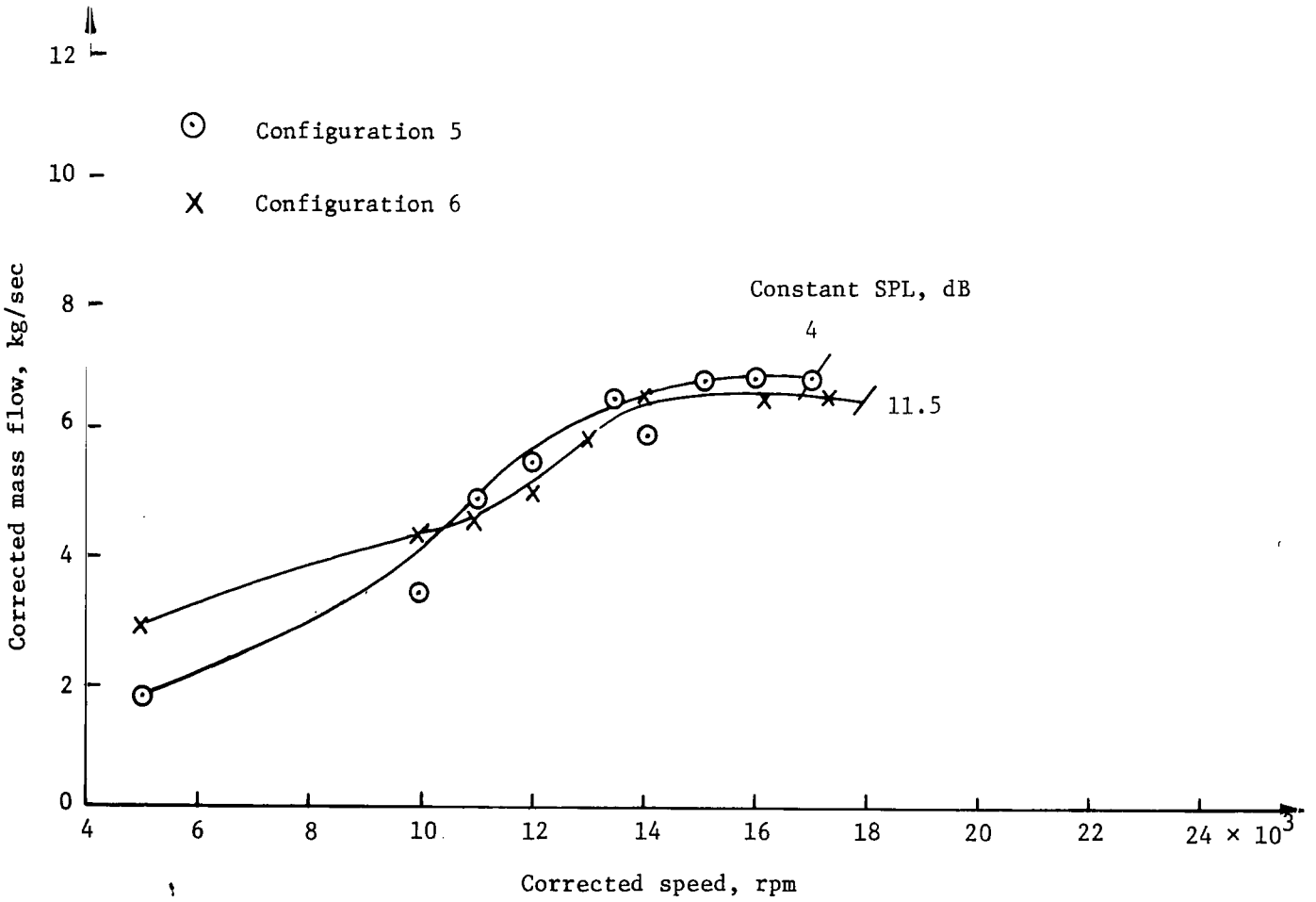

Figure 49.- Mass flow for inlet configurations 5 and 6.

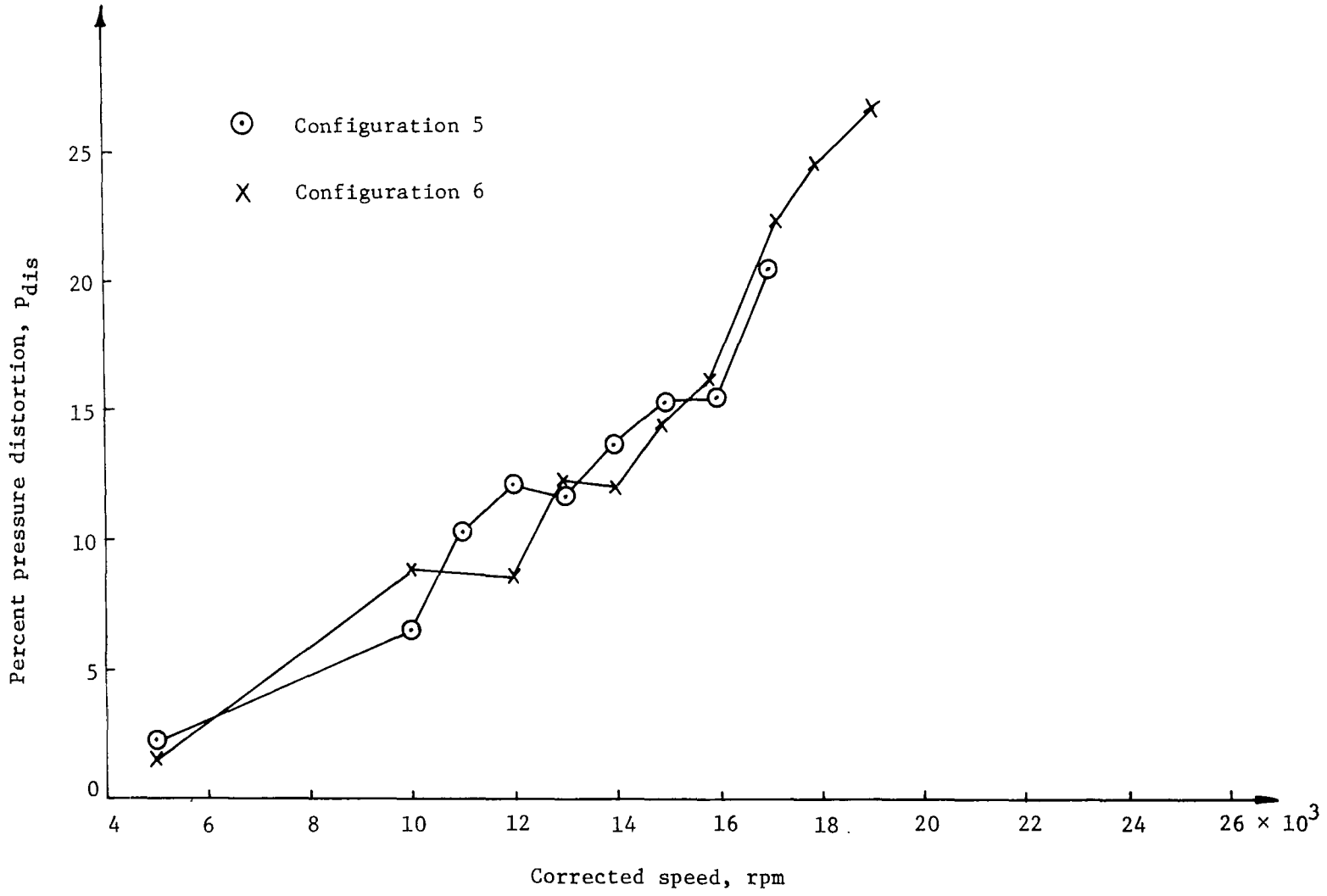

Figure 50.- Pressure distortion for inlet configurations 5 and 6.

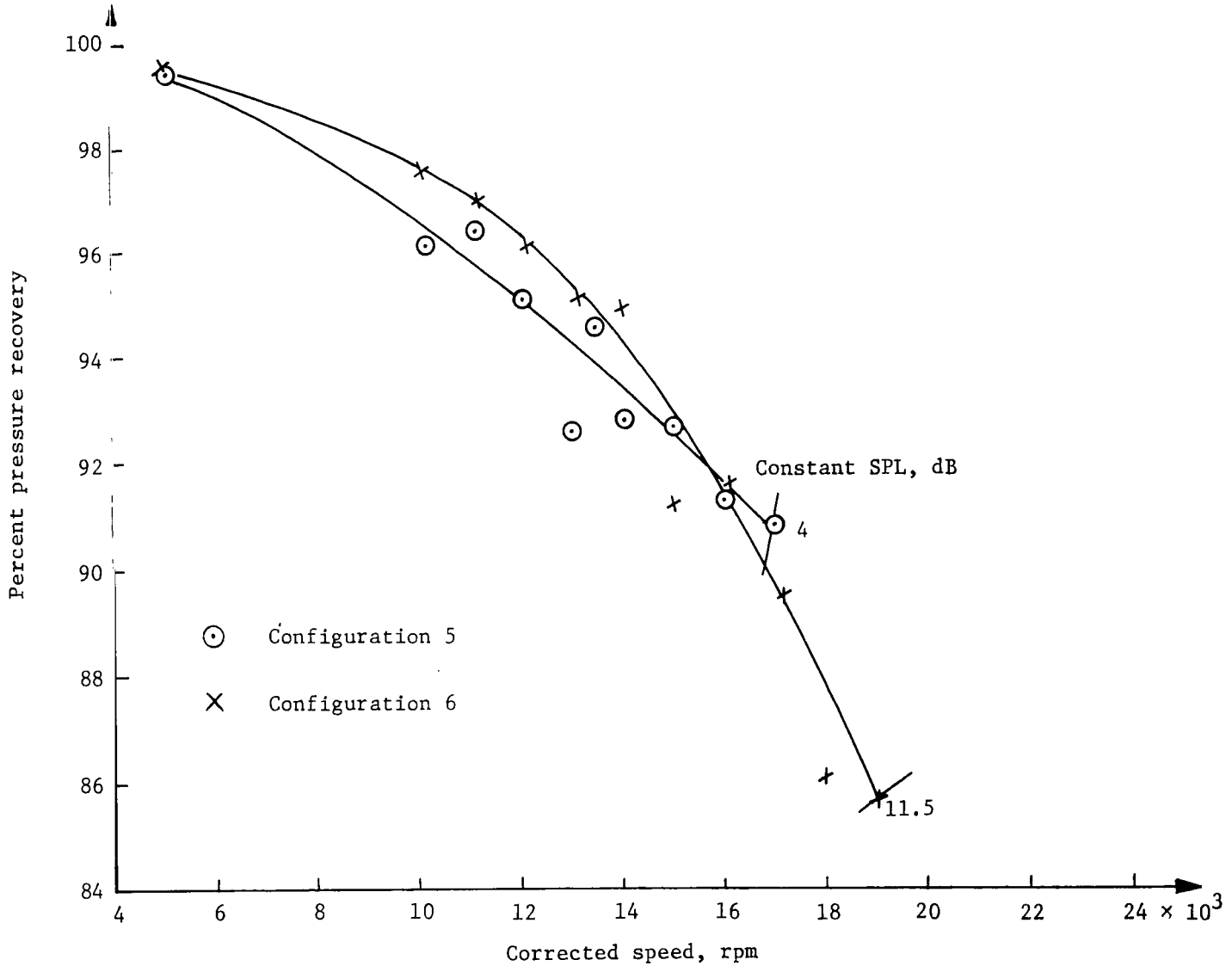

Figure 51.- Pressure recovery for inlet configurations 5 and 6. Inlet pressure recovery, $p_{t2,d}/p_{t1,d}$.

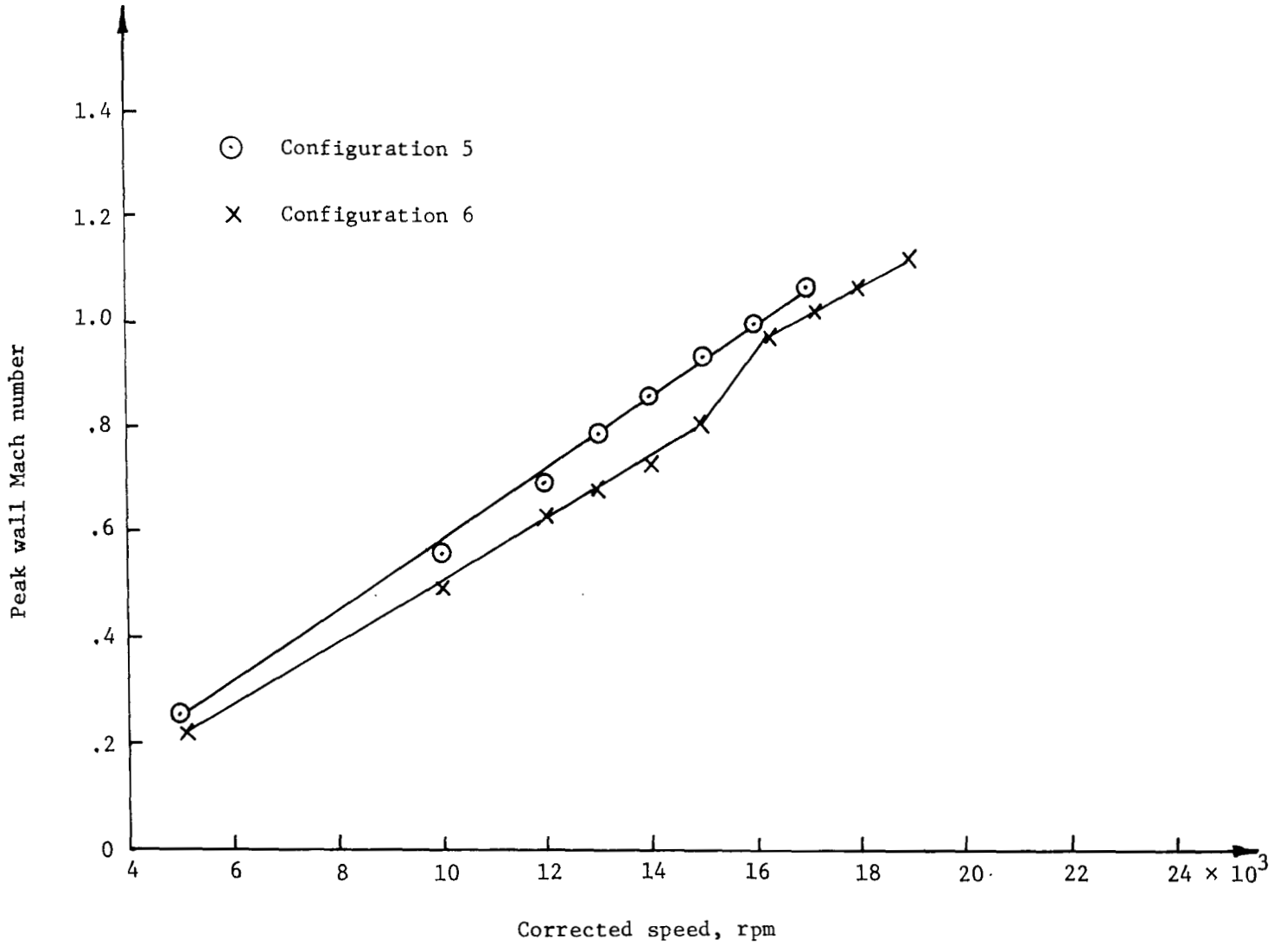

Figure 52.- Peak wall Mach number of inlet configurations 5 and 6.

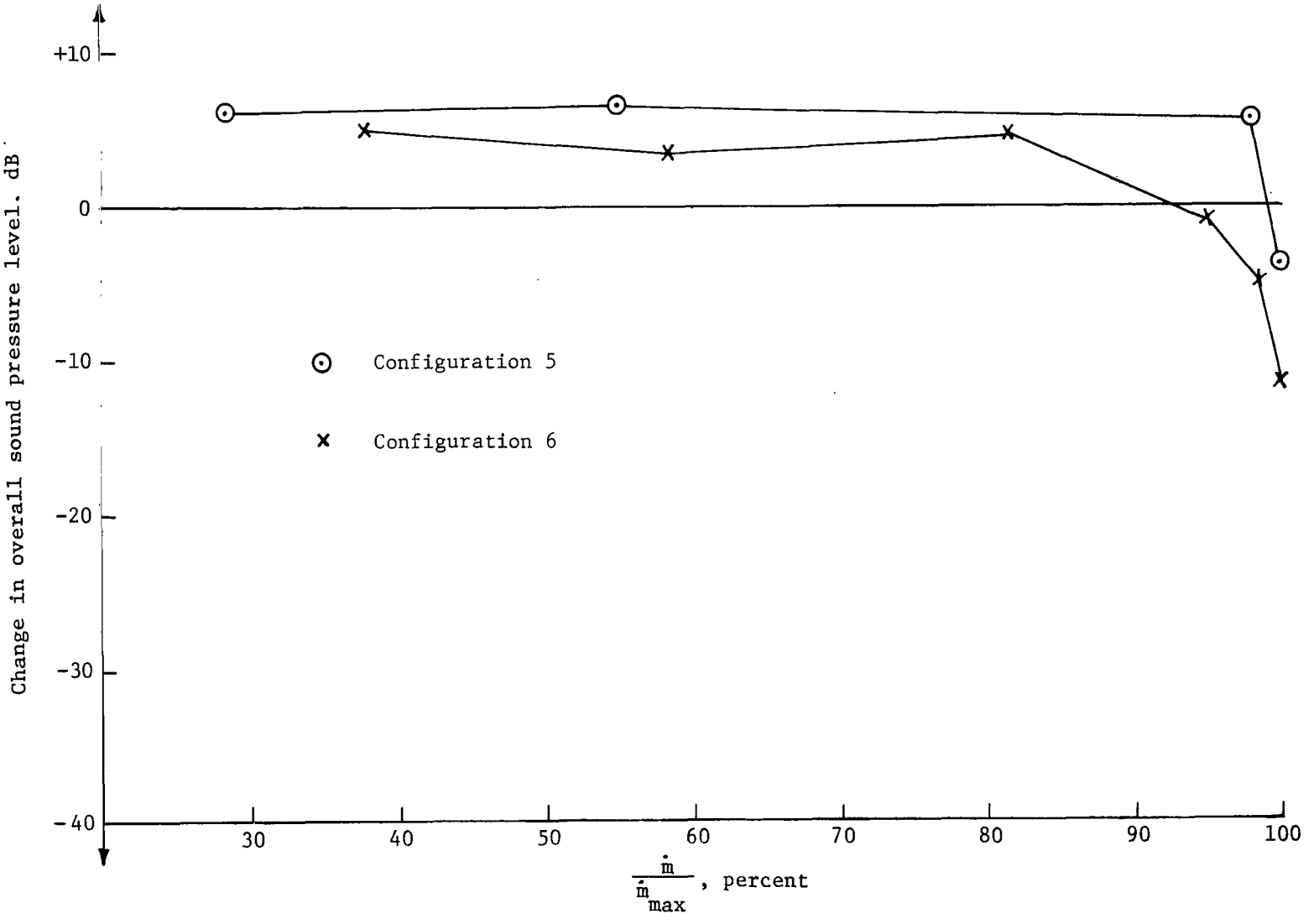

Figure 53.- Effect of percentage of maximum mass flow on noise attenuation for inlet configurations 5 and 6.

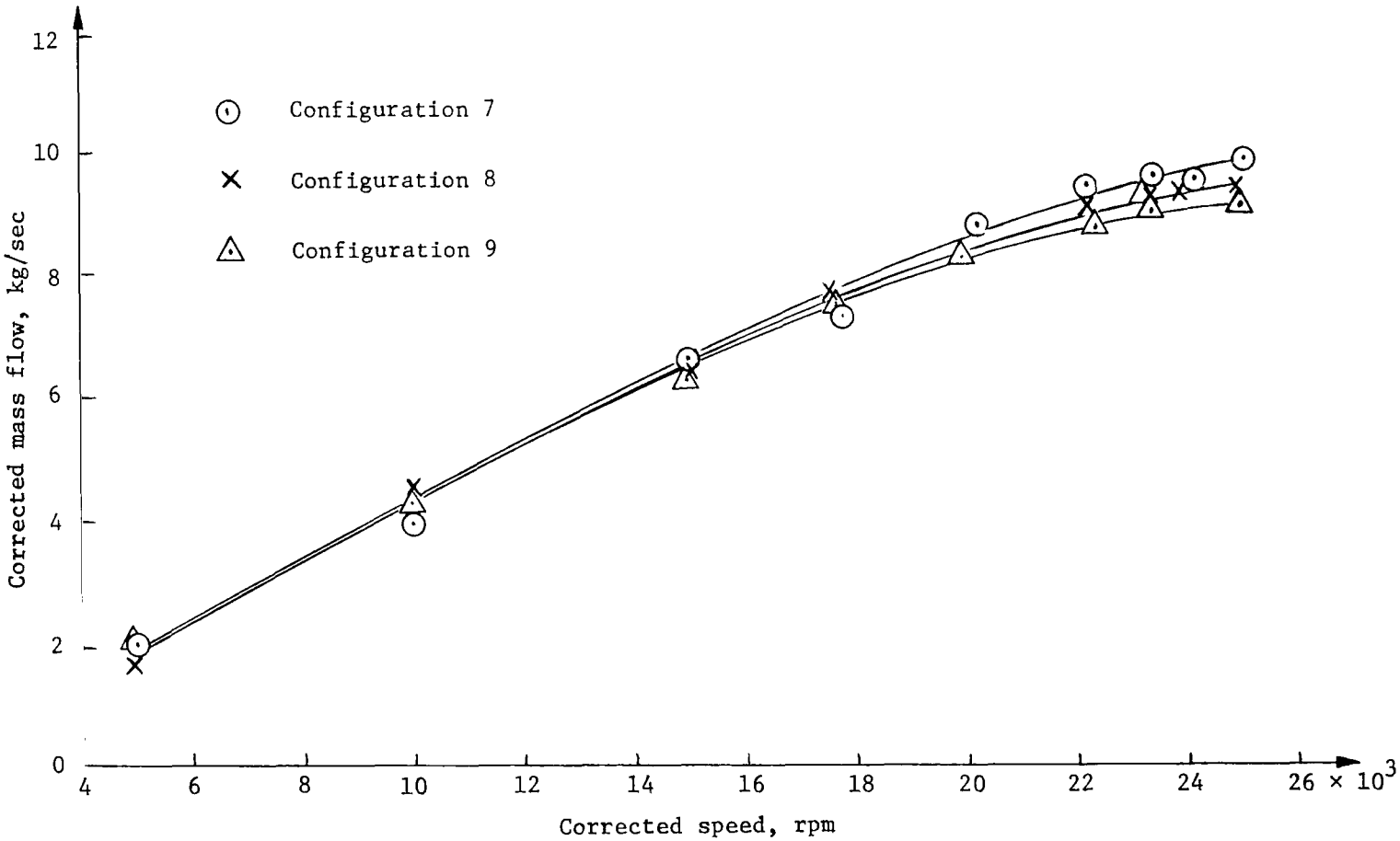

Figure 54.- Mass flow for inlet configurations 7, 8, and 9.

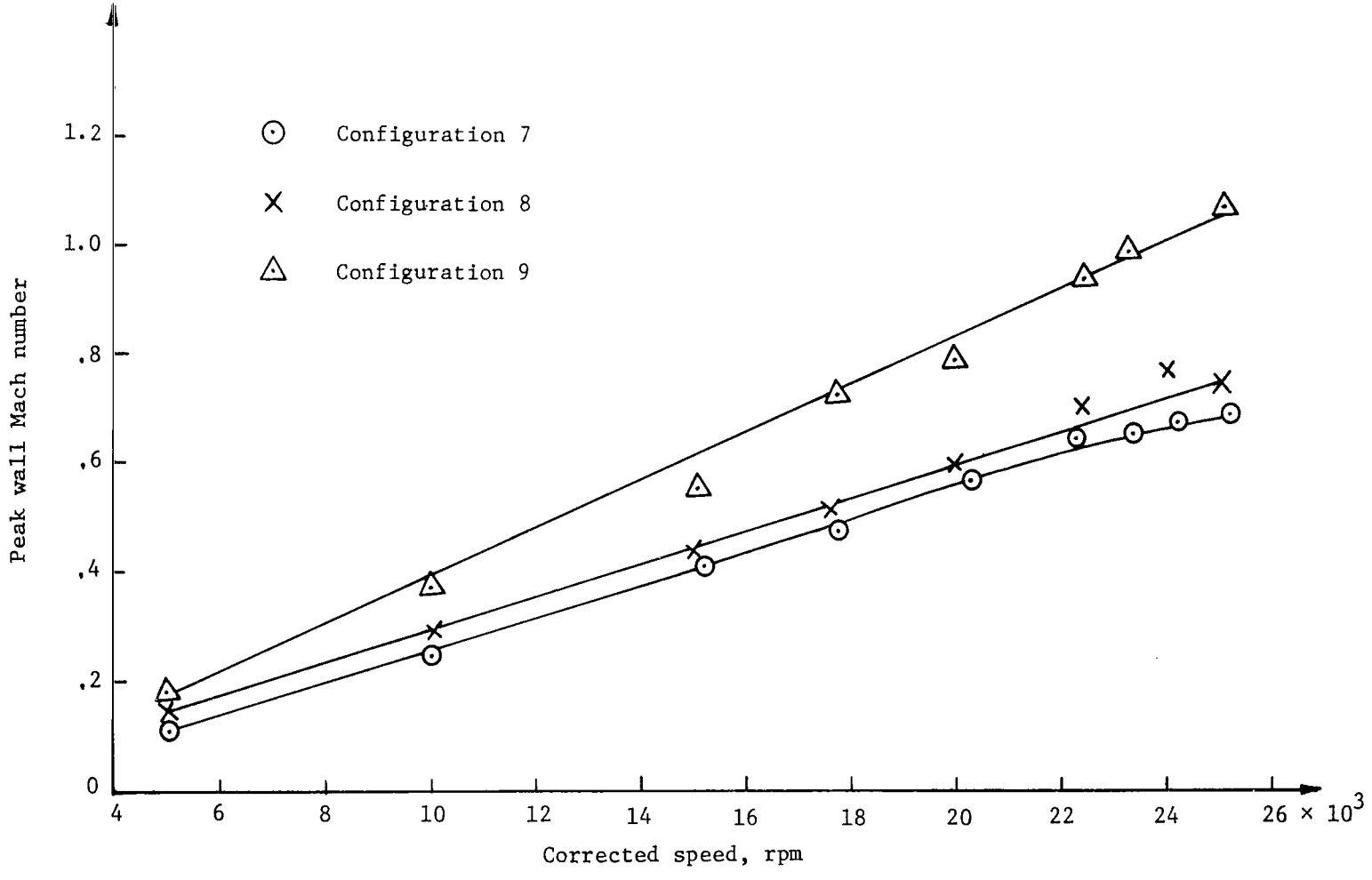

Figure 55.- Peak wall Mach number of inlet configurations 7, 8, and 9.

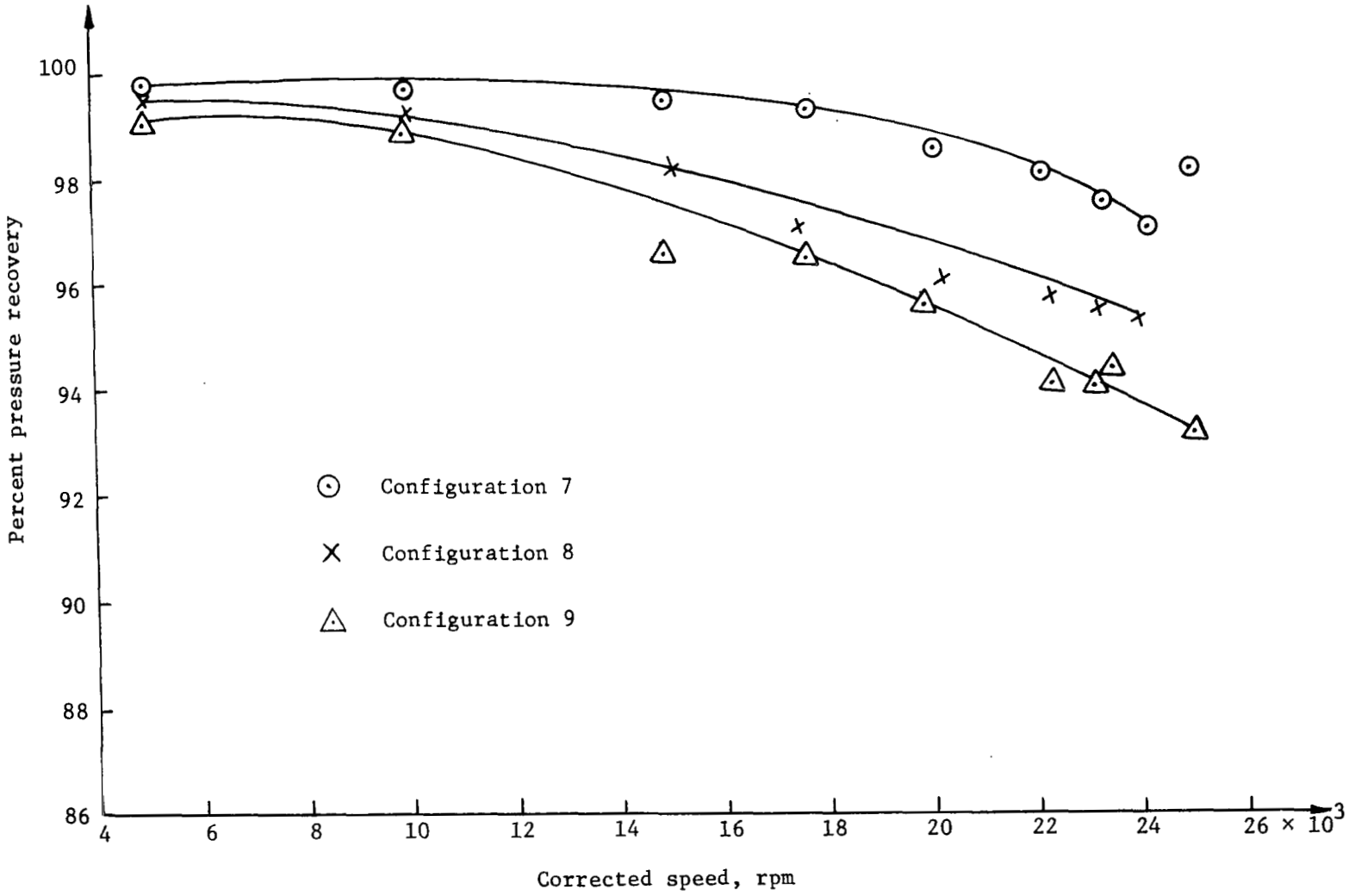

Figure 56.- Pressure recovery for inlet configurations 7, 8, and 9. Inlet pressure recovery, $p_{t2,d}/p_{t1,d}$.

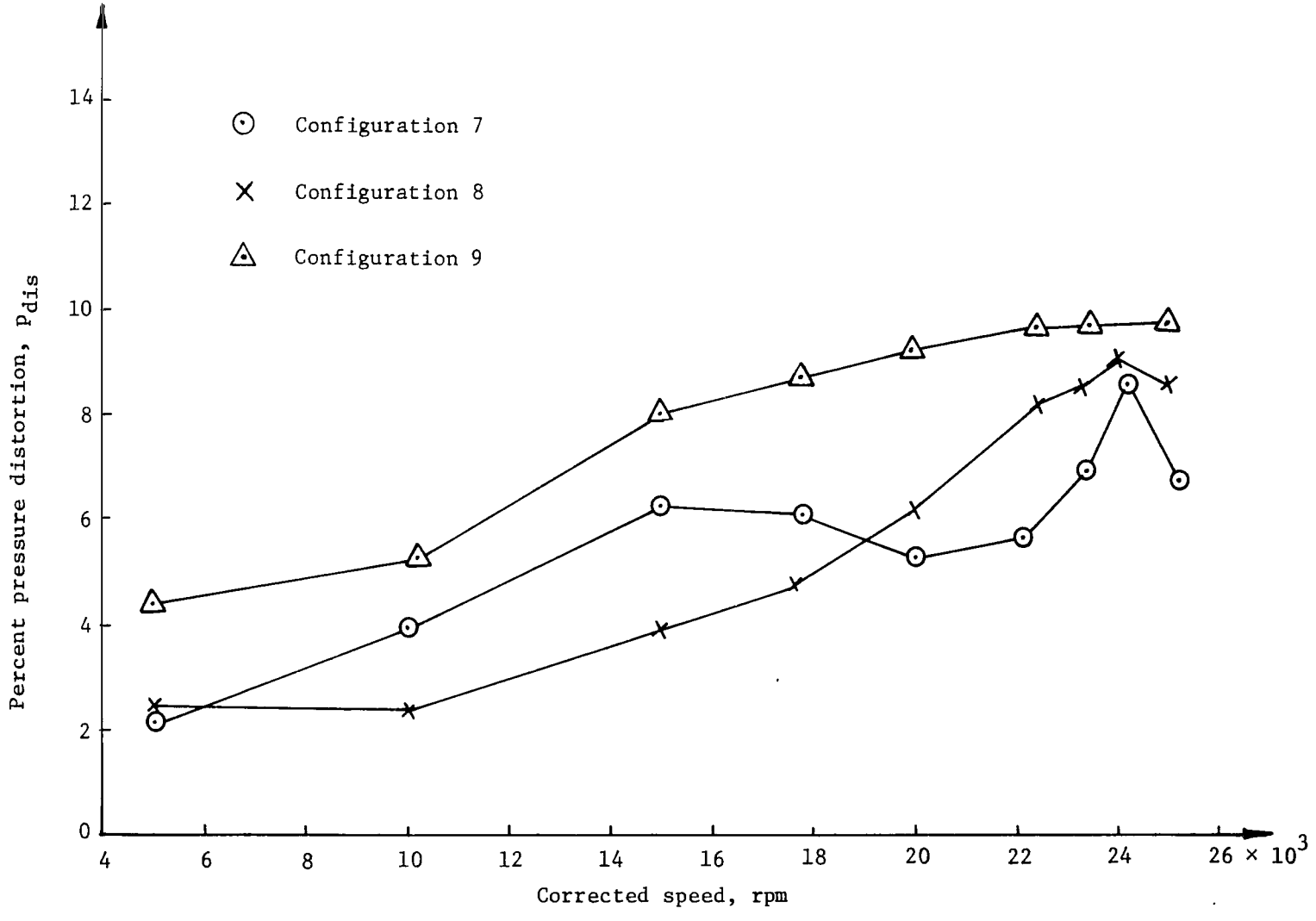

Figure 57.- Pressure distortion for configurations 7, 8, and 9.

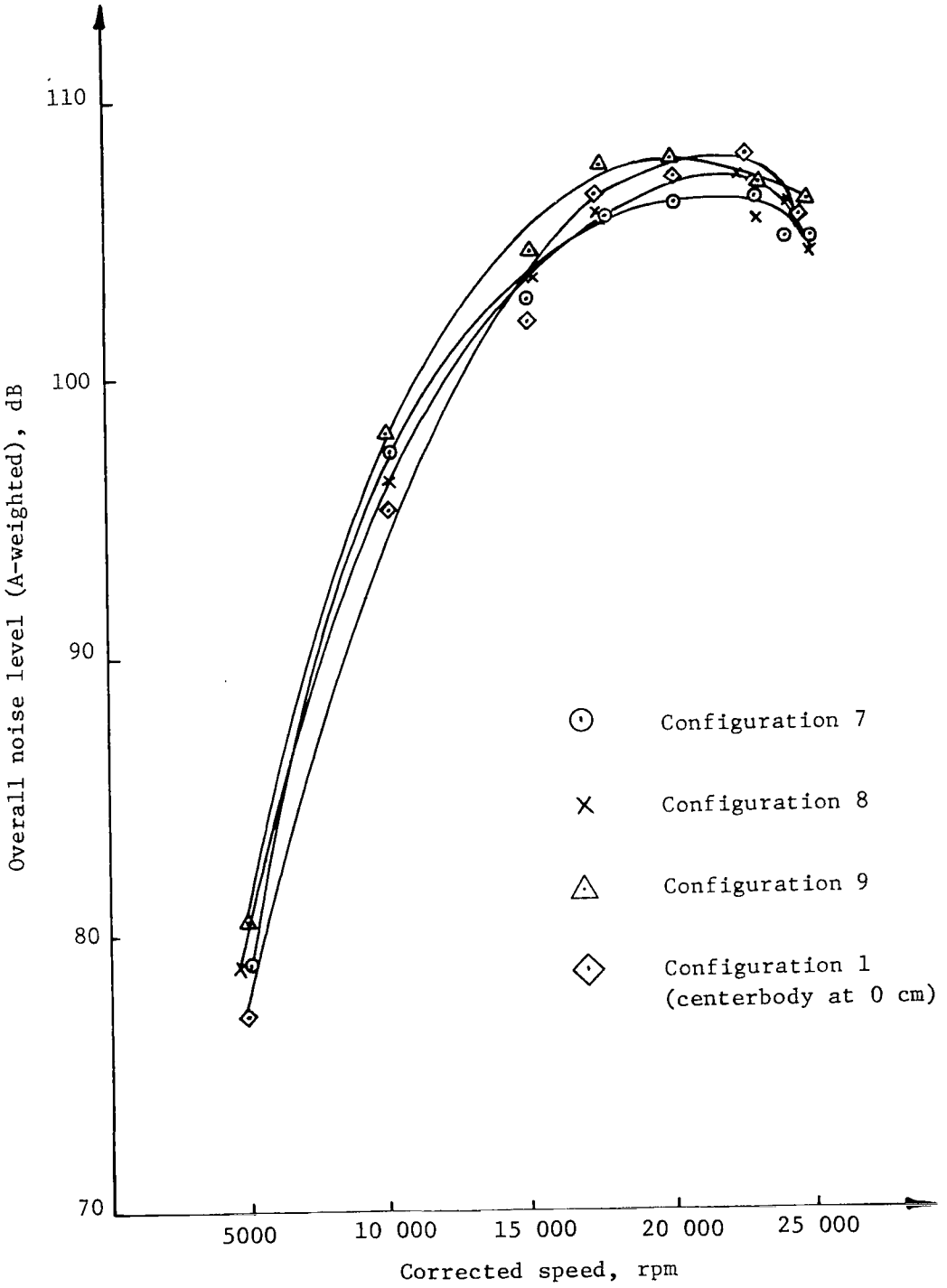

Figure 58.- Comparison of overall noise attenuation characteristics of inlets operating at subsonic Mach numbers; boom microphone at 45°.

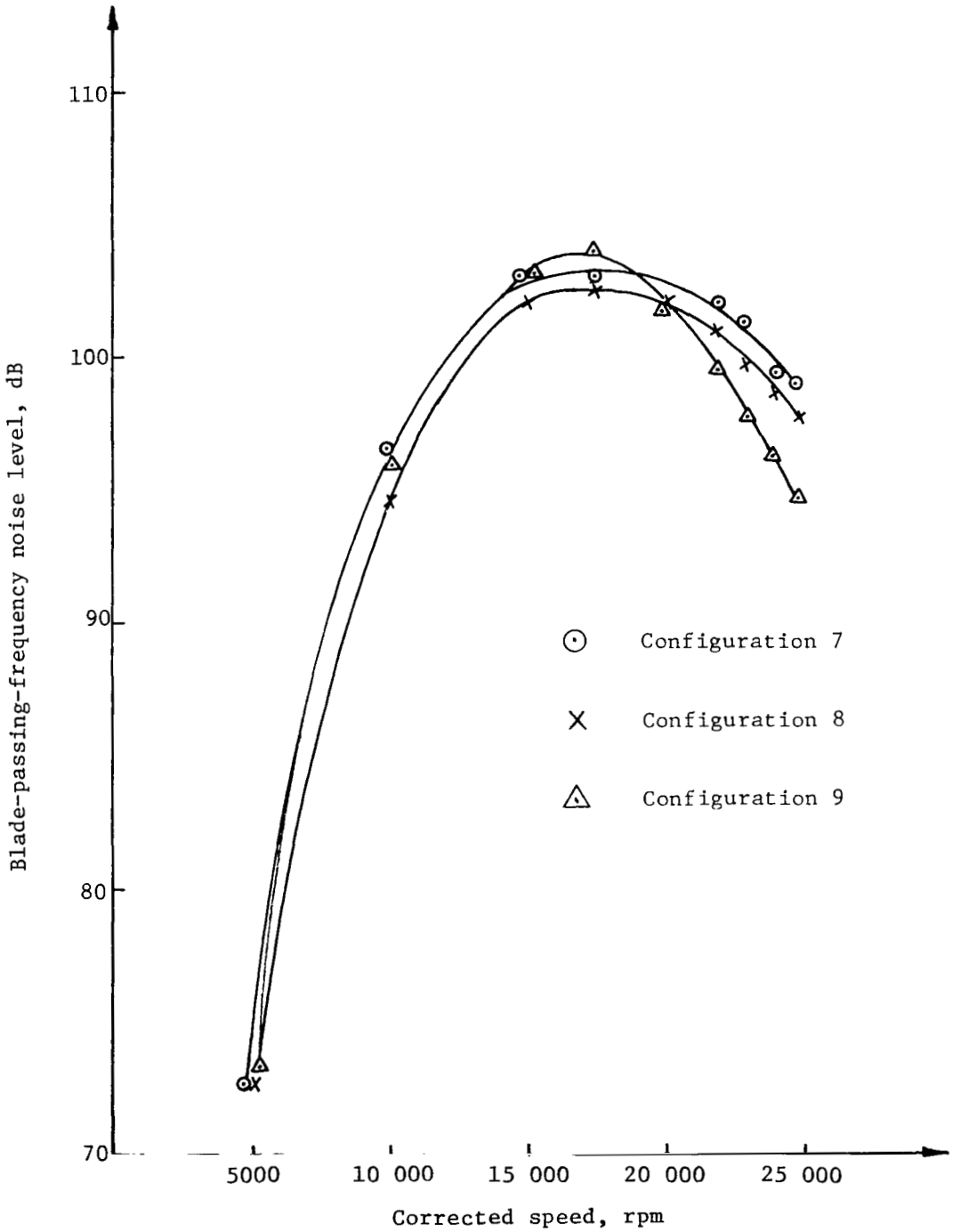

Figure 59.- Comparison of blade-passing-frequency attenuation characteristics of inlets operating at subsonic Mach numbers; boom microphone at 45°.

NATIONAL AERONAUTICS AND SPACE ADMINISTRATION
WASHINGTON, D.C. 20546

OFFICIAL BUSINESS
PENALTY FOR PRIVATE USE $300

SPECIAL FOURTH-CLASS RATE BOOK

POSTAGE AND FEES PAID
NATIONAL AERONAUTICS AND SPACE ADMINISTRATION
451

U.S.MAIL

"The aeronautical and space activities of the United States shall be conducted so as to contribute . . . to the expansion of human knowledge of phenomena in the atmosphere and space. The Administration shall provide for the widest practicable and appropriate dissemination of information concerning its activities and the results thereof."

—NATIONAL AERONAUTICS AND SPACE ACT OF 1958

NASA SCIENTIFIC AND TECHNICAL PUBLICATIONS

TECHNICAL REPORTS: Scientific and technical information considered important, complete, and a lasting contribution to existing knowledge.

TECHNICAL NOTES: Information less broad in scope but nevertheless of importance as a contribution to existing knowledge.

TECHNICAL MEMORANDUMS: Information receiving limited distribution because of preliminary data, security classification, or other reasons. Also includes conference proceedings with either limited or unlimited distribution.

CONTRACTOR REPORTS: Scientific and technical information generated under a NASA contract or grant and considered an important contribution to existing knowledge.

TECHNICAL TRANSLATIONS: Information published in a foreign language considered to merit NASA distribution in English.

SPECIAL PUBLICATIONS: Information derived from or of value to NASA activities. Publications include final reports of major projects, monographs, data compilations, handbooks, sourcebooks, and special bibliographies.

TECHNOLOGY UTILIZATION PUBLICATIONS: Information on technology used by NASA that may be of particular interest in commercial and other non-aerospace applications. Publications include Tech Briefs, Technology Utilization Reports and Technology Surveys.

Details on the availability of these publications may be obtained from:

SCIENTIFIC AND TECHNICAL INFORMATION OFFICE

NATIONAL AERONAUTICS AND SPACE ADMINISTRATION

Washington, D.C. 20546